Biogeosciences

Review: geological and experimental evidence for secular variation in seawater Mg/Ca (calcite-aragonite seas) and its effects on marine biological calcification

J. B. Ries

Department of Marine Sciences, 333 Chapman Hall, CB# 3300, University of North Carolina – Chapel Hill,
Chapel Hill, NC 27599, USA

Abstract. Synchronized transitions in the polymorph mineralogy of the major reef-building and sediment-producing calcareous marine organisms and abiotic $CaCO_3$ precipitates (ooids, marine cements) throughout Phanerozoic time are believed to have been caused by tectonically induced variations in the Mg/Ca ratio of seawater (molar Mg/Ca>2="aragonite seas", <2="calcite seas"). Here, I assess the geological evidence in support of secular variation in seawater Mg/Ca and its effects on marine calcifiers, and review a series of recent experiments that investigate the effects of seawater Mg/Ca (1.0–5.2) on extant representatives of calcifying taxa that have experienced variations in this ionic ratio of seawater throughout the geologic past.

Secular variation in seawater Mg/Ca is supported by synchronized secular variations in (1) the ionic composition of fluid inclusions in primary marine halite, (2) the mineralogies of late stage marine evaporites, abiogenic carbonates, and reef- and sediment-forming marine calcifiers, (3) the Mg/Ca ratios of fossil echinoderms, molluscs, rugose corals, and abiogenic carbonates, (4) global rates of tectonism that drive the exchange of Mg^{2+} and Ca^{2+} along zones of ocean crust production, and (5) additional proxies of seawater Mg/Ca including Sr/Mg ratios of abiogenic carbonates, Sr/Ca ratios of biogenic carbonates, and Br concentrations in marine halite.

Laboratory experiments have revealed that aragonite-secreting bryopsidalean algae and scleractinian corals and calcite-secreting coccolithophores exhibit higher rates of calcification and growth in experimental seawaters formulated with seawater Mg/Ca ratios that favor their skeletal mineral. These results support the assertion that seawater Mg/Ca

played an important role in determining which hypercalcifying marine organisms were the major reef-builders and sediment-producers throughout Earth history. The observation that primary production increased along with calcification within the bryopsidalean and coccolithophorid algae in mineralogically favorable seawater is consistent with the hypothesis that calcification promotes photosynthesis within some species of these algae through the liberation of CO_2.

The experiments also revealed that aragonite-secreting bryopsidalean algae and scleractinian corals, and bacterial biofilms that secrete a mixture of aragonite and high Mg calcite, began secreting an increased proportion of their calcium carbonate as the calcite polymorph in the lower-Mg/Ca experimental seawaters. Furthermore, the Mg/Ca ratio of calcite secreted by the coccolithophores, coralline red algae, reef-dwelling animals (crustacea, urchins, calcareous tube worms), bacterial biofilms, scleractinian corals, and bryopsidalean algae declined with reductions in seawater Mg/Ca. Notably, Mg fractionation in autotrophic organisms was more strongly influenced by changes in seawater Mg/Ca than in heterotrophic organisms, a probable consequence of autotrophic organisms inducing a less controlled mode of calcification simply through the removal of CO_2 via photosynthesis.

These results indicate that biomineralogical control can be partially overridden by ambient seawater Mg/Ca and suggest that modern aragonite-secreting organisms may have secreted a mixture of aragonite and low Mg calcite, and that modern high Mg calcite-secreting organisms probably secreted low Mg calcite, in calcite seas of the past. These effects of seawater Mg/Ca on the polymorph mineralogy and calcite Mg/Ca ratio of calcareous skeletons should be accounted for in thermal-chemical reconstructions of seawater that are based upon skeletal Mg/Ca.

Correspondence to: J. B. Ries
(jries@unc.edu)

Lastly, by identifying how marine calcifiers respond to changes in seawater Mg/Ca and absolute Ca^{2+} concentration, this work should enhance our interpretation of parallel studies investigating the effects of anthropogenic CO_2-induced ocean acidification on marine calcification.

1   Introduction

Chemical analyses of fluid inclusions derived from ancient primary marine halite indicate that the Mg/Ca ratio[1] of seawater has varied between 1.0 and 5.2 throughout the Phanerozoic Eon (Lowenstein et al., 2001, 2003, 2005; Horita et al., 2002; Brennan et al., 2004; Timofeeff et al., 2006). These secular variations in seawater Mg/Ca are thought to be responsible for systematic changes in the polymorph mineralogy of ooids and marine cements throughout Phanerozoic time (Sandberg, 1983). During intervals of low seawater Mg/Ca (<2), such as early Cambrian through late Mississippian time and Middle Jurassic through middle Paleogene time, the predominant form of abiotically produced calcium carbonate ($CaCO_3$) produced in shallow seas was low Mg calcite (i.e., "calcite seas"). During intervals of high seawater Mg/Ca (>2), such as during early Cambrian time, late Mississippian through Middle Jurassic time and middle Paleogene though Modern time, aragonite and high Mg calcite were the predominant polymorphs (i.e., "aragonite seas"). For convention, I refer to Sandberg's three aragonite sea intervals as Aragonite I, II, and III and his two calcite sea intervals as Calcite I and II.

Stanley and Hardie (1998, 1999) observed that the carbonate mineralogy of simple, hypercalcifying organisms has varied in concert with Sandberg's (1983) aragonite and calcite seas throughout Phanerozoic time (Fig. 1). From this, they conclude that certain hypercalcifying organisms were only able to function as major reef builders (corals, sponges and algae) and carbonate sediment producers (algae) when their $CaCO_3$ polymorph mineralogy was favored by the Mg/Ca ratio of seawater. Here, I evaluate the geological evidence in support of secular variation in seawater Mg/Ca and its effects on marine calcification and review experiments that explore the effects of seawater Mg/Ca on the biomineralization of extant representatives of the calcifying taxa that were subjected to the alternating calcite and aragonite seas of Phanerozoic time.

The experiments reviewed here investigate the effect of seawater Mg/Ca on: (1) algae that secrete aragonite in modern seas (three calcareous bryopsidalean algae *Penicillus capitatus* (Ries, 2005a), *Udotea flabellum* (Ries, 2006a), and *Halimeda incrassata* (Stanley et al., 2010); (2) algae that secrete calcite in modern seas [the encrusting coralline red alga *Neogoniolithon* sp. (Ries, 2006b), three species of branching

coralline red algae of the genus *Amphiroa* sp. (Stanley et al., 2002), and three species of coccolithophores, *Pleurochrysis carterae*, *Ochrosphaera neopolitana*, and *Coccolithus neohelis* (Stanley et al., 2005); (3) animals that secrete aragonite in modern seas (the scleractinian corals *Porites cylindrica*, *Montipora digitata*, and *Acropora cervicornis*; Ries et al., 2006); (4) animals that secrete calcite in modern seas (the echinoid *Eucidaris tribuloides*, the crab *Perchon gibbesi*, the shrimp *Palaemonetes pugio* and the calcareous serpulid worm *Hydroides crucigera*; Ries, 2004); and (5) microbial biofilms that secrete a mixture of aragonite and high Mg calcite in modern seas (Ries et al., 2008). The experiments on the bryopsidalean algae, the coccolithophores, and the scleractinian corals address mineralogy, Mg incorporation, and rates of calcification and growth, while the experiments on the coralline algae, calcite-secreting animals, and microbial biofilms focus solely on mineralogy and Mg incorporation.

1.1   Investigated organisms

1.1.1   Calcareous bryopsidalean algae (calcareous green algae)

Calcareous bryopsidalean algae have been primary sediment producers in tropical marine environments since the late Paleogene shift to Aragonite III seas (Fig. 1). Stanley and Hardie (1998, 1999) hypothesized that the dominance of these simple aragonitic hypercalcifiers was permitted by the transition to a seawater Mg/Ca ratio greater than two in the oceans, which would have favored precipitation of their preferred skeletal mineral – aragonite.

Specimens of *Penicillus capitatus*, *Udotea flabellum*, and *Halimeda incrassata* were grown in experimental seawaters formulated at Mg/Ca ratios of 1.0, 2.5 and 5.2, which correspond to calcite seawater, a boundary seawater, and aragonite seawater, respectively (Ries, 2005a, 2006a, 2009; Stanley et al., 2010). The effects of seawater Mg/Ca on algal growth and calcification, polymorph mineralogy, Mg fractionation, and crystal ultrastructure were investigated. Additionally, thallus stiffness was determined for the *Penicillus capitatus* specimens grown under the various seawater Mg/Ca ratios by subjecting them to a hydraulic stress-strain biomechanical analysis.

1.1.2   Coccolithophores

Coccolithophores flourished during the second half of Calcite II seas and were responsible for the deposition of the massive and widespread Cretaceous chalk deposits, from which the Cretaceous Period derives its name (*Creta-* is the Latin word for "chalk"). Some of these calcareous nannoplankton secrete high Mg calcite while others secrete low Mg calcite in modern seas (Stanley et al., 2005). The success of these algae in Late Cretaceous time has been attributed to the low Mg/Ca ratio of seawater at that time favoring the

---

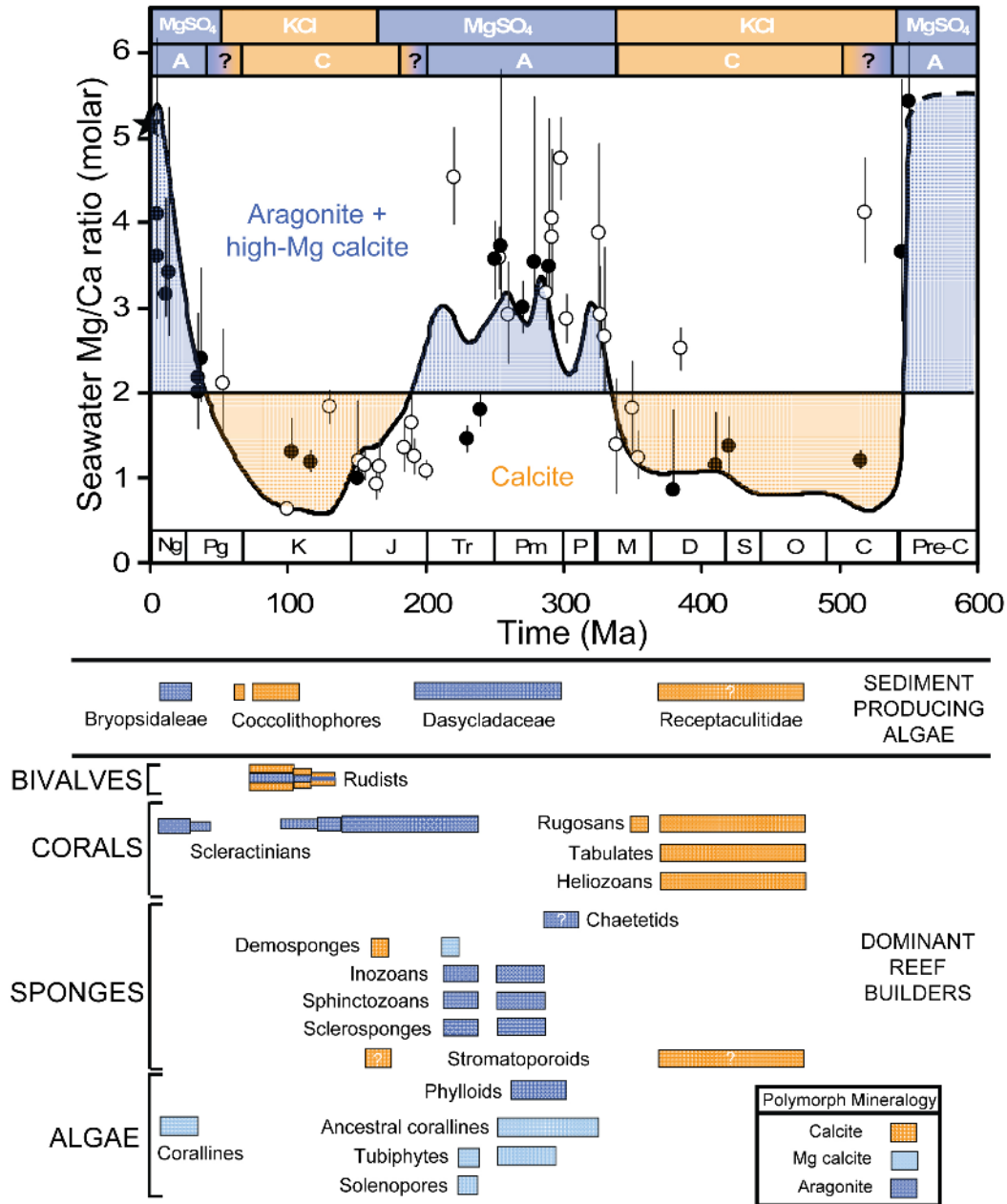[1] Here and throughout the manuscript, "Mg/Ca" represents a molar ratio.

Fig. 1. Synchronized transitions in the mineralogy of dominant reef-building and sediment-producing marine calcifiers, marine evaporites, nonskeletal carbonates, and seawater Mg/Ca ratios throughout Phanerozoic time. Curve is molar Mg/Ca ratio of seawater (Hardie, 1996; Demicco et al., 2005) estimated using a mid-ocean ridge hydrothermal flux/river water mixing model driven by global rates of ocean crust production. Closed circles correspond to seawater Mg/Ca ratios estimated from fluid inclusions in primary marine halite (Lowenstein et al., 2001, 2003, 2005; Brennan, 2002; Horita et al., 2002; Brennan and Lowenstein, 2002; Brennan et al., 2004; Timofeeff et al., 2006). Open circles are seawater Mg/Ca ranges estimated from the Mg content of fossil echinoids [recalculated from Dickson (2002) by Ries (2004) using available paleotemperature data and a nonlinear, empirically-derived Mg-fractionation algorithm]. Star represents modern seawater (Mg/Ca=5.2). Horizontal line divides the calcite (Mg/Ca<2) and aragonite + high Mg calcite (Mg/Ca>2) nucleation fields in seawater at 25 °C. Intervals of primarily aragonitic ("A") and calcitic ("C") abiotic precipitates (ooids, marine cements, seafloor precipitates; Sandberg, 1983; Lasemi and Sandberg, 2000) and KCl and MgSO₄ marine evaporites (Hardie, 1996) are plotted along top of figure. These data suggest that secular variation in seawater Mg/Ca ratios throughout Phanerozoic time supported three intervals of predominantly aragonite + high Mg calcite precipitation (seawater Mg/Ca>2) alternating with two intervals of predominantly calcite precipitation (seawater Mg/Ca<2). Adapted from Stanley and Hardie (1999).

coccolithophores' calcitic mineralogy (Stanley and Hardie, 1998, 1999).

To test this hypothesis, three species of coccolithophore (*Pleurochrysis carterae*, *Ochrosphaera neopolitana*, and *Coccolithus neohelis*) were cultured in seawater formulated with Mg/Ca ratios of 0.5, 1.0, 1.5, 2.5, 3.5 and 5.2 (Stanley et al., 2005). The effects of seawater Mg/Ca on coccolithophorid population growth, chalk production, Mg fractionation, and skeletal ultrastructure were investigated.

1.1.3 Scleractinian corals

Stanley and Hardie (1998, 1999) suggest that aragonitic scleractinian corals were major reef builders in Triassic, Jurassic, late Paleogene and Neogene time because the oceans maintained Mg/Ca ratios that were favorable for the secretion of the corals' inherently aragonitic skeleton during these intervals. The reign of the scleractinian corals was interrupted during the middle Cretaceous by the largely calcitic rudist bivalves, when Mg/Ca ratios dropped to their lowest levels of Phanerozoic time. The rudists retained their position as dominant carbonate producers through the end of Cretaceous time. Significantly, the scleractinian corals did not resume their dominance until Late Eocene time, well after the extinction of the rudists at the end of the Cretaceous Period, when the Mg/Ca ratio of seawater had transitioned back into the aragonite domain.

To test Stanley and Hardie's hypothesis (1998, 1999) that reef-building by scleractinian corals was enhanced when oceanic Mg/Ca ratios supported their aragonitic skeletal mineralogy, three species of scleractinian corals (*Porites cylindrica*, *Montipora digitata*, and *Acropora cervicornis*) were grown in experimental seawaters formulated at Mg/Ca ratios of 1.0, 1.5, 2.5, 3.5, and 5.2 (Ries et al., 2006). The effects of seawater Mg/Ca on calcification rate, polymorph mineralogy, skeletal Mg-fractionation, and skeletal ultrastructure were determined. To differentiate between the effects of Mg/Ca ratio and absolute concentration of Ca on coral growth, three additional seawaters were formulated with fixed Ca concentrations at Mg/Ca ratios of 1, 3.5 and 5.2. This also permits the comparison of coral growth rates in two sets of seawaters with fixed Mg/Ca ratios (1.0 and 5.2) and different absolute Ca^{2+} concentrations.

1.1.4 Coralline red algae

Stanley and Hardie (1998, 1999) hypothesized that organisms that secrete high Mg calcite in modern seas (Mg/Ca=5.2) would have secreted low Mg calcite in ancient seas of lower Mg/Ca ratios. Füchtbauer and Hardie (1976, 1980) showed experimentally that the amount of magnesium incorporated into non-skeletal calcite is proportional to the ambient Mg/Ca ratio as well as to the temperature of the precipitating solution. Therefore, if simple calcifiers such as coralline red algae merely induce the precipitation of calcite

through the removal of CO_2 via photosynthesis, one would expect their skeletal calcite to behave similarly to Füchtbauer and Hardie's (1976, 1980) non-skeletal calcite, with respect to the incorporation of Mg^{2+}. This expectation is also supported by earlier observations that the Mg/Ca ratio of calcite secreted by these algae varies as a function of other physicochemical parameters of seawater, including temperature (Chave, 1954; Agegian, 1985; Mackenzie and Agegian, 1989) and carbonate ion concentration (Moberly, 1968; Agegian, 1985; Mackenzie and Agegian, 1989).

To test this prediction, species of both encrusting and branching coralline red algae were grown over the range of seawater Mg/Ca ratios believed to have occurred throughout their geologic history (Stanley et al., 2002; Ries, 2006b). Magnesium fractionation curves for the various algae were developed from these experiments.

1.1.5 High Mg calcite-secreting animals

To investigate Stanley and Hardie's (1998, 1999) Mg fractionation hypothesis for more complex organisms, four animals that secrete high Mg calcite in modern seas (the echinoid *Eucidaris tribuloides*, the crab *Perchon gibbesi*, the shrimp *Palaemonetes pugio* and the calcareous serpulid worm *Hydroides crucigera*) were grown in experimental seawaters formulated at Mg/Ca ratios believed to have existed throughout the animals' geologic histories (Ries, 2004). Mg fractionation curves were derived for the organisms and the Mg content of fossil echinoderms was used to reconstruct oceanic Mg/Ca throughout the Phanerozoic Eon.

Chave (1954) showed that the effect of temperature on skeletal Mg is greatest for taxonomically simple organisms. The experiments reviewed here (Ries, 2004) evaluate whether the effect of seawater Mg/Ca on skeletal Mg incorporation is comparably correlated with taxonomic complexity.

1.1.6 Bacterial biofilms

Biofilms are highly diverse bacterial communities that can precipitate $CaCO_3$ extracellularly within their mm-to-cm thick matrices through various redox reactions that alter the $CaCO_3$ saturation state of the biofilm's intercellular fluid. Bacterial biofilms are the oldest biocalcifying systems on Earth, having been intimately involved in $CaCO_3$ mineralization on the seafloor for at least the past ca. 3.45 Gy (Knoll and Semikhatov, 1998; Grotzinger and Knoll, 1999; Grotzinger and James, 2000; Riding, 2000). The absence of grazing and bioturbation throughout most of Precambrian time enabled these biofilms to form laminated stromatolites, microbialites, and thrombolites throughout this interval (Awramik, 1971; Riding and Liang, 2005). Hardie's (2003) model of Precambrian seawater Mg/Ca – ultimately driven by the global rate of ocean crust production inferred from granitic pluton data – suggests that bacterial biofilms would have experienced

six intervals of aragonite seas and five intervals of calcite seas between late Archean and terminal Proterozoic time. If the polymorph mineralogy of the CaCO$_3$ precipitated within biofilms is strongly influenced by seawater Mg/Ca, then the original mineralogy of ancient microbial carbonates (i.e., stromatolites, microbialites, thrombolites) may prove to be a viable proxy for Precambrian seawater chemistry.

To evaluate the effect of Mg/Ca$_{sw}$ on microbial calcification (Ries et al., 2008), mixed-community marine sedimentary biofilms were cultured in experimental seawaters formulated over the range of Mg/Ca ratios predicted to have occurred since late Archean time (1.5, 2.5, 5.2; Hardie, 2003). Biofilm phylogenetic diversity, CaCO$_3$ polymorph mineralogy and distribution, and Mg fractionation in biofilm calcite were evaluated in response to these modifications in seawater Mg/Ca.

2 Background

2.1 Patterns of skeletal polymorph mineralogy throughout Phanerozoic time

Stanley and Hardie (1998, 1999) observed that the polymorph mineralogy of the primary reef-forming and sediment-producing marine calcifiers has varied in concert with Sandberg's (1983) aragonite and calcite seas throughout Phanerozoic time. This led them to assert that certain taxa have been able to function as major reef builders and sediment producers only when their mineralogy was favored by the Mg/Ca ratio of seawater (Fig. 1). The general patterns that they identified are briefly reviewed in the following section.

In Calcite I (early-middle Paleozoic), calcitic tabulate, heliolitid and rugose corals, and stromatoporoids (possibly calcitic) were the dominant reef builders, while receptaculitids (possibly calcitic) were the dominant sediment producers. As the Mg/Ca ratio increased in the middle Mississippian to cause the onset of Aragonite II (late Paleozoic-early Mesozoic), aragonitic groups of sponges, scleractinian corals and phylloid algae, and high Mg calcitic red algae, became major reef builders, while aragonitic dasycladaceans were important algal sediment producers. The Mg/Ca ratio then dropped again in the mid-Jurassic, shifting oceanic state to Calcite II (Middle Jurassic-late Paleogene). During the peak of Calcite II (highest Ca^{2+} concentrations) in Early- to mid-Cretaceous time, the bi-mineralic rudist bivalves (aragonite and calcite) replaced the aragonitic scleractinian corals as major carbonate producers, while calcitic nannoplankton (coccolithophores) became important chalk producers. Furthermore, as the absolute concentration of Ca^{2+} fell throughout Cenozoic time, individual coccoliths became less robustly calcified (Stanley and Hardie, 1998, 1999). The most recent increase in seawater Mg/Ca, which commenced in late Paleogene time, has advanced the oceans into Aragonite III,

where aragonitic scleractinian corals and high Mg calcitic red algae once again dominated reef construction and aragonitic green algae, such as *Halimeda*, *Penicillus*, and *Udotea*, control sediment production.

Stanley and Hardie (1998, 1999) investigated mineralogical trends in organisms that were hypercalcifiers and/or exhibited weak control over their calcification. Hypercalcifying organisms, defined either as individuals that produce massive calcium carbonate skeletons or as populations that produce excessive calcium carbonate material (e.g., reefs or sediment producers), probably require favorable seawater chemistry (i.e., Mg/Ca ratios that support their inherent mineralogy) to engage in such rapid calcification. Since hypercalcification is typically a warm-water phenomenon, most of the organisms analyzed in their study are warm-adapted taxa. Organisms that exhibit only minor control over their calcification, typically taxonomically simple organisms, are also likely to require favorable seawater chemistry to calcify. For example, Chave (1954) showed that the degree of correlation between skeletal Mg/Ca and temperature is inversely related to biological complexity. Therefore, one would expect the relationship between calcification rate and seawater Mg/Ca to be comparably linked to biological complexity.

Sandberg (1975) originally suggested that the Phanerozoic Eon exhibited only a single transition (now known to be incorrect) from "calcite seas" to "aragonite seas," which occurred during the Cenozoic Era. Milliken and Pigott (1977) pointed to a similar shift during the Carboniferous. Wilkinson (1979), using the relative diversities and biomasses of various taxa, suggested a corresponding one-time shift in the dominant mineralogy of calcareous marine organisms. However, Wilkinson's erroneous mineralogical assessments of several groups of organisms and lack of distinction between high Mg and low Mg calcite rendered his conclusions invalid.

Riding and Liang (2005) later observed that fluctuations in the calcium carbonate saturation state of seawater have generally been synchronized with fluctuations in the rate of shallow water limestone accumulation throughout the Phanerozoic Eon. From this they infer that fluctuations in seawater [CO$_3^{2-}$] (via atmospheric pCO$_2$) and in the mid-ocean ridge flux of [Ca^{2+}] have exerted strong control on the precipitation of marine carbonates throughout Phanerozoic time. They also conclude that calcium carbonate saturation states and rates of marine limestone formation were generally higher during calcite sea intervals of the geologic past, which contrasts with Tyrrell and Zeebe's (2005) conclusion that the calcium carbonate state of seawater during the calcite sea interval of Cretaceous time was lower than it is in the modern aragonite sea, as evidenced by a shallower carbonate compensation depth in Cretaceous time. Riding and Liang (2005), however, did not attribute secular shifts in the primary mineralogy of marine carbonates to CO$_2$-induced fluctuations in the calcium carbonate saturation state of seawater

– they simply attributed changes in the abundance of all marine carbonates (independent of polymorph) to such changes in seawater chemistry.

In a recent study, Kiessling et al. (2008) identified a statistically significant relationship between oceanic state (aragonite vs. calcite seas) and the polymorph mineralogy of reef-building organisms throughout Phanerozoic time. Critically, this relationship disappeared when their analysis was expanded to include all calcifying organisms – regardless of their inferred degree of biomineralogical control. However, an earlier study by Porter (2007) showed that the mineralogy of nearly all newly evolved CaCO$_3$ skeletons between Ediacaran and Ordovician time – for both hypercalcifying and non-hypercalcifying taxa – reflects the aragonite-calcite sea transition (Sandberg, 1983; Hardie, 1996) reported for that time. Thus, although most calcifying taxa appear to have been influenced by seawater Mg/Ca at the time that they evolved their calcareous skeleton (Porter, 2007), only the major reef-building and sediment-producing organisms appear to have been affected by subsequent changes in oceanic state (Kiessling et al., 2008).

Van de Poel and Schlager (1994) had previously recognized a weak correspondence between skeletal and non-skeletal carbonates over the Mesozoic-Cenozoic interval. However, they were unable to demonstrate that the shifts they observed were first-order changes in primary skeletal mineralogy, rather than second order oscillations imprinted upon Sandberg's (1975) one-time unidirectional shift from calcite-to-aragonite seas. The work by Kiessling et al. (2008) suggests that the reason Van de Poel and Schlager's (1994) skeletal data revealed only a weak correspondence with the non-skeletal data is because Van de Poel and Schlager's (1994) analysis included the skeletal remains of all calcifying taxa, including organisms whose biomineralization would not be expected to be strongly influenced by seawater chemistry, such as foraminifera and mollusks.

Zhuravlev and Wood (2009) have subsequently reiterated Sandberg's (1975) and Wilkinson's (1979) observation of a single low Mg calcite-to-aragonite shift in the primary mineralogy of marine carbonates throughout Phanerozoic time, adding that extinction events and secular variation in seawater Mg/Ca appear only to have imposed second- and third-order trends upon this unidirectional shift. They base this assertion on their observation that the proportional abundance of aragonitic calcifiers has been steadily increasing throughout Phanerozoic time.

However, the fact that the first half of the Phanerozoic Eon is dominated by a protracted calcite sea interval while the second half is dominated by two aragonite sea intervals (interspersed with a single calcite sea interval) would inevitably generate an apparent first-order increase in the proportional abundance of aragonitic calcifiers throughout Phanerozoic time, even if the actual trend in carbonate mineralogy is defined by alternating calcite-aragonite intervals.

This apparent unidirectional trend would have been exacerbated by Zhuravlev and Wood's (2009) exclusion of organisms from their analysis that are thought to have secreted high Mg calcite shells. Experiments (e.g., Ries, 2004) have shown that most, if not all, organisms that secrete high Mg calcite in high Mg/Ca waters (i.e., aragonite seas) begin secreting low Mg calcite in low Mg/Ca waters (i.e., calcite seas). Thus, by excluding high Mg calcite-secreting organisms from their analysis of aragonite sea intervals, yet including them in their analysis of calcite sea intervals (as they likely secreted low Mg calcite during those intervals), a bias may have inadvertently been introduced into their analysis that would have caused the proportional abundance of aragonitic calcifiers to be overestimated during aragonite sea intervals, thereby exacerbating the apparent unidirectional shift in primary mineralogy from calcite-to-aragonite throughout Phanerozoic time.

Furthermore, Zhuravlev and Wood's analysis [like Van de Poel and Schlager's (1994)] was based upon the inferred primary mineralogies of all marine calcifiers, rather than the dominant reef-builders and sediment-producers upon which Stanley and Hardie's (1998, 1999) calcite-aragonite sea hypothesis is based. Indeed, Stanley and Hardie (1999) state that there is no reason to suspect that the primary mineralogy of sophisticated biomineralizers would be influenced by secular variations in seawater Mg/Ca. And this assertion is supported by the findings of Kiessling et al. (2008), which only revealed a correlation between seawater Mg/Ca and skeletal polymorph mineralogy for the major reef-building organisms.

2.2 Cause of calcite-aragonite seas: atmospheric pCO$_2$ vs. seawater Mg/Ca

2.2.1 Atmospheric pCO$_2$

Sandberg (1975) suggested that his observed single shift from calcite to aragonite seas was caused by an increase in the Mg/Ca ratio of seawater throughout Mesozoic time, resulting from the selective removal of calcium ions from the ocean via flourishing calcareous nannoplankton and planktonic foraminifera. As more ancient oolite and early marine cement data became available, Sandberg abandoned the single-shift hypothesis in favor of the currently accepted four-fold shift in carbonate mineralogy, consisting of 3 aragonite intervals (late Precambrian to early Cambrian; late Mississippian to Late Triassic/Early Jurassic; early/middle Cenozoic to the present) and two calcite intervals (Cambrian to late Mississippian; Late Triassic/Early Jurassic to early/middle Cenozoic; Sandberg, 1983; Lasemi and Sandberg, 2000).

It should be noted here that Sandberg's (1983) identification of an oscillating trend in the polymorph mineralogy of ooids and marine cements has not gone unchallenged. For example, Bates and Brand (1990) reassessed the petrography

and elemental geochemistry of ooids and marine cements throughout Phanerozoic time and concluded that their primary mineralogies did not correlate with Sandberg's (1983) putative calcite and aragonite sea intervals. Instead, they attributed differences in the primary mineralogy of these abiogenic carbonate precipitates to local hydraulic, physicochemical, and environmental conditions that were only loosely influenced by tectonic, eustatic, climatic, and atmospheric effects.

Sandberg's oscillating trend in carbonate mineralogy caused him to abandon his initial hypothesis that Mg/Ca ratios were driven by planktonic removal of calcium ions in favor of Mackenzie and Pigott's (1981) hypothesis that the observed mineralogical shifts were driven by tectonically induced shifts in atmospheric pCO_2. Wilkinson and Given (1986) also argued that fluctuations in sea level, atmospheric pCO_2, and concomitant fluctuations in the saturation state of seawater with respect to calcium carbonate, were largely responsible for the observed secular shifts in the primary mineralogy of ooids and marine cements throughout Phanerozoic time.

However, atmospheric pCO_2 would only be expected to cause a shift to calcite seas if pCO_2 caused seawater to be simultaneously oversaturated with respect to calcite and undersaturated with respect to aragonite. Because the stoichiometric solubility coefficients (K_{sp}) of aragonite ($10^{-6.19}$) and calcite ($10^{-6.37}$) are relatively close, the range of $CaCO_3$ saturation states that yields simultaneous calcite oversaturation and aragonite undersaturation is correspondingly narrow ($1 < \Omega_{calcite} < 1.5$; $0.7 < \Omega_{aragonite} < 1$), and requires that seawater be near undersaturation with respect to calcite over protracted intervals of geologic time. Given the ubiquity and abundance of both biogenic and abiogenic limestone deposits throughout the calcite seas of early Cambrian – late Mississippian time and Late Jurassic – Middle Paleocene time, it seems improbable that the $CaCO_3$ saturation state of seawater during these intervals was regularly constrained to such a narrow range ($1 < \Omega_{calcite} < 1.5$), teetering on the edge of total undersaturation with respect to $CaCO_3$.

Furthermore, the effect of atmospheric pCO_2 on carbonate oceanic state will vary strongly with both latitude and depth. This is because temperature and pressure influences the solubility of CO_2 in seawater and, thus, the effect of atmospheric pCO_2 on calcite vs. aragonite stability. Modern upwelling waters are also known to have much higher levels of dissolved inorganic carbon and reduced pH than surface waters (Feely et al., 2007), which would further moderate the effects of atmospheric pCO_2 on carbonate oceanic state. These extreme variations in $CaCO_3$ saturation state throughout the oceans would likely preclude atmospheric pCO_2 from causing the oceans to systematically favor one polymorph of $CaCO_3$ over another, at least across spatial scales that would allow such patterns to be confidently inferred from the geologic record.

Hardie (1996) also observed that the timing of Sandberg's transitions between aragonite and calcite seas are in phase with transitions between $MgSO_4$ and KCl marine evaporites, respectively, throughout the Phanerozoic record. Hardie concluded that the synchronicity of these mineralogical shifts must have been caused by shifts in seawater chemistry that would have simultaneously influenced the mineralogy of both carbonate precipitates and marine evaporites. Atmospheric pCO_2 is not capable of causing these synchronized transitions in carbonate and evaporite mineralogy because it bears no influence on the mineralogy of marine evaporites.

More recently, Zhuravlev and Wood (2009) have revisited the hypothesis that atmospheric pCO_2 has played a major role in determining secular variations in the primary mineralogy of marine calcifiers. In this work, they invoke Sandberg's (1983) and Wilkinson's (1979) abandoned hypotheses that marine carbonates have exhibited a unidirectional shift from low Mg calcite to aragonite mineralogies throughout Phanerozoic time, and assert that this trend roughly parallels the general decline in atmospheric pCO_2 levels thought to have occurred throughout this time.

However, in addition to the problems noted in the previous section, Zhuravlev and Wood's (2009) assertions are not supported by recent experimental work (Ries et al., 2009) that revealed that skeletal mineral solubility (high Mg calcite and aragonite > low Mg calcite) does not play a major role in determining the relative abilities of marine calcifiers to build their shells and skeletons under conditions of elevated pCO_2. In fact, Ries et al.'s (2009) experiments showed that six species of the more soluble high Mg calcite-secreting (crabs, lobsters, shrimp, coralline red algae, and an urchin) and aragonite-secreting (calcareous green algae) marine organisms actually calcified more rapidly under conditions of elevated pCO_2. The experiments also showed that some of the less soluble low Mg calcite-secreting organisms, including oysters, bay scallops, and periwinkles, fared worst under the experimental high-CO_2 conditions. Ries et al. (2009) concluded that physiological attributes such as the ability to regulate pH at the site of calcification (thereby converting to HCO_3^- to CO_3^{2-}), the characteristics of the organic layer that organisms use to protect their shells or skeletons from ambient seawater, and whether organisms utilize photosynthesis, play more important roles than skeletal polymorph mineralogy does in determining the response of marine calcifiers to CO_2-induced ocean acidification.

Furthermore, as Zhuravlev and Wood (2009) point out, the total alkalinity of seawater would have also increased with rising atmospheric pCO_2 over geologic timescales, due to shoaling of the calcium carbonate compensation depth (CCD; Tyrrell and Zeebe, 2004). Thus, the effects of protracted, tectonically driven fluctuations in atmospheric pCO_2 would have been partially mitigated (over geologic timescales) in terms of their effects on the calcium carbonate saturation state of seawater (and, thus, primary carbonate mineralogy) by concomitant fluctuations in the total

alkalinity of seawater. This negative feedback loop is not expected to accompany future, anthropogenic CO_2-induced ocean acidification because the CO_2-induced reduction in the carbonate ion concentration of surface seawater occurs on the order of 100-year timescales, while the mitigating effects of increased total alkalinity (due to shoaling of the CCD) occurs over 1000-year timescales, consistent with the 1000-year mixing time of the oceans.

For these reasons, it is unlikely that atmospheric pCO_2 is the primary link explaining the synchronicity between carbonate mineralogy and rates of ocean crust production (inferred from first order changes in eustatic sea level) throughout Phanerozoic time. Nonetheless, fluctuations in atmospheric pCO_2 (as well as seawater temperature) have surely modulated the effect of seawater Mg/Ca on oceanic state (calcite vs. aragonite seas) throughout Phanerozoic time. The effect of pCO_2 would have been particularly pronounced during intervals in which seawater Mg/Ca remained near the boundary between calcite and aragonite seas (Mg/Ca=2; Morse et al., 1997). For example, Zhuravlev and Wood (2008) attribute a short-lived aragonite sea interval that occurred shortly after the onset of Calcite I seas in middle Cambrian time (late Atbadanian–Botoman) to seawater Mg/Ca remaining near the boundary value of two over that interval. They assert that these conditions would have supported high-frequency oscillations between calcite and aragonite sea intervals, since even minor changes in seawater Mg/Ca, atmospheric pCO_2, and/or temperature could have caused a shift in oceanic state (Morse et al., 1997; De Choudens-Sanchez and Gonzalez, 2009).

2.2.2 Seawater Mg/Ca

Experimental work by Leitmeier (1910, 1915), Lippman (1960), Müller et al. (1972) and Folk (1974) has shown that the precipitation of aragonite and high Mg calcite, rather than low Mg calcite, is caused by elevated concentrations on Mg^{2+}. Füchtbauer and Hardie (1976, 1980) showed that in laboratory experiments on the system $MgCl_2$-$CaCl_2$-Na_2CO_3-H_2O, the precipitation of calcite versus high Mg calcite and aragonite is determined by the solution's Mg/Ca ratio, ionic strength and temperature. Their experiments yielded a Mg/Ca mole ratio of 2 ($\pm$0.5) as the boundary between the low Mg calcite (Mg/Ca<0.04) and the aragonite + high Mg calcite (Mg/Ca>0.04) nucleation fields for chloride solutions under laboratory conditions approximating modern values of ionic strength (I=0.7), temperature (28 °C), pressure (1 atm total pressure) and atmospheric pCO_2 (~380 ppm). These results are in excellent agreement with Müller et al.'s (1972) carbonate nucleation fields (Mg/Ca vs. salinity) that were determined from observations of natural lakes. In two recent studies, De Choudens-Sanchez and Gonzalez (2009) and Lee and Morse (2010) showed that both solution Mg/Ca and the saturation state of the solution with respect to calcium carbonate influence the polymorph

mineralogy of the calcium carbonate minerals that precipitate from the solution. However, Morse et al. (1997) argued that for temperatures between 6° and 35 °C, the carbonate polymorph precipitated (calcite vs. aragonite + high Mg calcite) will be primarily determined by the Mg/Ca ratio of the solution, rather than by atmospheric pCO_2 and the calcium carbonate saturation state of the solution.

Experiments have also shown that the percentage of Mg incorporated into non-skeletal calcite precipitates increases in proportion to both the Mg/Ca ratio and temperature of the solution (Chave, 1954; Kitano and Kanamori, 1966; Glover and Sippel, 1967; Katz, 1973; Füchtbauer and Hardie, 1976, 1980; Devery and Ehlmann, 1981; Mucci and Morse, 1983; Mucci, 1987; Burton and Walter, 1991; Rushdi, 1992; Rimstidt et al., 1998). Other factors such as salinity (ionic strength; Muller et al., 1972; Folk, 1974; Füchtbauer and Hardie, 1976, 1980; Borremans et al., 2009) has also been shown to influence Mg incorporation in calcite. However, experiments conducted by Mucci and Morse (1983), Burton and Walter (1991), Hartley and Mucci (1996), De Choudens-Sanchez and Gonzalez (2009), and Lee and Morse (2010) revealed that atmospheric pCO_2 and solution saturation state had no statistically significant effect on the Mg-content of calcite that precipitated from experimental seawater solutions. Although variations in temperature, and salinity across latitude and depth are thought to cause regional differences in the Mg-content of marine calcite (Morse and Bender, 1990), global secular variation in these seawater parameters (T=20–30 °C; salinity = 30–40) would not have been sufficient to explain the observed global secular trends in the Mg-content of biogenic marine calcite (e.g., Dickson, 2002, 2004; Webb and Sorauf, 2002; Steuber and Rauch, 2005; Hasiuk and Lohmann, 2008) throughout Phanerozoic time.

Mg-incorporation in the calcite crystal lattice has long been known to slow the growth rate of calcite crystals (De Groot and Duyvis, 1966; Folk, 1974; Lahann, 1978). Davis et al. (2000) demonstrated that Mg-incorporation alters the step-geometry of the calcite crystal in ways that increase its solubility, thereby reducing its net rate of growth. They argue that because the Mg-content, geometry, and growth rate of aragonite crystals are less influenced by solution Mg/Ca, aragonite will be kinetically favored when solution Mg/Ca ratios are high. This observation provides mechanistic support for the experimental and geological evidence that a seawater Mg/Ca ratio of 2 divides the calcite (Mg/Ca<2) and aragonite (Mg/Ca>2) nucleation fields. Davis et al. (2004) later observed that Mg is preferentially incorporated into calcite crystal growth steps that propagate in specific crystallographic directions, which causes Mg-incorporation to also alter the morphology and habit of calcite crystals.

Spencer and Hardie (1990) showed that the primary factors that control seawater chemistry are river water (input), mid-ocean ridge hydrothermal brine (input), $CaCO_3$ precipitation (output), and SiO_2 precipitation (output). Using mid-ocean ridge/river water flux ratios to calculate ancient

seawater chemistry, Spencer and Hardie showed that small changes in the mid-ocean ridge flux can cause changes in the Mg/Ca, Na/K and Cl/SO$_4$ ratios of seawater that would result in the observed synchronized shifts in limestone and marine evaporite mineralogy (Fig. 1).

Hardie (1996) later proposed that such minor changes in mid-ocean ridge flux could be caused by changes in the rate of ocean crust production. Mid-ocean ridge basalt is converted to greenstone as it comes in contact with brine, thereby releasing Ca^{2+} and K^+ to the seawater and removing Mg^{2+} and SO_4^{2-} from it. Therefore, mid-ocean ridges act as massive ion exchange systems where high rates of ocean crust production result in relatively high concentrations of Ca^{2+} and low concentrations of Mg^{2+} in seawater (low Mg/Ca ratios). Using historical rates of ocean crust production (inferred from first order eustatic sea level changes), Hardie (1996) employed his ocean chemistry model to calculate ancient Mg/Ca ratios throughout Phanerozoic time. The combination of these historical Mg/Ca values with Füchtbauer and Hardie's (1976, 1980) experimentally determined carbonate polymorph nucleation fields predicts a pattern of aragonite and calcite seas over the Phanerozoic Eon that closely resembles Sandberg's (1983) pattern observed in the geologic record of ooids and marine cements.

Hardie's (1996) Phanerozoic Mg/Ca curve can also be combined with empirically derived brine evaporite models to predict a temporal pattern of late stage marine evaporites throughout the Phanerozoic Eon (Fig. 1). Elevated rates of ocean crust production, which cause gypsum stage CaCl$_2$ brines, would result in the dominance of KCl late stage evaporites. Depressed rates of ocean crust production, which cause gypsum stage MgSO$_4$ brines, would result in the dominance of MgSO$_4$ late stage evaporites. Hardie's model predicts a pattern of late stage marine evaporites that agrees very well with the pattern observed in the Phanerozoic record.

The ability of Hardie's (1996) model to predict synchronized variations in the mineralogies of late stage marine evaporites (Hardie, 1996), of abiogenic carbonates (Sandberg, 1983; Lasemi and Sandberg, 2000; Yan et al., 2005), and of reef- and sediment-forming marine calcifiers (Stanley and Hardie, 1998, 1999; Steuber, 2002; Porter, 2007; Kiessling et al., 2008) suggests that the principal tenants of the model are correct. Hardie's model is further supported by ancient seawater Mg/Ca ratios estimated from fluid inclusions in primary marine halite (Lowenstein et al., 2001, 2003, 2005; Brennan and Lowenstein, 2002; Brennan, 2002; Horita et al., 2002; Brennan et al., 2004; Timofeeff et al., 2006); secular variation in the Mg/Ca ratio of fossil molluscs (Steuber and Rauch, 2005), rugose corals (Webb and Sorauf, 2002), echinoderms (Dickson, 2002, 2004; Hasiuk and Lohmann, 2008), and abiogenic carbonates (Hasiuk and Lohmann, 2008); secular variation in the ratio of aragonite-to-calcite within bi-mineralic calcareous serpulid worm tubes (Railsback, 1993); secular variation in the Sr/Mg ratio of abiogenic marine carbonates throughout Phanerozoic time

(this evidence is more robust in early Phanerozoic time than in latter Phanerozoic time; Cicero and Lohmann, 2001); the occurrence of higher seawater Sr/Ca ratios during predicted calcite sea intervals than during predicted aragonite sea intervals, as recorded in low Mg calcite shells throughout Phanerozoic time (Sr would be depleted in seawater during aragonite sea intervals because Sr is more readily incorporated in aragonite than in calcite; Steuber and Veizer, 2002); and secular variation in concentrations of Br in marine halite (Siemann, 2003).

2.2.3 Other factors that influence the polymorph mineralogy of marine carbonates

Salinity (or ionic strength) is also known to influence the polymorph mineralogy of calcium carbonate precipitated from seawater solutions (Folk, 1974; Müller et al., 1972; Morse et al., 1997). However, it is unclear whether the oceans have undergone major secular variations in salinity throughout Phanerozoic time. However, variations in salinity with depth or across the surface of the ocean at any given time probably far exceed any temporal variations in average seawater salinity that have occurred.

Experiments have shown that sulphate ions inhibit the precipitation of both calcite and, to a lesser extent, aragonite in seawater-based solutions (Bischoff and Fyfe, 1968; Walter, 1986). However, the effect of seawater Mg/Ca on CaCO$_3$ polymorph nucleation (Leitmeier, 1910, 1915; Lippman, 1960; Müller et al., 1972; Berner, 1975; Morse et al., 1997; Stanley and Hardie, 1999; De Choudens-Sanchez and Gonzalez, 1999) is much stronger than that of [SO_4^{2-}] (Bischoff and Fyfe, 1968; Walter, 1986), at least across the range of seawater Mg/Ca ratios (1<Mg/Ca<5.2; Hardie, 1996; Lowenstein et al., 2003) and [SO_4^{2-}] (5<20–25 mmol kg-SW^{-1}; Canfield et al., 2000; Lowenstein et al., 2003) that are thought to have occurred throughout Phanerozoic time.

Temperature is also known to exert an influence on the polymorph mineralogy of marine carbonates (Morse et al., 1997; Burton and Walter, 1991). Experiments on solutions formulated to mimic modern seawater (salinity = 35, 1 atm pressure, modern open seawater total alkalinity, Mg/Ca=5.2) revealed that the kinetically favored CaCO$_3$ polymorph will switch from aragonite to calcite when temperature falls below 6±3 °C (Morse et al., 1997). Seawater temperature, like salinity, should exert a strong effect on CaCO$_3$ polymorph mineralogy with depth and latitude. Indeed, first-order calcite-aragonite sea patterns are generally only evident in the mineralogy of ooids, marine cements (Sandberg, 1983; Hardie, 1996), and reef- and sediment-producing marine calcifiers (Stanley and Hardie, 1998, 1999) within shallow, tropical carbonate-platform marine environments. This underscores the importance of restricting investigations of temporal patterns in the primary mineralogy of marine carbonates to facies, depths, and environments for which paleo-seawater temperature is reasonably well-constrained.
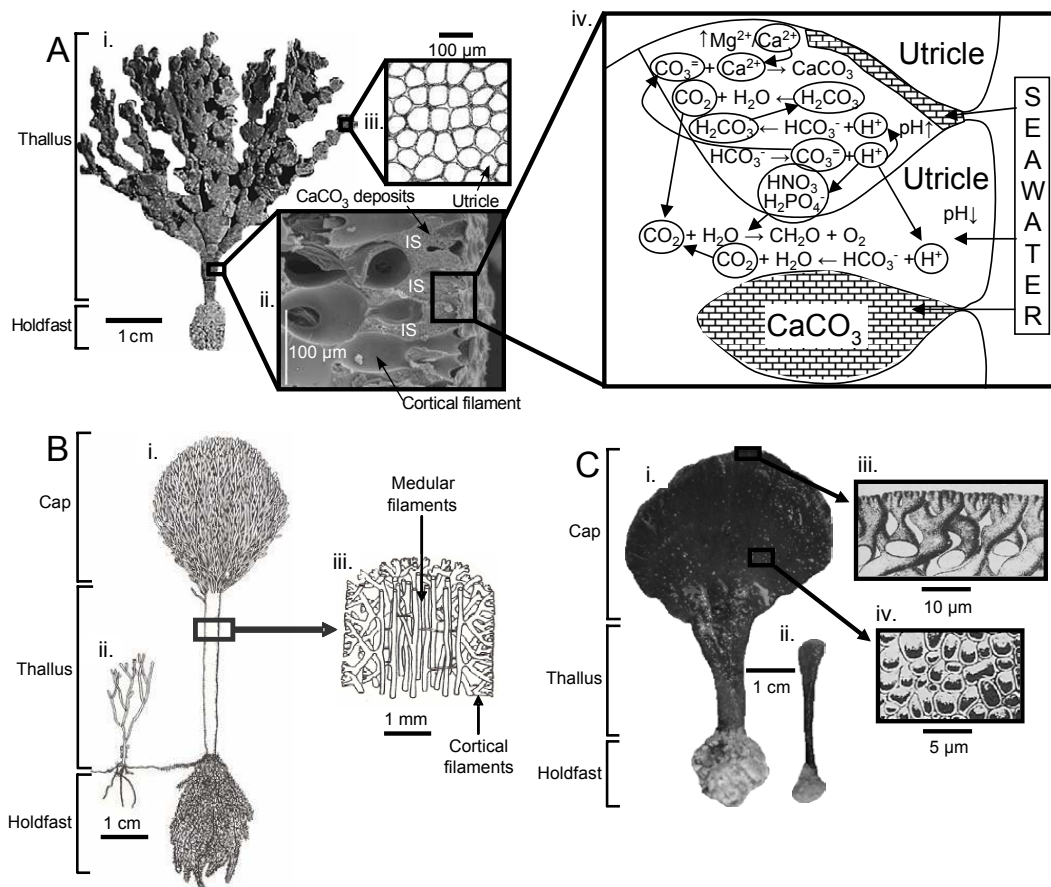
Fig. 2. Anatomy of the predominant CaCO$_3$-producing bryopsidalean algae in modern carbonate platform environments. **(A)** *Halimeda incrassata* showing (i) the thallus, the calcified segments, and the uncalcified holdfast; (ii) an SEM image of a vertical section through the cortical layer of the thallus, showing extracellular calcification in the interutricular space ("IS"), external to the outer algal wall; (iii) corticated surface of a calcified segment resulting from coalescence of utricles; (iv) diagram showing the chemical connectivity between the primary mass-forming reactions (calcification, photosynthesis), the primary carbonate system equilibria, nutrient shuttling, localized Mg/Ca ratios, and pH within and between the coalescing utricles that form the calcified cortex of the *Halimeda*, *Penicillus*, and *Udotea* algae. **(B)** *Penicillus capitatus* showing (i) a full grown plant revealing uncalcified holdfast, calcified thallus and calcified cap; (ii) an offspring alga sprouting from rhizoids; and (iii) magnified diagram of thallus revealing the constituent calcified medullar and cortical filaments. **(C)** *Udotea flabellum* showing (i) full-grown alga revealing uncalcified holdfast, calcified thallus, and calcified fan; (ii) an offspring alga; (iii) vertical section through the cortical layer of the fan, showing coalescence of the utricles; and (iv) corticated surface of the fan (from Ries, 2005a, b, 2006a, 2009; after Fritsch, 1948, and Böhm et al., 1978).

Secular fluctuations in seawater temperature may have also influenced the diversity and/or abundance of marine calcifiers for reasons that are unrelated to crystal growth kinetics. For example, Aguirre and Riding (2005) provided compelling evidence that the biodiversity of dasycladacean algae has generally tracked average global temperatures from Carboniferous through Pliocene time (excluding Late Cretaceous time). They attributed the relative success of the dasycladacean algae during greenhouse intervals to the elevation of seawater temperatures and to the expansion of euphotic epeiric seas, both of which should have supported enhanced primary production by these algae.

3 Calcareous bryopsidalean algae

Secular variation in seawater Mg/Ca would have subjected the sediment- and limestone-forming bryopsidalean algae (the "calcareous green algae" or the "codiacean algae") to at least 3 transitions between intervals favoring the precipitation of low Mg calcite and intervals favoring the precipitation of aragonite (their preferred mineralogy) and high Mg calcite since Permian time, which is the age of the oldest fossils assigned to the bryopsidalean order (Hillis, 2000). However, despite the order's Permian origin, the *Halimeda*, *Penicillus*, and *Udotea* genera of bryopsidalean algae (Fig. 2) did not assume their modern role as major contributors of aragonite sediments to carbonate platform environments until the
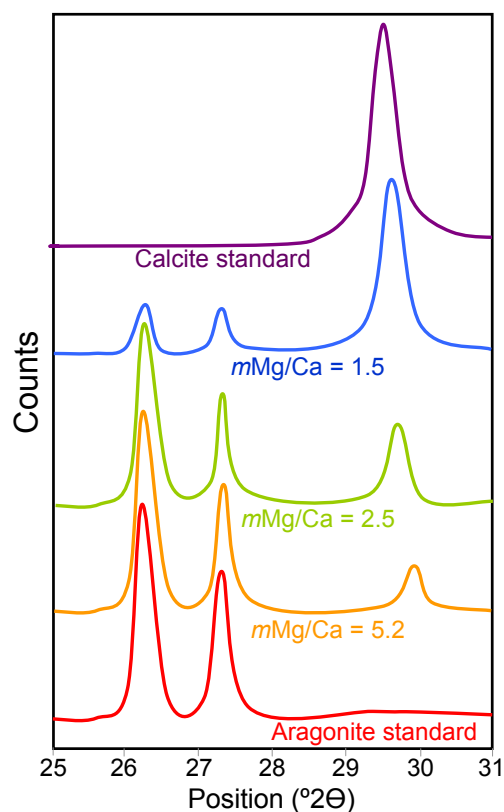
Fig. 3. Purple curve: X-ray diffraction pattern for pure calcite, revealing primary calcite peak [d(104); 3.03–3.04 Å; 2θ=29.4–29.5°]. Blue curve: X-ray diffraction pattern for a *H. incrassata* alga that produced 54% aragonite and 46% calcite when reared in the experimental calcite seawater (Mg/Ca=1.5; $[Ca^{2+}]$=25.3 mmol kg-SW^{-1}). Green curve: X-ray diffraction pattern for a *H. incrassata* alga that produced 84% aragonite and 16% calcite when reared in the boundary aragonite-calcite experimental seawater (Mg/Ca=2.5; $[Ca^{2+}]$=18.1 mmol kg-SW^{-1}). Orange curve: X-ray diffraction pattern for a *Halimeda incrassata* alga that produced 92% aragonite and 8% calcite when reared in experimental seawater that favors the nucleation of the aragonite polymorph (Mg/Ca=5.2; $[Ca^{2+}]$=10.2 mmol kg-SW^{-1}). Red curve: X-ray diffraction pattern for pure aragonite, revealing primary aragonite peak [d(111)] at 2θ=26.2° (3.40 Å) (data from Ries, 2005a, b, 2006a; Stanley et al., 2010).

Eocene, around the time that the oceans transitioned into the most recent aragonite sea interval (Mg/Ca>2). Multiple studies have been published over the past several years investigating the effects of seawater Mg/Ca and absolute $[Ca^{2+}]$ on the polymorph mineralogy, primary production, and calcification of calcareous bryopsidalean algae (Ries, 2005a, 2006a, 2009; Stanley et al., 2010).

Specimens of *Halimeda incrassata* (Stanley et al., 2010), *Penicillus capitatus* (Ries, 2005a), and *Udotea flabellum* (Ries, 2006a) were grown for up to 90 days in 38-l glass aquaria filled with 30 l of experimental seawater (Bidwell and Spotte, 1985) formulated with Mg/Ca ratios of 1.0–1.5,

2.5, and 5.2, corresponding to "calcite sea", "boundary calcite-aragonite sea", and "aragonite sea" conditions, respectively. In the experiments on *Halimeda*, an additional set of tanks was set up to investigate the effects of absolute $[Ca^{2+}]$. These aquaria were formulated with identical Mg/Ca ratios and differed only in absolute $[Ca^{2+}]$, which was fixed at 25.3, 18.1, and 10.2 mmol kg-SW^{-1}, as well as $[Mg^{2+}]$, which was adjusted to maintain the prescribed Mg/Ca ratio, and $[Na^{2+}]$, which was adjusted to offset the prescribed variations in $[Mg^{2+}]$ and $[Ca^{2+}]$, such that salinity was maintained at the modern value of 35.

3.1 Effect of seawater Mg/Ca on polymorph mineralogy of calcareous bryopsidalean algae

Powder X-ray diffraction (XRD) of the mineral precipitates (Fig. 3; Table 1) derived from the *Halimeda*, *Penicillus*, and *Udotea* offspring algae from the normal seawater treatments (Mg/Ca=5.2) confirms that these algae produce the majority of their CaCO$_3$ as aragonite (*Halimeda*=92% aragonite, 8% Mg-calcite; *Penicillus* and *Udotea*=100% aragonite) under these conditions. However, all three species of algae began producing a substantial portion of their CaCO$_3$ as low Mg calcite (*Halimeda*=46%; *Penicillus*=22%; and *Udotea*=25%) under the experimental calcite sea conditions (Mg/Ca=1.0–1.5; Table 1). The proportion of calcite produced by the *Halimeda* algae increased significantly ($p \ll 0.001$) as the Mg/Ca ratio of the experimental seawater treatment decreased into the calcite stability field (Table 1). Furthermore, the Mg/Ca ratio of the calcite produced by the *Halimeda* specimens (*Halimeda* actually produced small amounts of high Mg calcite in the boundary and aragonite sea conditions, as well) increased proportionately ($p \ll 0.001$) with the Mg/Ca ratio of the experimental seawater treatment (Fig. 4).

Backscatter electron images of the *Halimeda* (Fig. 5) and *Udotea* (Fig. 6) offspring algae from each of the seawater treatments reveal the distribution of aragonite and calcite precipitates within the interutricular space of the algae (Fig. 2). The aragonite crystals are acicular and euhedral, ranging in length from 1 to 10 μm, and packed in apparently random orientations. The calcite crystals are rhombic and subhedral, less than one micron in diameter, and generally clustered between the aragonite bundles. The two mineral phases tend to exhibit clumped distribution throughout the interutricular space.

These results suggest that calcifying bryopsidalean algae inhabiting calcite seas of the geologic past may have secreted a portion or all of their CaCO$_3$ as the calcite polymorph. However, no study to date has endeavored to evaluate secular transitions in the primary mineralogy of these algae throughout their geologic past.

Table 1. Summary of mineralogy, linear growth, calcification, and primary productivity for *Halimeda incrassata*, *Penicillus capitatus*, and *Udotea flabellum* algae grown in experimental seawater treatments formulated at different Mg/Ca ratios.

Alga	SW mMg/Ca[a]	Mineralogy (%cal:%arag)	Linear growth $\pm$SE (mm d^{-1})	Calcification $\pm$SE (mg d^{-1})	Primary production $\pm$SE (mg d^{-1}))	Study
Halimeda incrassata	5.2	8:92$\pm$2	0.41$\pm$0.04	0.83$\pm$0.07	0.73$\pm$0.02	Stanley et al. (2010)
Halimeda incrassata	2.5	16:84$\pm$2	0.28$\pm$0.03	0.52$\pm$0.03	0.43$\pm$0.05	Stanley et al. (2010)
Halimeda incrassata	1.5	46:54$\pm$8	0.21$\pm$0.03	0.40$\pm$0.04	0.33$\pm$0.04	Stanley et al. (2010)
Penicillus capitatus	5.2	0:100$\pm$3	1.00$\pm$0.11	0.70$\pm$0.06	0.87$\pm$0.10	Ries (2006a)
Penicillus capitatus	2.5	0:100$\pm$3	0.75$\pm$0.07	0.42$\pm$0.07	0.36$\pm$0.04	Ries (2006a)
Penicillus capitatus	1.0	22:78$\pm$3	0.14$\pm$0.02	0.06$\pm$0.03	0.15$\pm$0.04	Ries (2006a)
Udotea flabellum	5.2	0:100$\pm$3	0.29$\pm$0.05	0.55$\pm$0.04	0.38$\pm$0.05	Ries (2005a)
Udotea flabellum	2.5	0:100$\pm$3	0.20$\pm$0.02	0.30$\pm$0.03	0.14$\pm$0.03	Ries (2005a)
Udotea flabellum	1.0	25:75$\pm$3	0.10$\pm$0.02	0.12$\pm$0.03	0.09$\pm$0.03	Ries (2005a)

[a] mMg/Ca=1.0, [Ca^{2+}]=31.6 mmol kg-SW^{-1}; mMg/Ca=1.5, [Ca^{2+}]=25.3 mmol kg-SW^{-1}; mMg/Ca=2.5, [Ca^{2+}]=18.1 mmol kg-SW^{-1}; mMg/Ca=5.2, [Ca^{2+}]=10.2 mmol kg-SW^{-1}
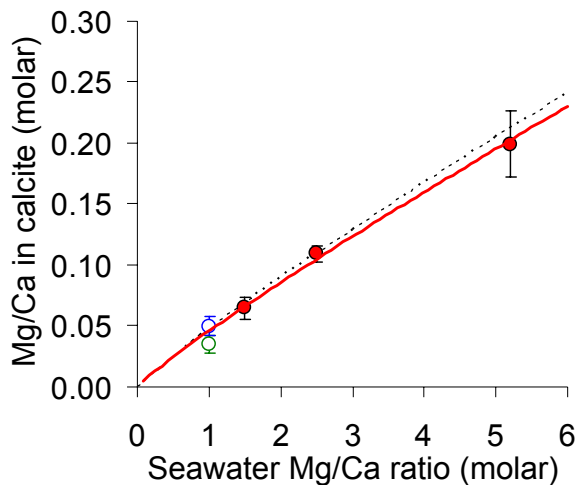

Fig. 4. Mg/Ca ratio of calcite precipitated by *Halimeda incrassata* (solid red circles), *Penicillus capitatus* (open blue circle), and *Udotea flabellum* (open green circle) algae in the experimental seawaters (*H. incrassata*: Mg/Ca=1.5, [Ca^{2+}]=25.3 mmol kg-SW^{-1}; Mg/Ca=2.5, [Ca^{2+}]=18.1 mmol kg-SW^{-1}; Mg/Ca=5.2, [Ca^{2+}]=10.2 mmol kg-SW^{-1}; *P. capitatus* and *U. flabellum*: Mg/Ca=1.0, [Ca^{2+}]=31.6 mmol kg-SW^{-1}), as determined by powder X-ray diffraction and energy dispersive spectrometry. Mg fractionation algorithm (solid red curve) is calculated for *H. incrassata* using a least squares regression and is defined as Mg/Ca$_C$=0.0460Mg/Ca$_{sw}$$^{0.899}$ (R^2=0.996) at 25 °C. Dashed black curve is Mg fractionation curve for calcite precipitated abiotically from seawater at 25 °C (Mg/Ca$_C$=0.0482 Mg/Ca$_{sw}$$^{0.898}$, R^2=0.930; Füchtbauer and Hardie, 1976). Error bars represent instrument error and variation within and amongst specimens (data from Ries, 2005a, b, 2006a; Stanley et al., 2010).
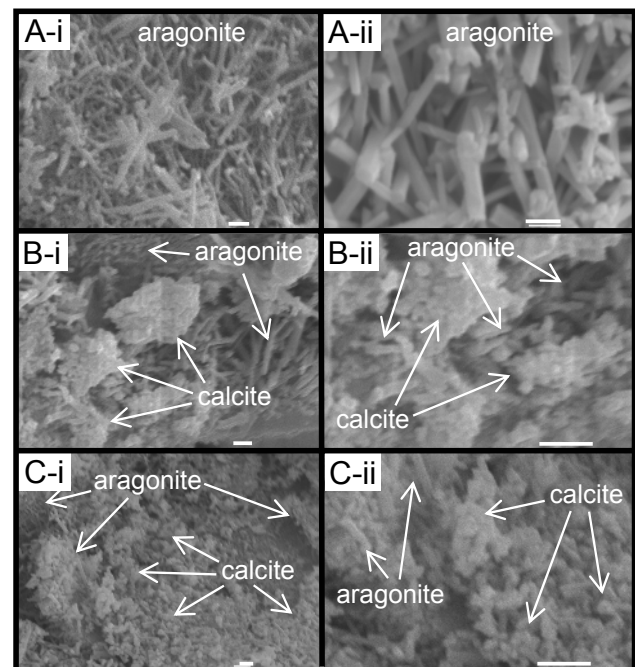

Fig. 5. Back-scatter electron images showing the distribution of the aragonite and calcite precipitated within the interutricular space of segments comprising the thalli of *Halimeda incrassata* algae reared in experimental seawaters with Mg/Ca=5.2 and [Ca^{2+}]=10.2 mmol kg-SW^{-1} (aragonite seawater; **A-i**, **A-ii**), Mg/Ca=2.5 and [Ca^{2+}]=18.1 mmol kg-SW^{-1} (aragonite-calcite boundary seawater; **B-i**, **B-ii**), and Mg/Ca=1.5 and [Ca^{2+}]=25.3 mmol kg-SW^{-1} (calcite seawater; **C-i**, **C-ii**). Scale bars are 1 μm.
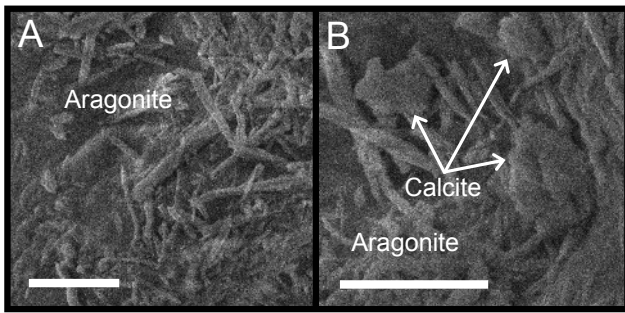
Fig. 6. Back-scatter electron images showing the distribution of the aragonite needles and calcite rhombs (indicated by arrows) precipitated within the interutricular space of segments comprising the thalli of *Udotea flabellum* algae reared in experimental seawaters with Mg/Ca=5.2 and $[Ca^{2+}]$=10.2 mmol kg-SW^{-1} (aragonite seawater, **A**) and Mg/Ca=1.0 and $[Ca^{2+}]$=31.6 mmol kg-SW^{-1} (calcite seawater, **B**). Note that calcite is only evident within algae grown in the experimental calcite seawater. Scale bars are 1 μm (modified from Ries, 2005b, 2006a).

3.2 Effect of seawater Mg/Ca on reproduction of calcareous bryopsidalean algae

The total number of offspring algae produced by the parent algae varied amongst the different experimental seawater treatments. In the calcite, boundary, and aragonite seawater treatments, *Halimeda* produced 18, 37, and 45 offspring algae, *Penicillus* produced 13, 29, and 16 offspring algae, and *Udotea* produced 16, 17, and 23 offspring algae, respectively. That the algae generally produced more offspring under increasingly elevated Mg/Ca ratios suggests that the algae were stressed by producing a large portion of their CaCO$_3$ as aragonite in the seawater favoring the nucleation of calcite. If the precipitation of aragonite under such conditions required extra energy to manipulate the composition of the algae's calcifying fluid (e.g., to elevate Mg/Ca; Fig. 2a), then this energy may have been diverted away from other physiological activities, such as reproduction and tissue growth.

3.3 Effect of seawater Mg/Ca on linear extension, calcification, and primary production of calcareous bryopsidalean algae

Rates of linear extension, calcification, and primary production for the *Halimeda*, *Penicillus*, and *Udotea* algae decreased significantly ($p < 0.05$) with reductions in Mg/Ca of the experimental seawaters (Table 1). This observation is consistent with the assertion that the steady elevation of seawater Mg/Ca ratios (from 1.0 to 5.2) over the past 65 My, since the major diversification of the calcareous bryopsidalean algae (Fig. 1), has fostered their increasingly important role as contributors of CaCO$_3$ sediments to carbonate platform environments throughout this interval.
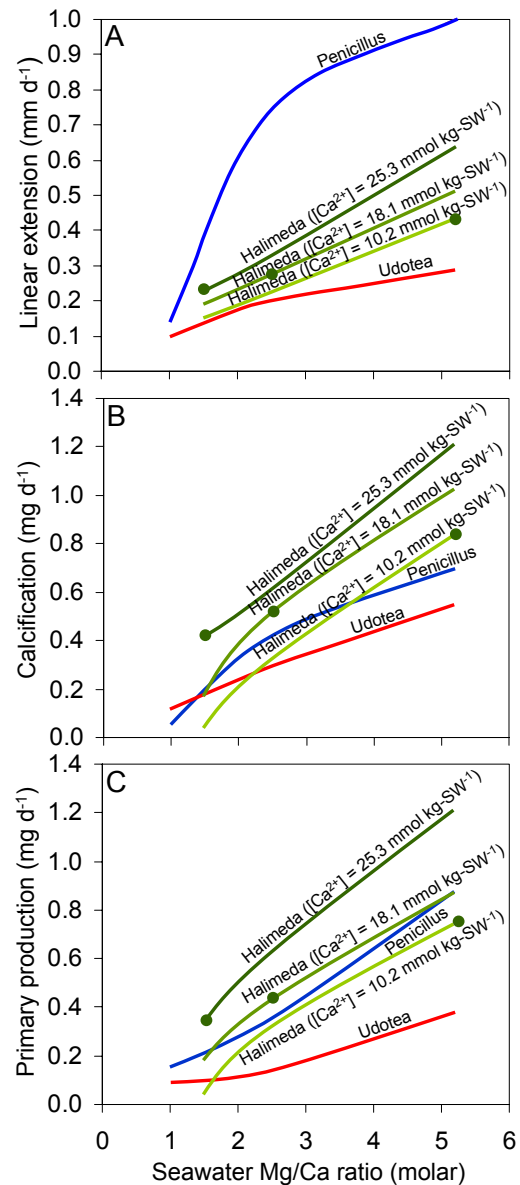

Fig. 7. Rates of linear extension (**A**), calcification (**B**), and primary production (**C**) for *Halimeda incrassata* (dark green curve: $[Ca^{2+}]$=25.3 mmol kg-SW^{-1}; medium green curve: $[Ca^{2+}]$=18.1 mmol kg-SW^{-1}; light green curve: $[Ca^{2+}]$=10.2 mmol kg-SW^{-1}), *Penicillus capitatus* (blue curve), and *Udotea flabellum* (red curve) algae reared in experimental seawaters of modified Mg/Ca and $[Ca^{2+}]$. Rates of linear extension, calcification, and primary production increase significantly ($p < 0.05$) for *H. incrassata* with both increasing seawater Mg/Ca ($[Ca^{2+}]$ fixed) and increasing seawater $[Ca^{2+}]$ (Mg/Ca fixed). Rates of linear extension, calcification, and primary production also increase significantly ($p < 0.05$) with elevations in seawater Mg/Ca that are formulated with geologically realistic (Hardie, 1996; Demicco et al., 2005) reductions in $[Ca^{2+}]$ for all three species of calcifying algae (*H. incrassata* = closed green circles; *P. capitatus* = blue curve; *U. flabellum* = red curve). Primary production is calculated as total dry weight minus weight of CaCO$_3$. Data from Ries (2005a, b, 2006a); Stanley et al. (2010).

Although the observed relationship between seawater Mg/Ca and calcification within the *Halimeda*, *Penicillus*, and *Udotea* algae may be expected, it is less intuitive why seawater Mg/Ca would also affect primary production and linear extension of these algae.

It has been proposed that photosynthesis in some calcareous bryopsidalean algae and coccolithophores is enhanced by CO_2 liberated by calcification (Paasche, 1968; Borowitzka and Larkum, 1976b; Borowitzka, 1977; Sikes et al., 1980; Reiskind et al., 1988, 1989; Ries, 2005a, 2006a, 2009; Stanley et al., 2005, 2010). The equilibrium reactions that govern the aqueous carbonate system can be summarized as follows:

$$CO_2 + H_2O \leftrightarrow H_2CO_3; \tag{R1}$$

$$H_2CO_3 \leftrightarrow HCO_3^- + H^+; \text{ and} \tag{R2}$$

$$HCO_3^- - \leftrightarrow H^+ + CO_3^{2-}. \tag{R3}$$

Calcification has the net effect of shifting the aqueous carbonate system towards elevated $[CO_2]$ and $[H^+]$ (Fig. 2a). Thus, elevated rates of calcification may increase CO_2 within the interutricular calcification space of the *Halimeda*, *Penicillus*, and *Udotea* algae (Fig. 2), thereby increasing the algae's rate of photosynthesis and primary production. Although calcification is certainly not the sole source of CO_2 for photosynthesis within calcareous bryopsidalean algae (as many non-calcifying bryopsidalean algae exist), its role in CO_2 liberation may be sufficient to explain the observed correlation between calcification, primary production, and linear extension.

An alternative mechanism that explains why algal linear extension and primary production would track calcification is based upon the release of H^+ ions during calcification (Fig. 2a). In one model, H^+ ions complex with HCO_3^- ions within the algae's interutricular space, thus facilitating CO_2 extraction by dehydration of H_2CO_3 within the algal cell (McConnaughey and Whelan, 1997; Hellblom et al., 2001; Hellblom and Axelsson, 2003). In another model, H^+ ions liberated by calcification are utilized by the alga as symporters or co-transporters of HCO_3^- and nutrients, such as NO_3^- and PO_4^{-3}, across the algal cell wall (Price and Badger, 1985; Price et al., 1985; McConnaughey and Whelan, 1997; Hellblom et al., 2001). Increased rates of assimilation of these typically limiting substrates could cause the algae's rate of photosynthesis and primary production to vary commensurately with their rate of calcification.

3.4 Effect of absolute $[Ca^{2+}]$ on linear extension, calcification, and primary production of the *Halimeda* alga

Because elevations in seawater Mg/Ca throughout the geologic past were partially driven by reductions in $[Ca^{2+}]$ (Hardie, 1996), there exists the potential that the positive effects of elevated seawater Mg/Ca favoring the nucleation of the algae's preferred aragonite mineral would have been

outweighed by the corresponding negative effects of reduced $CaCO_3$ saturation state resulting from reduced $[Ca^{2+}]$. To isolate the effects of $[Ca^{2+}]$ and Mg/Ca, *Halimeda* algae were reared in an array of experimental seawaters, specifically formulated to test for the effects of $[Ca^{2+}]$ when Mg/Ca is held constant, and vice versa (Fig. 7). When Mg/Ca was held constant (at 1.5, 2.5, and 5.2), increases in $[Ca^{2+}]$ from 10.2, to 18.1, to 25.3 mmol kg-SW^{-1} resulted in increased rates of linear extension, calcification, and primary production (Fig. 7). And when $[Ca^{2+}]$ was held constant (at 10.2, 18.1, and 25.3 mmol kg-SW^{-1}), increases in Mg/Ca from 1.5, to 2.5, to 5.2 resulted in increased rates of linear extension, calcification, and primary production (Fig. 7).

Thus, the results of the study on *Halimeda* reveal that both elevated Mg/Ca ratios and elevated $[Ca^{2+}]$ promote calcification, primary production, and linear extension within this alga. The elevated Mg/Ca ratios evidently translate to higher rates of calcification by creating ambient chemical conditions favorable for the precipitation of the alga's preferred aragonite biomineral. Elevated $[Ca^{2+}]$ probably fosters higher rates of calcification by increasing the $CaCO_3$ saturation state of the alga's ambient seawater.

Critically, over the range of Mg/Ca ratios (1.0–5.2) and absolute $[Ca^{2+}]$ (10.2–25.3 mmol kg-SW^{-1}) that are believed to have occurred throughout Phanerozoic time, the favorable effects of elevated Mg/Ca on bryopsidalean calcification were greater in magnitude than the unfavorable effects of reduced $CaCO_3$ saturation state that resulted from corresponding reductions in $[Ca^{2+}]$. Thus, Mg/Ca ratio appears to be the primary determinant of how calcareous bryopsidalean algae would have responded to calcite-aragonite sea transitions. However, at least one scenario was identified in which increasingly favorable Mg/Ca ratios were concomitantly outweighed by increasingly unfavorable $CaCO_3$ saturation states (via decreasing $[Ca^{2+}]$), in terms of their relative effects on calcification rate. This was evident (Fig. 7) when comparing the algae's responses to the Mg/Ca=1.5, $[Ca^{2+}]$=25.2 mmol kg-SW^{-1} and the Mg/Ca=2.5, $[Ca^{2+}]$=10.2 mmol kg-SW^{-1} experimental treatments.

3.5 Effect of seawater Mg/Ca on thallus stiffness of the *Penicillus* alga

Stress-strain curves were generated for the *Penicillus* specimens subjected to varying hydraulic current stresses within a flume tank by plotting current stress against the resulting deflection, or strain, of the algae's thalli (Figs. 8–10). Strain was measured as thallus deflection because all deflection was due solely to current stress. The thallus stiffness for each *Penicillus* thallus was then calculated as the slope of the least squares linear regression through this stress-strain curve (Fig. 10a). Thallus stiffness was averaged for each of the seawater treatments and plotted against corresponding seawater Mg/Ca (Fig. 10b).
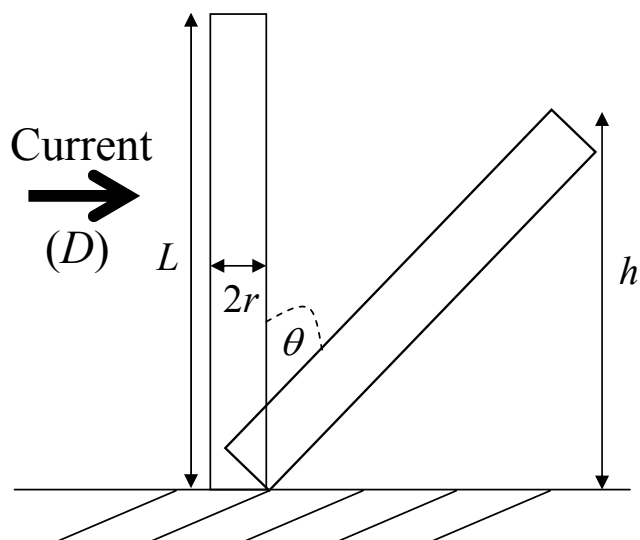
Fig. 8. Free body diagram of a decapitated *Penicillus capitatus* alga modeled as a cantilever beam stressed by a unidirectional current. Stress (σ) is calculated as $4Dh/(\pi r^3)$, where D is the current velocity, h is the height of the stalk and r is the radius of the stalk. Note that height (h) decreases as a function of $L\cos\theta$, where L is the length of the stalk and θ is the angle of stalk deflection. From Ries (2005a).

The stiffness of the *Penicillus* thalli increased significantly ($p < 0.001$) with Mg/Ca ratio of the ambient seawater (Fig. 10b). Algae reared in the experimental seawater favoring their inherently aragonitic mineralogy were nearly twice as stiff as those reared in the experimental seawater that favored the nucleation of calcite.

3.6 Biomineralogical control within the calcareous bryopsidalean algae

The observation that the *Halimeda*, *Penicillus* and *Udotea* algae each precipitate the majority of their $CaCO_3$ as the aragonite polymorph in the experimental calcite seawater suggests that these algae exhibit substantial control over the Mg/Ca ratio of their interutricular calcifying fluid. However, since these algae commence producing a portion of their $CaCO_3$ as the kinetically favored calcite polymorph under these conditions, it is evident that their biomineralogical control can be partially overridden by ambient seawater Mg/Ca.

The distribution of aragonite and calcite precipitates within the *Halimeda* (Fig. 5), *Penicillus*, and *Udotea* (Fig. 6) algae reared in the experimental calcite seawater occurs on a spatial scale that is comparable to that of the purported acid and alkaline zones within these algae (De Beer and Larkum, 2001). Both conditions may reflect the algae's spatially limited control over the chemical milieu of their interutricular fluid

It has been suggested that *Halimeda* algae control calcification solely through pH regulation (Borowitzka, 1987; De
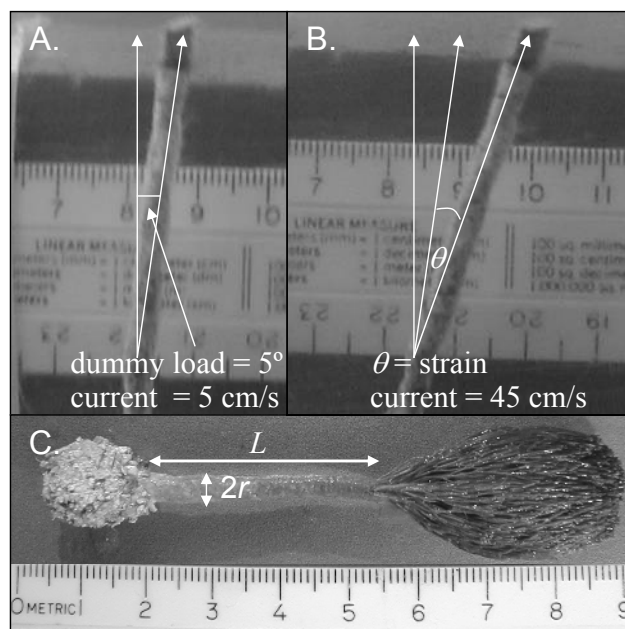

Fig. 9. **(A)** Decapitated *Penicillus capitatus* alga pre-strained to 5° deflection with the dummy load (current velocity = 5 cm/s). **(B)** Decapitated *P. capitatus* alga strained beyond the 5° pre-strain dummy load (current velocity = 45 cm/s). Angles of deflection (θ) beyond the 5° pre-strain were employed in the stress-strain analyses. **(C)** Photograph of a *P. capitatus* alga depicting the length (L) and radius (r) dimensions employed in modeling its thallus as a cantilever beam. From Ries (2005a).

Beer and Larkum, 2001). If this assertion is correct, then *Halimeda* algae grown in the experimental calcite seawater should precipitate exclusively calcite – which they did not. DeBeer and Larkum's (2001) conclusion that Ca^{2+} is not actively transported into the interutricular space of *Halimeda* is based on their observation that the alga's rate of calcification is unaffected by inhibition of the Ca-ATPase enzyme. Although their findings show that *Halimeda* do not actively transport Ca^{2+} *into* the calcifying space, their results do not preclude the possibility that *Halimeda*, as well as *Penicillus and Udotea*, pump Ca^{2+} *out of* the interutricular space, thereby maintaining the Mg/Ca ratio of certain regions of the algae's interutricular space within the aragonite nucleation field (Mg/Ca > 2), even when ambient seawater remains within the calcite nucleation field (Mg/Ca < 2). This, of course, requires that the $CaCO_3$ saturation state of the interutricular fluid is maintained at a level sufficient to promote calcification, even after Ca^{2+} is transported out, perhaps by increasing $[CO_3^{2-}]$ by removing CO_2 via photosynthesis (Borowitzka, 1982b, 1987) or by increasing pH through H^+-pumping (De Beer and Larkum, 2001). It is also possible that the Mg/Ca ratio of the algae's calcifying fluid is elevated into the aragonite stability field simply through the removal of Ca^{2+} ions via calcification. Alternatively, the same result
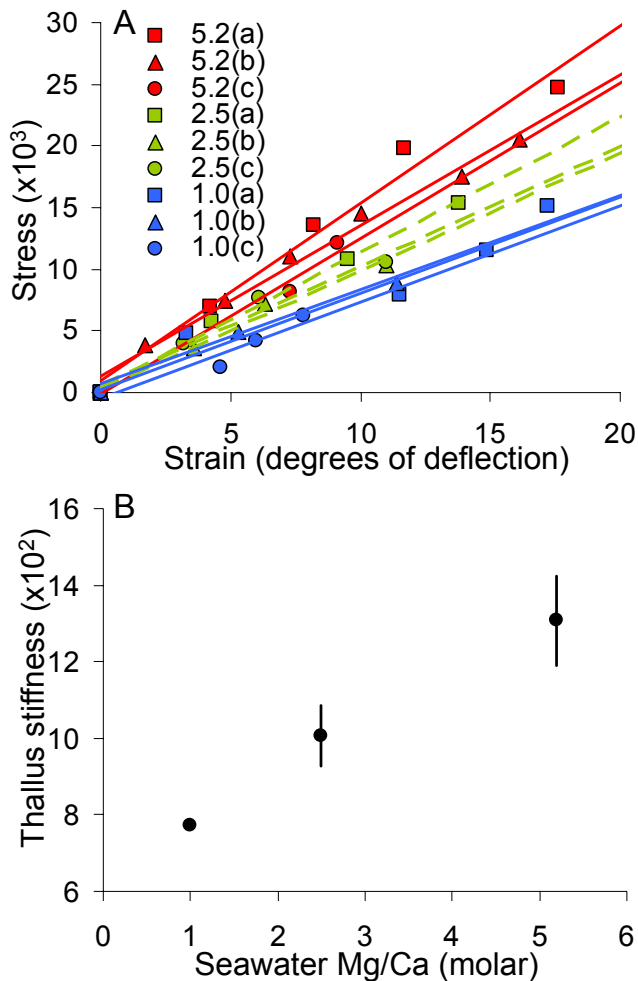
Fig. 10. (A) Stress-strain data generated for the thalli of nine *Penicillus capitatus* algae reared in the three seawater treatments (from Ries, 2005a). Stress-strain curves were generated by fitting linear regressions to the data using the least squares method. The solid red, dashed green, and solid blue curves correspond to *P. capitatus* algae reared in experimental seawaters formulated with Mg/Ca of 5.2, 2.5 and 1.0, respectively. Average stiffnesses were calculated from the slopes of these stress-strain curves and plotted against seawater Mg/Ca in panel **(B)**. Thallus stiffness decreased significantly ($p < 0.001$) with reductions in seawater Mg/Ca, such that algae were most stiff when reared in seawater that supports precipitation of their inherent aragonite skeletal mineral (Mg/Ca=5.2) and least stiff in seawater that supports the nucleation of calcite (Mg/Ca=1.0). Error bars represent standard deviation.

could be achieved by actively transporting Mg^{2+} ions into the algae's interutricular space, thereby elevating the Mg/Ca ratio into the aragonite nucleation field. However, a mechanism capable of such rapid transport of Mg^{2+} across the algal cell wall has yet to be identified in the *Halimeda*, *Penicillus*, or *Udotea* algae.

3.7 Paleoecological implications for the calcareous bryopsidalean algae

The results of the experimental studies suggest that the predominant carbonate-producing bryopsidalean algae in modern aragonite seas – *Halimeda*, *Penicillus*, and *Udotea* – would have been slower growing, smaller, and less calcified during calcite seas of the geologic past. Such geochemically induced reductions in the fitness of these algae would have had significant ecological implications for these algae and for carbonate platform environments, in general. Their slower growth rates and smaller size would have reduced their ability to compete for space and sunlight on the substrate-limited shallow tropical seafloor. And their reduced calcification would have rendered them more susceptible to predation by grazing fish, which in modern aragonite seas are deterred by the algae's high $CaCO_3$ content, as well as their secondary metabolic toxins (Wray, 1977; Paul and Fenical, 1984; Paul and Hay, 1986; Hay et al., 1988, 1994; Paul and Van Alstyne, 1988, 1992; Schupp and Paul, 1994). The algae's contribution of biogenic $CaCO_3$ to shallow tropical carbonate platforms would have been comparably diminished by such reductions in calcification, primary production, and population density during calcite sea intervals.

3.8 Conclusions – calcareous bryopsidalean algae

1. Observed reductions in the calcification, primary production, and linear extension of *Halimeda*, *Penicillus*, and *Udotea* algae grown in experimental seawater that favors the calcite polymorph over the aragonite polymorph indicate that the fitness of these algae is reduced when grown in mineralogically unfavorable seawater. These experimental studies suggest that calcareous bryopsidalean algae would have been smaller, less abundant, less competitive for space on the seafloor, and less resistant to grazing when seawater Mg/Ca did not favor their inherently aragonitic mineralogy. This is consistent with the assertion (Stanley and Hardie, 1998, 1999) that a shift from calcite-to-aragonite seas in the early-to-middle Cenozoic enabled the aragonite-secreting bryopsidalean algae to flourish and to become the important producers of $CaCO_3$ sediments that they are today.

2. Thallus stiffness decreased for specimens of *P. capitatus* grown in seawater that does not favor the aragonite polymorph. This physiological consequence of reduced Mg/Ca appears to result from decreased calcification and associated reductions in primary production.

3. Elevated Mg/Ca ratios and elevated $[Ca^{2+}]$ both result in increased rates of calcification, primary production, and linear extension in *Halimeda* algae. Therefore, the inherently inverse relationship between Mg/Ca and $[Ca^{2+}]$ causes their effects on *Halimeda* algal calcification, primary production, and linear extension to

partially counteract one another. However, over the range of coupled seawater Mg/Ca ratios and $[Ca^{2+}]$ that are believed to have occurred throughout the geologic history of the bryopsidalean algae, these experiments reveal that seawater Mg/Ca is the controlling variable. Inverse variations in $[Ca^{2+}]$ appear only to moderate the effects of seawater Mg/Ca.

4. The concomitant variations in calcification, primary production, and linear extension of the *Halimeda*, *Penicillus*, and *Udotea* algae suggest that there are important connections amongst these processes within the algae. Seawater Mg/Ca appears to directly influence calcification via $CaCO_3$ polymorph compatibility. Calcification, in turn, may influence primary production and linear extension by supplying CO_2 for photosynthesis and/or supplying H^+ ions for various cellular functions that support photosynthesis, such as the transcellular proton-shuttling of nutrients or HCO_3^- and the formation of intracellular H_2CO_3, from which CO_2 can be efficiently extracted via dehydration

5. The precipitation of predominantly aragonite by *Halimeda*, *Penicillus*, and *Udotea* algae in experimental seawater that kinetically favors the precipitation of calcite (Mg/Ca<2) indicates that these algae actively specify nucleation of the aragonite polymorph. This may be accomplished by controlling internal Mg/Ca through cation pumping or with chemical and/or mechanical templates that specify nucleation of the aragonite polymorph (Borowitzka, 1987). However, precipitation of a portion of the algae's $CaCO_3$ as calcite in the experimental calcite seawater reveals that their biomineralogical control can be partially overridden by ambient seawater Mg/Ca.

4 Coccolithophores

The formation of the massive, coccolithic chalk deposits in Late Cretaceous time (Hattin, 1988) has been attributed to the low oceanic Mg/Ca ratios reported for that interval (Stanley and Hardie, 1998, 1999), which would have favored the coccolithophores' inherently calcitic mineralogy. Experiments were conducted to evaluate the effect of seawater Mg/Ca on skeletal Mg/Ca, calcification, and population growth rate of these calcifying nannoplankton (Stanley et al., 2005).

Coccolithophore strains (CCMP645, CCMP2119, CCMP298) of *Pleurochrysis carterae*, *Ochrosphaera neopolitana*, and *Coccolithus neohelis* were cultured for 15 days in 500 mL experimental seawaters (contained in 1 l beakers) formulated at Mg/Ca ratios of 0.5, 1.0, 1.5, 2.5, 3.5, and 5.2, thereby encompassing the range of values (Hardie, 1996) believed to have existed throughout the coccolithophores' existence. To differentiate between the
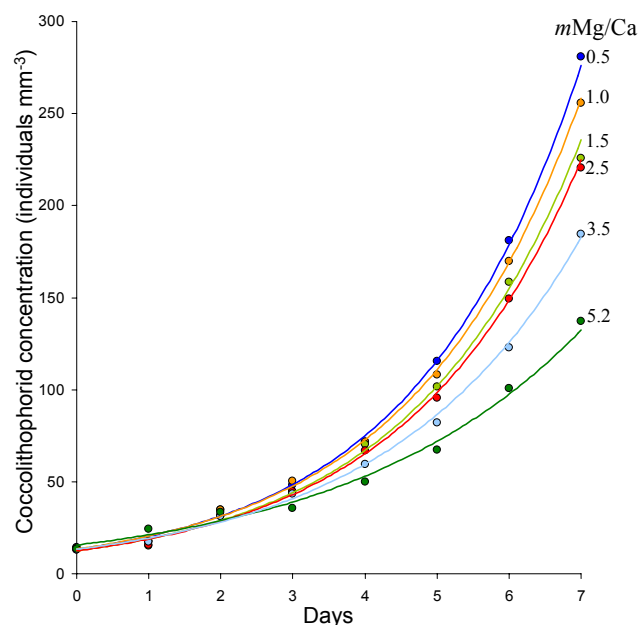

Fig. 11. Exponential population growth for the coccolithophore *Pleurochrysis carterae* as a function of seawater Mg/Ca. Rates of population growth increased significantly ($p < 0.05$) as seawater Mg/Ca declined into the calcite stability field, which favors precipitation of the coccolithophores' calcite skeletal mineral. For modern seawater, Mg/Ca is 5.2 and the absolute concentration of Ca^{2+} is 10 mmol kg-SW^{-1}; for the imputed Late Cretaceous seawater, the Mg/Ca ratio is between 0.5 and 1.5 and the absolute concentration of Ca^{2+} is between 42 and 25 mmol kg-SW^{-1}. R^2 is between 0.98 and 0.99 for exponential fitted curves. Spearman rank correlation (r_s)=0.99 for growth rates. From Stanley et al. (2005).

effects of Mg/Ca ratio and absolute $[Ca^{2+}]$ on the coccolithophores, three additional seawaters were formulated with fixed $[Ca^{2+}]$ at Mg/Ca ratios of 1, 3.5 and 5.2 (see experimental design for experiments on calcareous bryopsidalean algae for details). The *Pleurochrysis carterae* and *Coccolithus neohelis* cultures were fertilized with 8.8×10^{-4} mol l^{-1} nitrogen (as nitrate), 2.3×10^{-4} mol l^{-1} phosphorus (as phosphate), and 1.45×10^{-5} mol l^{-1} iron (as Fe^{3+}), as specified by the P-G CCMP f/2 culture medium. The *Ochrosphaera neopolitana* culture was fertilized with 3.5×10^{-5} mol l^{-1} nitrogen (as nitrate), 9.2×10^{-6} mol l^{-1} phosphorus (as phosphate), and 5.8×10^{-7} mol l^{-1} iron (as Fe^{3+}), as specified by the P-G CCMP f/50 culture medium.

4.1 Effect of seawater Mg/Ca and $[Ca^{2+}]$ on population growth of coccolithophores

The rate of population growth for each of the three species of coccolithophore was greatest in the experimental seawaters that favored the nucleation of the coccolithophores' calcite skeletal mineral (Mg/Ca<2) and systematically decreased as seawater Mg/Ca increased towards the aragonite stability
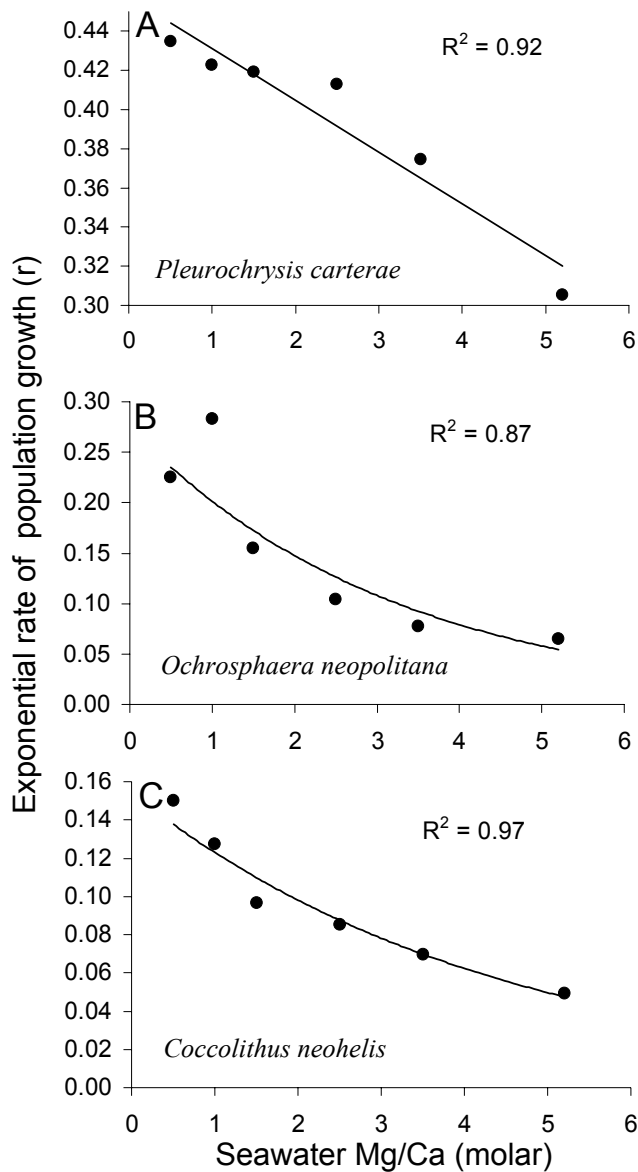
Fig. 12. Exponential rates of population growth (r) as a function of seawater Mg/Ca ratio for the coccolithophore species *Pleurochrysis carterae* (**A**), *Ochrosphaera neopolitana* (**B**), and *Coccolithus neohelis* (**C**). Rates of population growth increased significantly ($p < 0.05$) for each of the three species as seawater Mg/Ca declined into the calcite stability field, which favors precipitation of the coccolithophores' calcite skeletal mineral. Fitted curve in (A) is linear, while fitted curves in (B) and (C) are exponential. Spearman rank correlation (r_s)=0.99 for all three species. From Stanley et al. (2005).

field (Figs. 11, 12). Experiments that held the Mg/Ca ratio constant while varying Ca^{2+} concentrations (Fig. 13a–b), and the concentration of Ca^{2+} constant while varying Mg/Ca ratios (Fig. 13c–d), revealed that population growth rates increased with increasing absolute concentrations of Ca^{2+}, as well as with decreasing seawater Mg/Ca ratios.

4.2 Effect of seawater Mg/Ca on chalk production by coccolithophores

Chalk production increased significantly as seawater Mg/Ca decreased (Fig. 14), resulting in the greatest amount of chalk being formed in the experimental calcite seawater treatment. Significantly, the composition of this experimental calcite seawater treatment is believed to be representative of the oceans in Late Cretaceous time – when coccolithophores were producing the massive chalk deposits (e.g., White Cliffs of Dover) after which the Cretaceous Period is named (*Creta-* is the Latin word for "chalk"). These results are consistent with the population data obtained from the daily turbidimeter measurements (Figs. 11, 12).

Backscatter electron images (Fig. 15) also reveal that individual coccoliths are more heavily calcified when grown in the low Mg/Ca seawater treatments, which favor nucleation of the coccolithophores' inherently calcitic biomineral. The observed correlation between rates of calcification (Fig. 15) and rates of population growth (Figs. 11–13) is consistent with the hypothesis that calcification enhances photosynthesis within some species of coccolithophores via the liberation of CO_2 (Paasche, 1968; Sikes et al., 1980). However, this appears not to be the case for all species of coccolithophores, as other experiments have revealed that photosynthesis within *Emiliania huxleyi* is not diminished when the coccolithophore's calcification is reduced under low-[Ca^{2+}] conditions (Leonardos et al., 2009).

These results support the assertion that coccolithophore chalk production that was widespread throughout Cretaceous time was facilitated by the low seawater Mg/Ca ratios known to have existed throughout this interval, which would have supported precipitation of the coccolithophore's inherently calcitic skeletal mineral. However, it should be noted that the enhanced chalk production by coccolithophores that occurred in Late Cretaceous time (Hattin, 1988) was not perfectly synchronized with the seawater Mg/Ca minimum that occurred in mid-Late Cretaceous time (Fig. 1). Thus, it is possible that other physicochemical factors, such as elevated atmospheric pCO$_2$, elevated seawater alkalinity, or warmer surface seawater temperatures, acted in concert with the low (yet not lowest) seawater Mg/Ca ratios in order to support the intense coccolithophorid chalk production that occurred in Late Cretaceous seawater.

4.3 Effect of seawater Mg/Ca on coccolithophorid mineralogy

The Mg/Ca ratios of the calcitic coccoliths secreted by the *Ochrosphaera neopolitana* and *Pleurochrysis carterae* coccolithophores (Fig. 16b–c) varied proportionately with the Mg/Ca ratio of their ambient seawater. Coccolithophores reared under calcite sea conditions secreted low Mg calcite, while those reared under aragonite sea conditions secreted high-Mg calcite. These results are particularly striking given
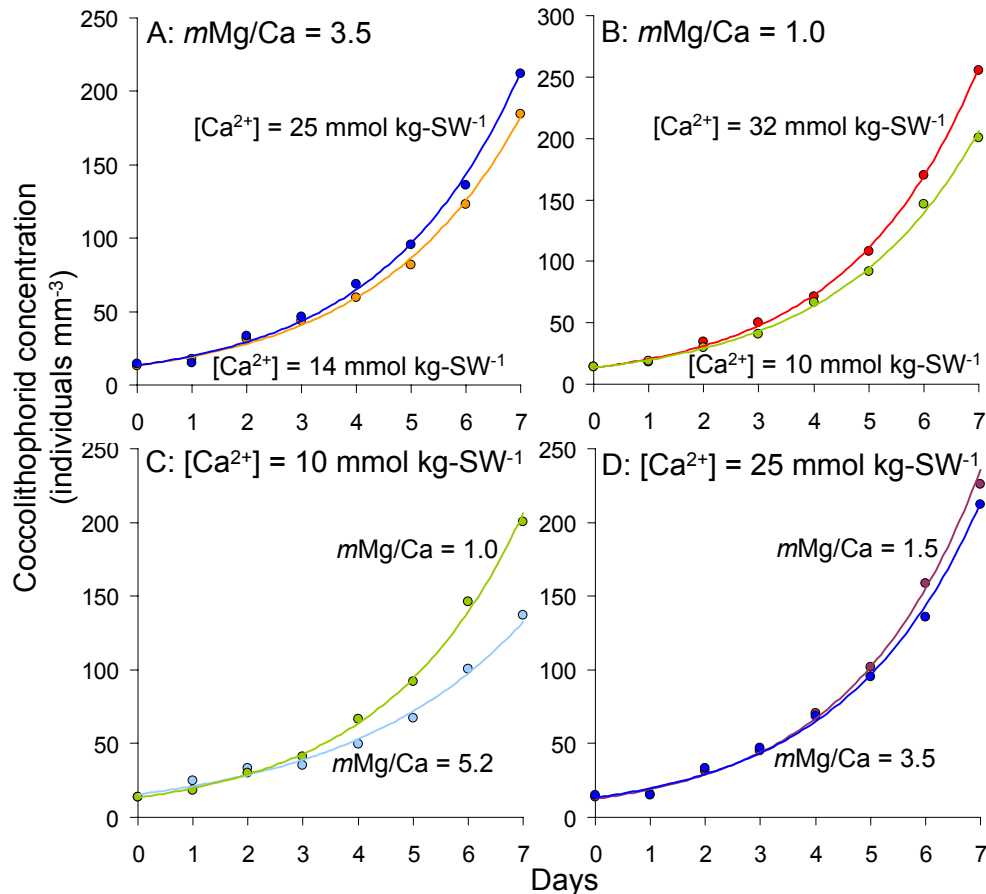
Fig. 13. Effect of seawater Mg/Ca ratio and absolute Ca^{2+} concentration on population growth rate of *Pleurochrysis carterae*. **(A)** With Mg/Ca ratio fixed at 3.5, elevation of Ca^{2+} concentration from 14.1 mmol kg-SW^{-1} (orange curve) to 25.3 mmol kg-SW^{-1} (dark blue curve) produced faster population growth. **(B)** With Mg/Ca ratio fixed at 1.0, reduction of Ca^{2+} concentration from 31.6 mmol kg-SW^{-1} (red curve) to 10.2 mmol kg-SW^{-1} (green curve) produced slower population growth. **(C)** With Ca^{2+} fixed at 10.2 mmol kg-SW^{-1}, reduction of Mg/Ca from 5.2 (light blue curve) to l.0 (green curve) produced faster population growth. **(D)** With Ca^{2+} fixed at 25.3 mmol kg-SW^{-1}, elevation of the Mg/Ca ratio from 1.5 (purple curve) to 3.5 (dark blue curve) yielded slower population growth. Experiments with *Coccolithus neohelis* yielded similar results. From Stanley et al. (2005).

that all modern coccolithophores are thought to secrete exclusively low Mg calcite (Milliman, 1974). This was the first study to show that, indeed, at least two modern species of coccolithophores secrete high Mg calcite in modern aragonite seawater (Mg/Ca=5.2). The coccolithophore *Coccolithus neohelis* (Fig. 16a), however, produced low Mg calcite in each of the experimental seawater treatments, regardless of prescribed seawater Mg/Ca.

The observation that two of the three species of coccolithophores incorporated Mg into their calcitic coccoliths in proportion to the Mg/Ca ratio of the seawater in which they were grown suggests that, despite their ability to dictate precipitation of highly intricate coccoliths, their mineralogical control is limited in its capacity to control Mg incorporation in the calcite crystal lattice. The third species, however, which precipitates low Mg calcite regardless of ambient seawater Mg/Ca, is apparently more adept at regulating skeletal Mg incorporation.

4.4   Conclusions – coccolithophores

1. Increased rates of population growth and calcification exhibited by coccolithophores grown under low Mg/Ca ratios and high Ca^{2+} concentrations suggest that the existence of these conditions in Cretaceous time likely enabled coccolithophores to produce the massive chalk deposits from which that interval derives its name. This is particularly striking given that the coccolithophores flourished in the most modified experimental seawaters, to which they were naturally the least accustomed.

2. Conversely, the high Mg/Ca ratio and low Ca^{2+} concentration of modern seawater probably prevents chalk production by most extant species.

3. The correlation between rates of calcification and rates of population growth observed for *P. carterae*, *O. neopolitana*, and *C. neohelis*, but not for *E. huxleyi*,
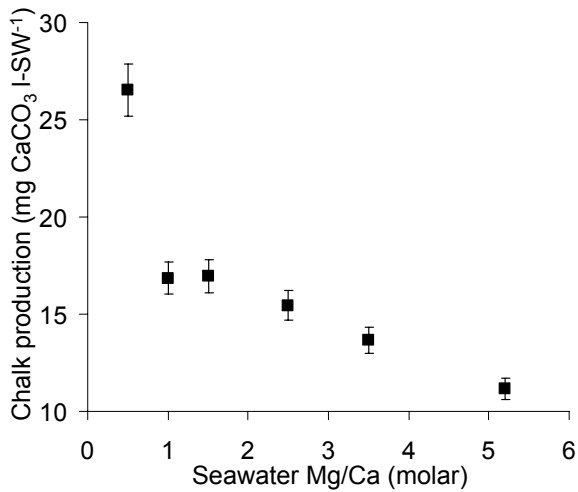
Fig. 14. Chalk production by *Pleurochrysis carterae* after seven days of growth in the six experimental seawater treatments. Chalk production increases as seawater Mg/Ca declines into the calcite stability field. Low seawater Mg/Ca favors precipitation of the coccolithophores' calcite skeletal mineral and is believed to have characterized seawater in Cretaceous time (Fig. 1) – when chalk production by coccolithophores was at its apex. Vertical bars represent measurement error. From Stanley et al. (2005).
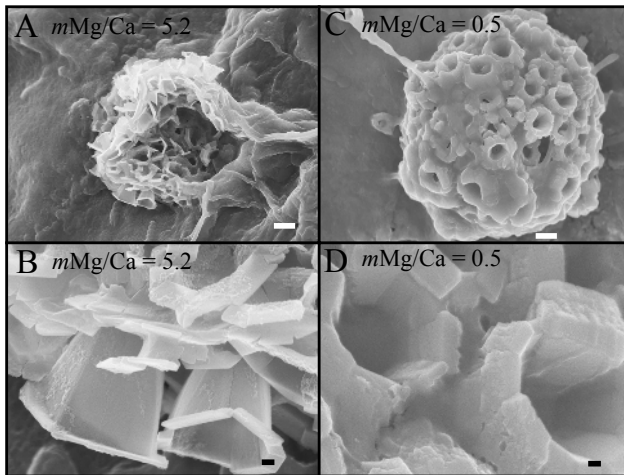

Fig. 15. Backscatter electron images of the coccolithophore *Ochrosphaera neopolitana* after growth in experimental modern (Mg/Ca=5.2; **A, B**) and Cretaceous (Mg/Ca=0.5; **C, D**) seawaters. Coccoliths precipitated in experimental Cretaceous seawater appear to be larger and more heavily calcified than those precipitated in modern seawater. White bars are 1 μm; black bars are 100 nm. From Stanley et al. (2005).

suggests that calcification enhances photosynthesis via the liberation of CO_2 for some – but not all – species of coccolithophores (Paasche, 1968; Sikes et al., 1980; Leonardos et al., 2009).
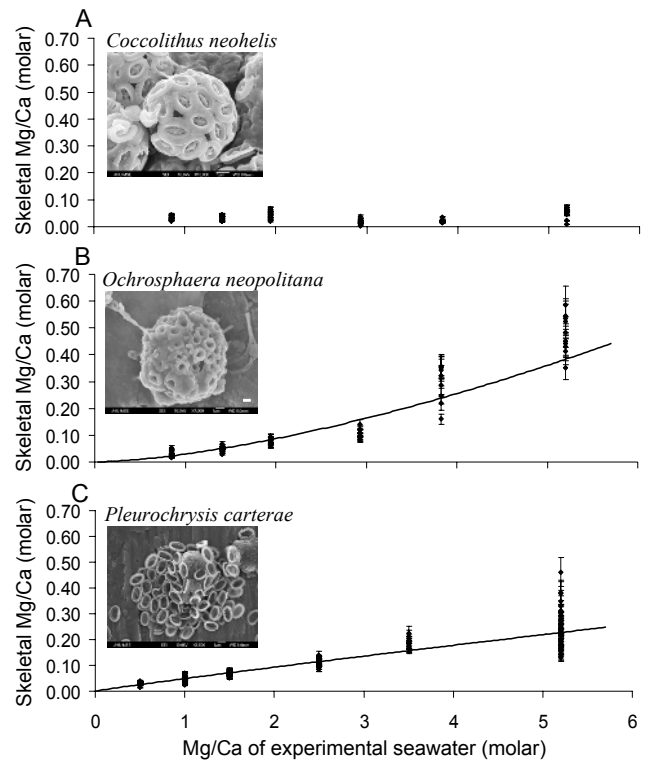

Fig. 16. Mg/Ca ratio of calcite secreted by coccolithophore species *Coccolithus neohelis* (**A**), *Ochrosphaera neopolitana* (**B**), and *Pleurochrysis carterae* (**C**) as a function of the Mg/Ca ratio of the experimental seawater in which they were reared. Error bars represent standard error of microprobe analysis. Fitted curves are power functions fit to the data using least squares regressions. From Stanley et al. (2005).

4. The decrease in skeletal Mg/Ca in response to reduced seawater Mg/Ca for two of the species studied suggests that their biomineralogical control can be partially overridden by ambient seawater chemistry. That the third species did not exhibit a change in skeletal Mg/Ca in response to reduced seawater Mg/Ca may be evidence of stronger biomineralogical control.

5. Correlation between skeletal Mg/Ca and seawater Mg/Ca for two of the three species of coccolithophores, but not for the third species, suggests that the mineralogy (low Mg calcite vs. high Mg calcite) of some, but not all, species of coccolithophores has varied significantly with seawater Mg/Ca throughout their geological history.

5   Scleractinian corals

Scleractinian corals, which secrete massive aragonitic skeletons, have been major reef frame builders from Late Triassic (Stanton and Flügel, 1987; Bernecker, 1996) through Early

Cretaceous time (Stanley and McRoberts, 1993) and from Early Oligocene through to present time (Frost, 1977, 1981; Fig. 1). During these intervals, the Mg/Ca ratio of the oceans favored the inorganic precipitation of aragonite (Mg/Ca > 2, Hardie, 1996). The reign of the scleractinian corals was interrupted during mid-Cretaceous time by the ascendance of the largely calcitic rudist bivalves (Scott, 1984; Kauffman and Johnson, 1988; Fig. 1) close to the time when the Mg/Ca ratio of seawater dropped to its lowest Phanerozoic level and favored the precipitation of calcite (Mg/Ca < 2).

The rudists continued as primary reef builders through the end of the Cretaceous Period. Significantly, however, the scleractinian corals did not resume forming massive, widespread reefs until early in Oligocene time, just after the Mg/Ca ratio of seawater shifted back into the aragonite stability field (Fig. 1), despite the global climate cooling that had occurred at that time (Wolfe, 1978).

It has been proposed that shifts in the Mg/Ca ratio of seawater, which alternately favored the precipitation of calcite or aragonite throughout Phanerozoic time (Fig. 1), may have influenced the success of scleractinian corals as primary reef builders throughout their existence (Stanley and Hardie, 1998, 1999). Experiments have been conducted (Ries et al., 2006) to evaluate the influence of seawater Mg/Ca on the mineralogy and growth rates of three species of modern zooxanthellate scleractinian corals, *Acropora cervicornis*, *Porites cylindrica*, and *Montipora digitata*.

Sixty comparably sized individuals of each of the three coral species (180 total) were grown for 60 days in six experimental seawaters that were identical except for their Mg/Ca ratios, which were formulated at 1.0, 1.5, 2.5, 3.5, and 5.2, thereby encompassing the range of values (Hardie, 1996) believed to have existed throughout the scleractinian corals' existence (Fig. 1). To differentiate between the effects of Mg/Ca ratio and absolute concentration of Ca^{2+} on coral growth, three additional seawaters were formulated with Ca^{2+} concentrations fixed at 14.1 mmol kg-SW^{-1} and Mg/Ca ratios of 1, 3.5 and 5.2.

5.1 Effect of seawater Mg/Ca on scleractinian coral mineralogy

Backscatter electron imaging (Fig. 17) and X-ray diffraction of new skeletal growth revealed that the three species of corals each secreted approximately one-third of their skeleton as low Mg calcite (Fig. 18a) when grown in the low Mg/Ca experimental calcite seawater (Mg/Ca = 1.0). As seawater Mg/Ca increased towards the aragonite stability field, the proportion of calcite within the coral skeletons decreased (Fig. 18a). Concentrations of Sr and Mg in the corals' skeletons were mapped to approximate the distribution of aragonite and calcite, respectively (Fig. 17).

Notably, the Mg/Ca ratio of the calcite secreted by the corals increased proportionally with the Mg/Ca ratio of the experimental seawater, such that low Mg calcite
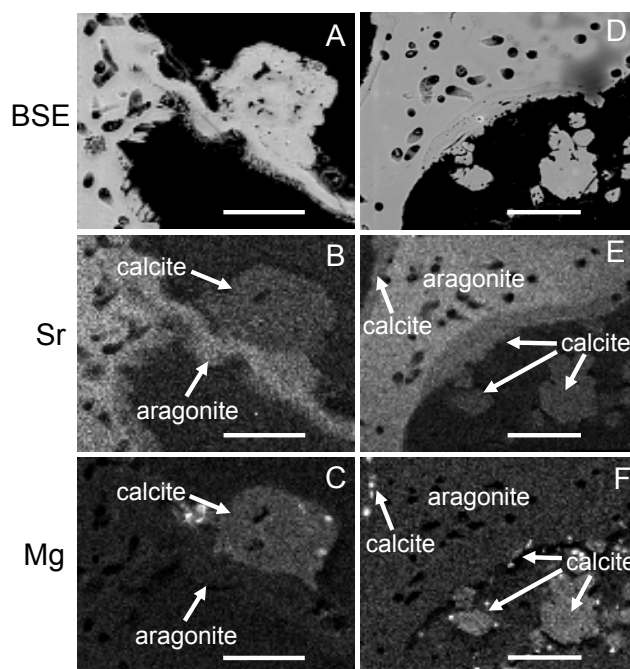

Fig. 17. Backscatter electron images (**A**, **D**), Sr/Ca maps (**B**, **E**) and Mg/Ca maps (**C**, **F**) showing, respectively, skeletal microstructure, aragonite, and calcite in two specimens of *Porites cylindrica* (A–C, D–F) reared for 60 days in experimental seawater that favors the abiotic precipitation of calcite over aragonite (Mg/Ca = 1.0). Light areas (molar Sr/Ca = 0.011–0.016) of the Sr/Ca maps (B, E) correspond to aragonite in the coral skeleton, while dark areas (molar Sr/Ca = 0.001–0.005) correspond to calcite. Light areas (molar Mg/Ca = 0.03–0.04) of the Mg/Ca maps (C, F) correspond to calcite in the coral skeleton, while dark areas (molar Mg/Ca = 0.004–0.008) correspond to aragonite. Aragonite typically incorporates about an order of magnitude more Sr^{2+} in its crystal lattice than does calcite, while calcite incorporates about one order of magnitude more Mg^{2+} in its crystal lattice than does aragonite. These characteristics make Sr/Ca and Mg/Ca reliable proxies for mapping the distribution of aragonite and calcite, respectively, within coral skeletons. Scale bars are 100 μm. From Ries et al. (2006).

(Mg/Ca < 0.04) was secreted in seawater of Mg/Ca < 2, and high Mg calcite (Mg/Ca > 0.04) was secreted in seawater of Mg/Ca > 2 (Fig. 18b). This relationship is consistent with that observed for Mg incorporation in calcite secreted by four species of reef-dwelling animals (echinoids, crabs, shrimp, serpulid worms; Ries, 2004), coralline red algae (Ries, 2006b; Stanley et al., 2002), some species of coccolithophores (Stanley et al., 2005), and the calcareous green alga *Halimeda* (Stanley et al., 2010). The Mg/Ca ratio of the aragonite secreted by the corals, which was roughly one-tenth the magnitude of the Mg/Ca ratio of the calcite secreted by the corals, also increased with seawater Mg/Ca (Fig. 18b).

It has been proposed that organic matter detected within the centers of calcification of scleractinian corals (up to 1% by volume) is a vestige of the organic matrices and templates
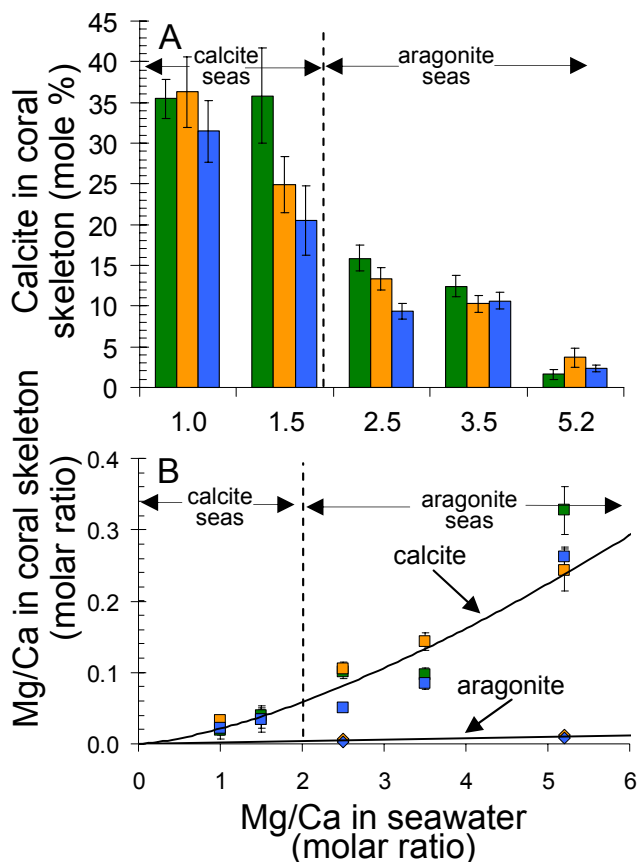
Fig. 18. Mineralogy and geochemistry of *Acropora cervicornis*, *Montipora digitata*, and *Porites cylindrica* reared in experimental seawaters with Mg/Ca ratios ranging from 1.0 to 5.2 (from Ries et al., 2006). **(A)** Molar percentage of calcite in coral skeletons versus Mg/Ca ratio of experimental seawater. Green bars = *A. cervicornis*, orange bars = *M. digitata*, and blue bars = *P. cylindrica*. **(B)** Mg/Ca ratio of calcitic (green squares = *A. cervicornis*, orange squares = *M. digitata*, and blue squares = *P. cylindrica*) and aragonitic (orange diamonds = *M. digi*tata, blue diamonds = *P. cylindrica*) portions of coral skeleton. Solid black lines represent Mg fractionation curves for coral calcite ($Mg/Ca_C=0.02129Mg/Ca_{sw}^{1.4628}$, $R^2=0.9458$, $n=43$) and coral aragonite ($Mg/Ca_C=0.002007Mg/Ca_{sw}$, $R^2=0.7537$, $n=43$), calculated using least squares regressions. Error bars correspond to instrument error plus specimen variation. Mg/Ca<2 = calcite seas; Mg/Ca>2 = aragonite + high Mg calcite seas.

that specify nucleation of the aragonite polymorph (Cuif et al., 1999). That the corals grown in the experimental seawater with a Mg/Ca ratio favoring the inorganic precipitation of low Mg calcite still precipitated two-thirds of their skeleton as aragonite supports the hypothesis that corals do exert significant control over their skeletal mineralogy (Cuif et al., 1999). However, the discovery that scleractinian corals precipitate approximately one-third of their skeleton as low Mg calcite, instead of aragonite, in the experimental calcite seawater suggests that CaCO$_3$ polymorph control within certain

portions of the coral skeleton can be partially overridden by ambient seawater chemistry.

Additional evidence that scleractinians are limited in their mineralogical control is their tendency to incorporate Mg, as observed in this study, and other trace elements (Cohen and McConnaughey, 2003), into their skeletons in proportions that reflect their abundance in seawater. Furthermore, the acicular morphology and spherulitic organization of the aragonitic crystals in the sclerodermites of coral skeletons closely resembles the spherulitic aragonite that forms inorganically in marine cements, suggesting that they could be deposited in a manner similar to that of abiotic precipitation (Barnes, 1970).

Seawater reaches the coral's region of calcification, beneath the calicoblastic ectoderm, by moving through cells, between cells, and by diffusion through the porous skeleton. An ATPase pump elevates Ca^{2+} in the region of calcification only slightly above the level of ambient seawater (Al-Horani et al., 2003), thereby suggesting that corals precipitate their skeletons from a medium with a Mg/Ca ratio that is very similar to that of ambient seawater. The accelerated precipitation rate of the coral skeleton, nearly 100 times that of inorganic CaCO$_3$ precipitation (Cohen and McConnaughey, 2003), can instead be attributed to the pumping of protons from the calcification medium (Al-Horani et al., 2003). It therefore seems reasonable that the Mg/Ca ratio of ambient seawater would have a significant effect on the chemistry of the coral's calcification medium, and therefore on its skeletal polymorph mineralogy.

Additionally, there is a secondary mode of calcification in scleractinians that occurs beneath the coral's ectoderm-bounded calcification space that fills pore spaces formerly occupied by living tissue. In modern scleractinians, this secondary growth is aragonite but its morphology, organization and trace element chemistry differs from that of the primary skeleton secreted (Enmar et al., 2000). Ries et al. (2006) hypothesized that the mineralogy of these secondary crystals is determined solely by the Mg/Ca ratio of the ambient seawater, and that these crystals may account for the relatively large amount of calcite produced by the scleractinians in the lower Mg/Ca experimental seawaters.

The discovery that coral skeleton polymorph mineralogy varies with the Mg/Ca of seawater suggests that scleractinian corals may have secreted at least part of their skeleton as low Mg calcite in the calcite seas of Late Cretaceous and early Cenozoic time, when they existed as isolated colonies and did not build the massive, widespread reefs that they do today. This is supported by recent geochemical and petrographic analyses of fossil scleractinia from the Cretaceous Period, which suggest that some species of scleractinian corals produced largely calcitic skeletons during calcite seas of the geologic past (Stolarski et al., 2007).

The tendency for both the aragonitic and calcitic portions of the coral skeletons to incorporate Mg in proportion to its abundance in seawater suggests that the Mg/Ca

of fossil corals (Mg/Ca in calcite = Mg/Ca_C; Mg/Ca in aragonite = Mg/Ca_A) may be an archive of past oceanic Mg/Ca (Mg/Ca_{sw}) throughout their geologic record. Mg fractionation algorithms for coral calcite and aragonite were derived from the experiments on the three scleractinian species:

$$Mg/Ca_A = 0.002007(Mg/Ca_{sw}) \text{ (aragonite)}; \qquad (1)$$

$$Mg/Ca_C = 0.02129(Mg/Ca_{sw})^{1.4628} \text{ (calcite)}. \qquad (2)$$

These algorithms were combined with temperature-based Mg fractionation algorithms (species-normalized; Chave, 1954):

$$Mg/Ca_A = 0.0003227T + 0.002430 \text{ (aragonite)}; \qquad (3)$$

$$Mg/Ca_C = 0.004453T + 0.07004 \text{ (calcite)}. \qquad (4)$$

to yield single algorithms that define the Mg/Ca ratio of skeletal aragonite and calcite as a function of the Mg/Ca ratio (Mg/Ca_{sw}) and temperature (T) of seawater, and a species coefficient (S) equal to the skeletal Mg/Ca of a wild representative of the given species in nature, which secreted $CaCO_3$ at Mg/Ca_{sw}=5.2 and some known temperature, divided by the skeletal Mg/Ca predicted by the algorithm for Mg/Ca_{sw}=5.2 and the given temperature:

$$Mg/Ca_A = S[0.00006244(T)(Mg/Ca_{sw})$$
$$+0.0004702(Mg/Ca_{sw})] \text{ (aragonite)}; \qquad (5)$$

$$Mg/Ca_C = S[0.0005227(T)(Mg/Ca_{sw}^{1.4628})$$
$$+0.008222(Mg/Ca_{sw}^{1.4628})] \text{ (calcite)}. \qquad (6)$$

These algorithms could theoretically be used to calculate historical oceanic Mg/Ca ratios from the skeletal Mg/Ca and paleoenvironmental temperature of unaltered coral fossils. Likewise, paleotemperature reconstructions based on the Mg/Ca ratio of fossil coral skeletons must correct for the effect of seawater Mg/Ca on skeletal Mg/Ca (Hart and Cohen, 1996; Mitsuguchi et al., 1996).

5.2 Effect of seawater Mg/Ca on calcification rates within scleractinian corals

Each of the three species of scleractinian corals grew fastest in the aragonite seawater treatments (Fig. 19a). There was a significant decrease in growth rates when seawater crossed into the calcite nucleation field (Mg/Ca<2). The slow growth rates for corals in the experimental calcite seawater is likely due to difficulties in precipitating aragonite, which still formed roughly two-thirds of their skeleton in this medium, from seawater that favors the nucleation of calcite (Ries et al., 2006).

These results support the empirical evidence that the Early Cretaceous through Early Oligocene hiatus of the aragonitic scleractinians' reign as primary reef builders from Late Triassic through present time (Frost, 1977, 1981; Stanton
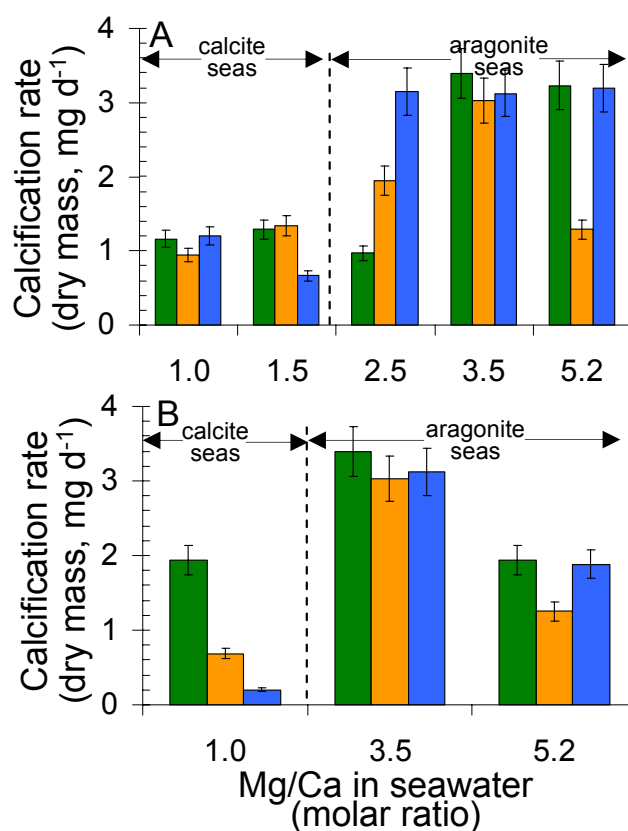

Fig. 19. Calcification rates of *Acropora cervicornis* (green bars, n=60), *Montipora digitata* (orange bars, n=60), and *Porites cylindrica* (blue bars, n=60) reared in eight chemically unique experimental seawater treatments (from Ries et al., 2006). **(A)** Calcification rates versus Mg/Ca ratio of experimental seawater. Ca^{2+} concentration of seawater decreases as Mg/Ca increases. **(B)** Calcification rates versus Mg/Ca ratio of seawater treatments. Ca^{2+} concentration held constant at $14.1 \, \text{mmol kg-SW}^{-1}$ in all three treatments, to isolate the effect of Mg/Ca ratio on coral growth rates. Error bars correspond to instrument error plus specimen variation. Mg/Ca<2 = calcite seas; Mg/Ca>2 = aragonite + high Mg calcite seas.

and Flügel, 1987; Stanley and McRoberts, 1993; Bernecker, 1996), was caused at least in part by a drop in oceanic Mg/Ca over this interval such that seawater no longer favored the precipitation of the scleractinians' inherently aragonitic mineralogy (Stanley and Hardie, 1998, 1999). Such depressed growth rates over this interval would have opened up low-latitude benthic marine environments to the bi-mineralic rudist bivalves, which were important carbonate producers throughout most of the Cretaceous Period (Scott, 1984; Kauffman and Johnson, 1988). However, the scleractinians did not resume their role as primary reef builders until early in Oligocene time (Frost, 1977, 1981), long after the decline of the rudists, when seawater Mg/Ca ratios had risen back into the aragonite stability field. Significantly, the highest growth rates for the scleractinians in this experiment occurred not in modern seawater (Mg/Ca=5.2), but rather

in seawater with a Mg/Ca=3.5. This is consistent with the dramatic resurgence of the scleractinians in Early Oligocene time, when the Mg/Ca of seawater was between 3 and 3.5. Ries et al. (2006) hypothesize that the occurrence of maximum growth rates in seawater with Mg/Ca=3.5 resulted from the optimal combination of elevated [Ca^{2+}], relative to modern seawater, along with Mg/Ca ratios that were well within the aragonite stability field.

Stanley and Hardie's (1998, 1999) calcite-aragonite sea hypothesis is somewhat problematical for the calcite sea interval of Early Cretaceous time because (1) the aragonite-secreting scleractinia continued forming large reefs at this time and (2) the rudist bivalves formed shells that were predominantly aragonitic at this time (Steuber, 2002). This apparent flourishing of largely aragonite-secreting organisms in the calcite seas of Early Cretaceous time suggests either that the Mg/Ca ratios reported for this interval are not accurate or that major carbonate producers exhibited a delayed response to the putative reduction in seawater Mg/Ca that occurred in Jurassic through Early Cretaceous time.

5.3   Effect of absolute [Ca^{2+}] on calcification rates within scleractinian corals

Experimental seawater treatments were formulated at Mg/Ca ratios of 1.0, 3.5, and 5.2 and with absolute Ca^{2+} concentrations fixed at 14 mmol kg-SW^{-1} to differentiate between the effects of Mg/Ca and absolute Ca^{2+} on coral growth rates. Again, the corals exhibited maximum growth rates in seawater formulated at Mg/Ca=3.5, slightly decreased growth rates in seawater formulated at Mg/Ca=5.2, and minimum growth rates in seawater formulated at Mg/Ca=1.0 (Fig. 19b). The similarity between these results and those from the experiments with variable absolute Ca^{2+} suggests that, regardless of the absolute concentration of Ca^{2+}, 3.5 is the optimal Mg/Ca ratio of seawater for the production of scleractinian coral skeleton.

In pioneering experiments on the influence of Mg^{2+} and Ca^{2+} concentrations on coral biomineralization (Swart, 1980), specimens of *Acropora aquamosa*, *Pocillopora damicornis*, *Acropora cuneata* and *Porites lutea* were grown for 10 days in seawater with Mg^{2+} concentrations 100 and 200 mg/l higher than modern values and Ca^{2+} concentrations 100, 200, and 400 mg/l higher than modern values. Seawater Mg^{2+} concentrations significantly higher than that of modern seawater prevented new skeletal growth, while Ca^{2+} concentrations twice those of modern seawater resulted in reduced rates of growth. These results are consistent with the findings that coral growth rates decreased significantly in experimental seawaters formulated with low Mg/Ca ratios, relative to modern values. However, the short duration of these experiments and the anomalously high concentrations of Mg^{2+} and Ca^{2+} used – higher than have ever characterized Phanerozoic seawater – preclude interpretation of the results in the context of actual past marine conditions.

Other experiments on specimens of *Acropora* sp., *Stylophora pistillata*, *Acropora cervicornis* and *Acropora formosa* show that calcification rates increase as Ca^{2+} concentrations are elevated from approximately 20% to 80% of normal marine values (Chalker, 1976; Gattuso et al., 1998, 2000). At Ca^{2+} concentration above 80%, calcification rates level out and, in some cases, decline. However, these experiments do not adjust Mg^{2+} concomitantly with Ca^{2+}, and therefore do not control for the kinetic effects of ambient seawater Mg/Ca. When the observed variation in calcification rate is correlated with the implicit variation in the Mg/Ca ratio of the experimental seawaters, the results generally conform to those observed in the Ries et al. (2006) study. Furthermore, the short durations (2–2.5 h) of the experiments (Chalker, 1976; Gattuso et al., 1998) did not allow sufficient time for the corals to fully acclimate to the substantially altered ambient conditions, thereby limiting the biological significance of the results.

The Gattuso et al. (2000) experiment also revealed that the reduced calcification observed for the zooxanthellate scleractinian coral *Stylophora pistillata* reared under low-[Ca^{2+}] conditions was not accompanied by reduced photosynthesis. Thus, in contrast to some species of bryopsidalean (Ries, 2005a, 2006a, 2009; Stanley et al., 2010) and coccolithophorid algae (Stanley et al., 2005), calcification appears not to stimulate photosynthesis within zooxanthellate scleractinian corals.

Experiments have also shown that the CO$_3^{2-}$ concentration of seawater can limit the rate of coral calcification (e.g., Langdon et al., 2000; Marubini et al., 2003). Therefore, it is conceivable that the rapid ocean crust production and accompanying volcanism that characterized the Cretaceous Period would have elevated pCO$_2$ in the atmosphere and oceans and reduced the aragonite saturation state of seawater. One could therefore deduce that it was the reduced aragonite saturation state of seawater during Cretaceous time, and not the low oceanic Mg/Ca favoring the precipitation of calcite over aragonite, which resulted in the scleractinian hiatus over this interval. However, as discussed above, the rapid ocean crust production of the Cretaceous Period resulted in an enrichment in oceanic Ca^{2+} that would have mostly offset the accompanying decline in CO$_3^{2-}$ (Hardie, 1996; Berner, 1997; Demicco et al., 2005), thereby maintaining seawater near the 3–4 times aragonite supersaturation state that exists today.

5.4   Paleoecological implications of reduced and bi-mineralic scleractinian coral calcification

The apparent lability of coral skeletal polymorph mineralogy begs the question whether there is a biomechanical advantage for a coral skeleton built from aragonite needles versus one built from calcite rhombs. The obvious difference between the two skeletons concerns crystal packing and can be likened to the advantages of trabecular (low density) and cortical (high density) bone in vertebrates. Assuming that

calcitic rhombs would be more closely packed than aragonite needles, the calcitic skeletons would presumably be denser and, therefore, less successful at taking up space on the seafloor, which could be a significant disadvantage in the highly competitive, substrate-limited tropical reef environment. The increased density of the close-packed calcitic skeleton would likely make the coral's surface more resistant to abrasion from minor impact, such as that delivered by grazing parrotfish, while its overall skeleton would probably be more susceptible to major impacts, such as that associated with hurricane surf, which would result in cross-skeletal fractures propagating along the calcite rhombs' perfect cleavage planes. Conversely, coral skeletons built from aragonite would be more resistant to major fracturing, as propagating fractures would be interrupted by the spherulitic organization of the aragonitic sclerodermites, and less resistant to minor surficial abrasion due to lower skeletal density.

5.5 The rise of rudist bivalves and seawater Mg/Ca ratios

Stanley and Hardie (1998) hypothesized that seawater Mg/Ca would have most strongly influenced calcification within rapidly calcifying marine organisms – so-called hypercalcifiers, and within simple marine calcifiers. Bivalves – the class to which rudists belong – appear to be neither rapid nor simple calcifiers. They are thought to exercise relatively strong control over the composition of their calcifying fluid, as evidenced by the ability of certain bivalves to interlaminate aragonite and calcite within their shell and to deposit nacreous aragonite at the location of muscle attachment (Checa et al., 2007). Bivalves are also known to maintain the pH of their calcifying fluid (mantle fluid) at relatively low pH and reduced calcium carbonate saturation (pH=7.33–8.53 (Crenshaw, 1972; Wada, 1976)). Instead of inducing the nucleation of calcium carbonate by elevating the pH of their mantle fluid, as scleractinian corals do (Al-horani, 2003), they are thought to employ sophisticated organic templates to control the nucleation and distribution of calcium carbonate polymorphs (Watabe and Wilbur, 1960).

Thus, although the largely calcitic rudists thrived during the Cretaceous calcite sea interval, the strong control that bivalves are known to exert over their biomineralization casts doubt over the role that seawater Mg/Ca played in the rise of the rudists as primary calcium carbonate producers in Cretaceous time. Furthermore, the rudists initially secreted a predominantly aragonitic shell at the time of their origin in the Early Cretaceous, when seawater Mg/Ca is thought to have favored the nucleation of calcite.

However, Harper et al. (1997) showed that the familial diversity of predominantly aragonite-secreting bivalves was generally lower during calcite sea intervals than during aragonite sea intervals throughout Phanerozoic time. From this they concluded that predominantly aragonite-secreting

molluscs were at a selective disadvantage during calcite sea intervals.

Checa et al. (2007) reared three species of scallops (*Aequipecten opercularis*, *Chlamys varia*, *Pecten maximus*), two species of oyster (*Anomia ephippium*, *Ostrea edulis*), and one species of mussel (*Mytilus galloprovincialis*), each of which secretes predominantly the low Mg calcite form of $CaCO_3$ in experimental seawaters with Mg/Ca ratios formulated at the modern level (5.2) and at elevated levels (8.3–9.2). They found that bivalves reared under the elevated Mg/Ca conditions began secreting a greater proportion of aragonite along the interior portions of their shell, as well as more high Mg calcite along the marginal portion of their shell, than under the control conditions. However, workers have yet to conduct experiments to evaluate Harper et al.'s (1990) hypothesis that predominantly aragonite-secreting molluscs are at a selective disadvantage when seawater Mg/Ca supports the nucleation of low Mg calcite, which would require rearing predominantly aragonitic molluscs in experimental seawater formulated with a Mg/Ca<2. Future experimental studies on this subject are needed to elucidate the role that seawater Mg/Ca played in the evolution and biomineralization of molluscs throughout Phanerozoic time.

5.6 Conclusions – scleractinian corals

1. Scleractinian corals changed their skeletal mineral from aragonite in modern aragonite seawater to a mixture of approximately one-third low Mg calcite and two-thirds aragonite when grown in experimental calcite seawater – indicating that although corals do specify nucleation of the aragonite polymorph, this mineralogical control can be partially overridden by ambient seawater chemistry.

2. The polymorph mineralogy of portions of scleractinian corals' skeletons may have varied with seawater Mg/Ca throughout geologic time. It now seems conceivable that they would have produced at least part of their skeleton from low Mg calcite during the calcite seas of mid-Late Cretaceous time.

3. Scleractinian corals exhibit reduced rates of calcification relative to the control when grown in experimental calcite seawaters that do not favor precipitation of the coral's preferred aragonite mineral.

4. These results support the hypothesis that the scleractinian corals' hiatus from primary reef building in Early Cretaceous through Early Oligocene time may have been caused, at least in part, by the transition to calcite seas over this interval. Likewise, their reappearance in Early Oligocene time and continued dominance as reef builders through to the present may have been facilitated by the concomitant transition back to aragonite

seas, which favors the scleractinians' preferred arago-nitic mineralogy.

6 Coralline red algae

Coralline algae have been important producers of $CaCO_3$ in the oceans throughout most of Phanerozoic time (Wray, 1977). Branching corallines have been major contributors of carbonate sediments to lower energy back-reef and fore-reef environments while encrusting corallines have been impor-tant cementers of reefs on the high-energy reef crest (Alexan-dersson, 1977; James et al., 1988; Berner, 1990; Aguirre et al., 2000; Littler, 1973; Macintyre, 1997; Wray, 1977; Chisholm, 2003). In modern seawater with a Mg/Ca of 5.2, these algae produce exclusively high Mg calcite. However, it has been asserted that the Mg/Ca ratio of the calcite se-creted by these algae may have varied throughout geologic time in lock-step with secular variations in seawater chem-istry (Stanley and Hardie, 1998, 1999). This assertion was based on two sets of earlier observations: (1) that the Mg/Ca ratio of calcite secreted by coralline algae, along with a wide range of other calcite-secreting organisms, is strongly influ-enced by seawater temperature (Chave, 1954); and (2) that the Mg/Ca ratio of abiotically-precipitated calcite is deter-mined by the temperature and Mg/Ca ratio of the precipi-tating solution (Berner, 1975; Füchtbauer and Hardie, 1976, 1980; Mucci and Morse 1983; Morse et al., 1997). Here, I review two sets of experiments that were conducted to inves-tigate the effects of seawater Mg/Ca on Mg incorporation in the encrusting (Ries, 2006b) and branching (Stanley et al., 2002) coralline red algae.

Specimens of three branching species of coralline algae of the genus *Amphiroa* (*A. fragilissima* and two unknown species, *Amphiroa* A and *Amphiroa* B) and one encrusting species of the genus Neogoniolithon were grown for 100 days in experimental seawaters that were identical (Bidwell and Spotte, 1985) except for their Mg/Ca ratios, which were formulated at 1.0, 1.5, 2.5, 2.5, 5.2 and 7.0, thereby encom-passing the range of values thought to have existed through-out the algae's geologic history (1.0–5.2; Fig. 1; Hardie, 1996). To differentiate between the effects of Mg/Ca ratio and absolute Mg^{2+} concentration on skeletal Mg fractiona-tion in the encrusting coralline algae, a second set of exper-imental seawaters were formulated with Mg/Ca ratios of 1.0 and 5.2 and corresponding absolute concentrations of Mg^{2+} (and Ca^{2+}) that were lower and higher, respectively, than those employed in the first set of experimental seawaters that were formulated with corresponding Mg/Ca ratios.

6.1 Mg fractionation in coralline algal calcite

Specimens of the branching and encrusting specimens of coralline algae precipitated exclusively the calcite poly-morph in each of the experimental seawaters. Significantly,
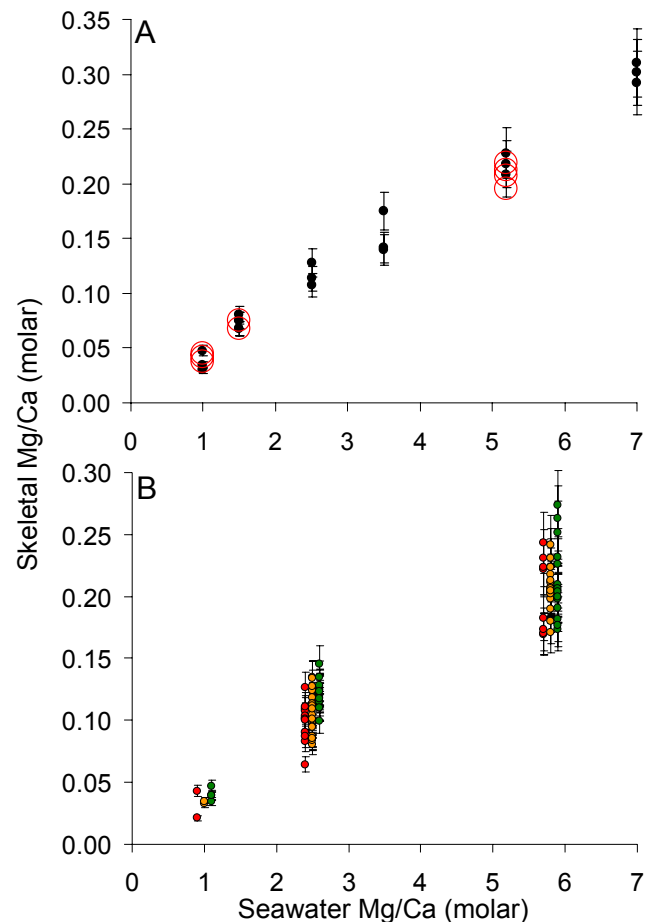

Fig. 20. Mg fractionation data for **(A)** the encrusting coralline alga *Neogoniolithon* sp. and for **(B)** the three species of branch-ing coralline algae *Amphiroa* A (closed red circles), *Amphiroa* B (closed orange circles), and *Amphiroa rigida* (closed green circles) reared in experimental seawater treatments formulated at Mg/Ca ra-tios ranging from 1.0 to 7.0 (from Ries, 2006b; Stanley et al., 2002). Skeletal Mg/Ca ratios increase in lock-step with seawater Mg/Ca ratios. Large open red circles in (A) correspond to skeletal Mg/Ca ratios for specimens of *Neogoniolithon* sp. reared in a second set of experimental seawaters with Mg/Ca ratios of 1.0, 1.5, and 5.2, that have reduced (1.0, 1.5) and elevated (5.2) absolute concentrations of Mg^{2+} and Ca^{2+}. Changes in the absolute Mg^{2+} concentration of seawater had no significant ($p < 0.05$) effect on algal skeletal Mg fractionation at fixed ambient Mg/Ca ratios.

however, the Mg/Ca of the calcite secreted by each of the four species of coralline algae declined proportionately with the Mg/Ca of the experimental seawater in which they were grown (Fig. 20). Specimens grown in seawater formulated with the lowest Mg/Ca ratio of 1.0 changed their mineral-ogy from high Mg to low Mg calcite (Mg/Ca<0.04). En-crusting coralline algae grown in the experimental seawaters with Mg/Ca ratios of 1.0 and 5.2 with reduced and elevated absolute Mg^{2+} concentrations, respectively, showed no sig-nificant differences in skeletal Mg/Ca ratios from the algae
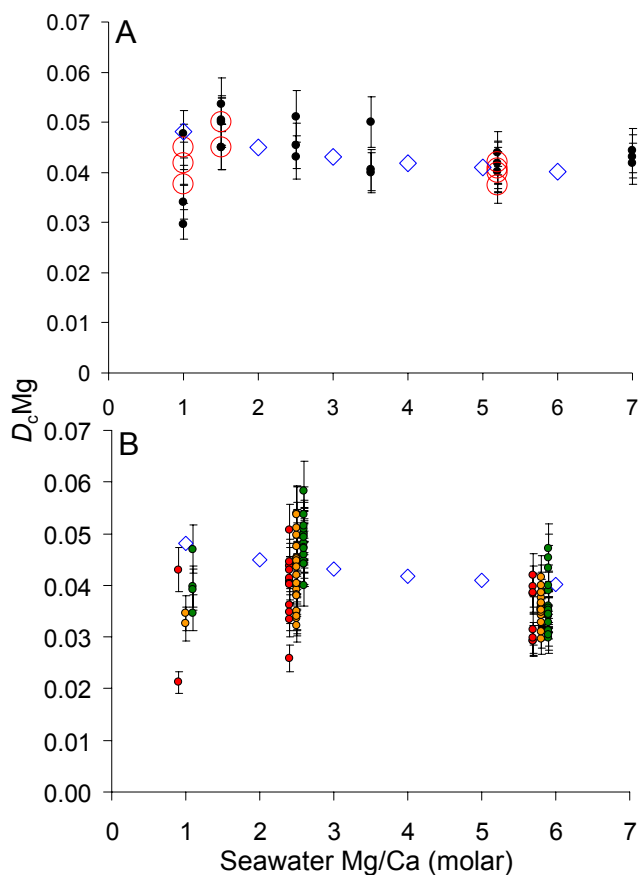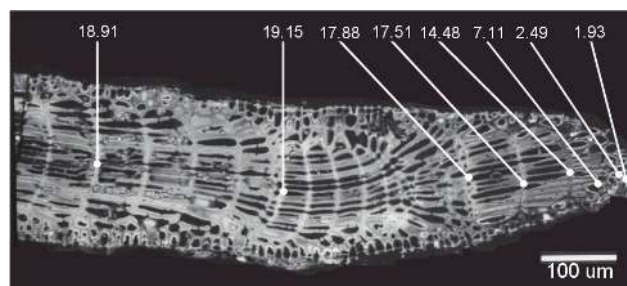
Fig. 22. Backscatter electron image of a longitudinal section through the tip of the branching coralline alga *Amphiroa* sp. A reared in seawater with the estimated Late Cretaceous Mg/Ca ratio of 1.0. Numbers are mole percentages of magnesium in substitution for calcium in cell wall calcite. Measurements are at junctures of four cells along cell rows, one of which is added daily. Percentages in the 17.51 to 19.15 range are for calcification in modern seawater. During 4 days of growth in the Late Cretaceous experimental seawater, the percentage of Mg progressively declined, ultimately reaching 1.93 (low Mg calcite; from Stanley et al., 2002).

Fig. 21. Mg fractionation coefficients (D_cMg) for **(A)** the encrusting coralline alga *Neogoniolithon* sp. and for **(B)** the three species of branching coralline algae *Amphiroa* A (closed red circles), *Amphiroa* B (closed orange circles), and *Amphiroa rigida* (closed green circles) reared in the experimental seawater treatments formulated at Mg/Ca ratios ranging from 1.0 to 7.0 (from Ries, 2006b; Stanley et al., 2002). D_cMg is calculated as Mg/Ca$_C$ divided by Mg/Ca$_{sw}$. Large open red circles in (A) correspond to D_cMg for the second set of experimental seawaters with Mg/Ca ratios of 1.0, 1.5, and 5.2 that have reduced (1.0, 1.5) and elevated (5.2) absolute concentrations of Mg^{2+} and Ca^{2+}, respectively. These results indicate that D_cMg varies with Mg/Ca$_{sw}$. However, changes in the absolute Mg^{2+} concentration of seawater had no significant ($p < 0.05$) effect on D_cMg when Mg/Ca$_{sw}$ was fixed with proportional elevations in [Ca^{2+}]. Large open blue diamonds correspond to the D_cMg of abiotic calcite (Füchtbauer and Hardie, 1976).

grown in seawater treatments formulated with corresponding Mg/Ca ratios and normal absolute Mg^{2+} concentrations (Fig. 20a).

Critically, Mg fractionation coefficients (D_cMg) calculated for both encrusting and branching coralline algae grown in the various experimental seawaters varied with seawater Mg/Ca (Fig. 21). Excluding the lowest seawater Mg/Ca condition (Mg/Ca=1), D_cMg generally decreased as Mg/Ca$_{sw}$ increased.

The proportionality between the Mg/Ca of the algal calcite and the Mg/Ca of experimental seawater indicates that the Mg content of the calcite produced by both branching and encrusting coralline red algae is variable, and that this variability can be driven by ambient seawater chemistry (Fig. 20). The similarity between the Mg/Ca ratios of algae grown in the two sets of experimental seawaters of identical Mg/Ca ratios (1.0 and 5.2) and differing absolute concentrations of Mg^{2+} reveals that the incorporation of Mg in algal calcite is, in fact, determined by the Mg/Ca ratio of seawater, rather than the absolute concentration of Mg^{2+} in seawater.

This proportionality between the Mg/Ca of the algal calcite and the Mg/Ca of the experimental seawaters (Fig. 20) also suggests that the Mg content of branching and encrusting coralline algae has fluctuated along with seawater Mg/Ca throughout Phanerozoic time. Furthermore, the production of low Mg calcite in experimental seawater with Mg/Ca=1 suggests that these algae, which produce exclusively high Mg calcite in modern seawater (Mg/Ca=5.2), probably produced low Mg calcite in middle and Late Cretaceous seas, when Mg/Ca ratios are believed to have been near unity.

A backscatter electron image of a longitudinal section through the tip of the branching coralline alga *Amphiroa* sp. (Fig. 22) reveals that skeletal mole-% MgCO$_3$ progressively declined from 19% (i.e., high Mg calcite) to 2% (i.e., low Mg calcite) over a four day period following immersion of the alga in the experimental calcite seawater (Mg/Ca=1.0).

Backscatter electron images of the *Neogoniolithon* sp. algae reveal that specimens grown in the low Mg/Ca experimental seawater (Mg/Ca=1.5; Fig. 23a–i) produced a more heavily calcified and less organized skeleton than algae grown in the high Mg/Ca experimental seawater (Mg/Ca=5.2; Fig. 23j–l), which produced well-defined cell
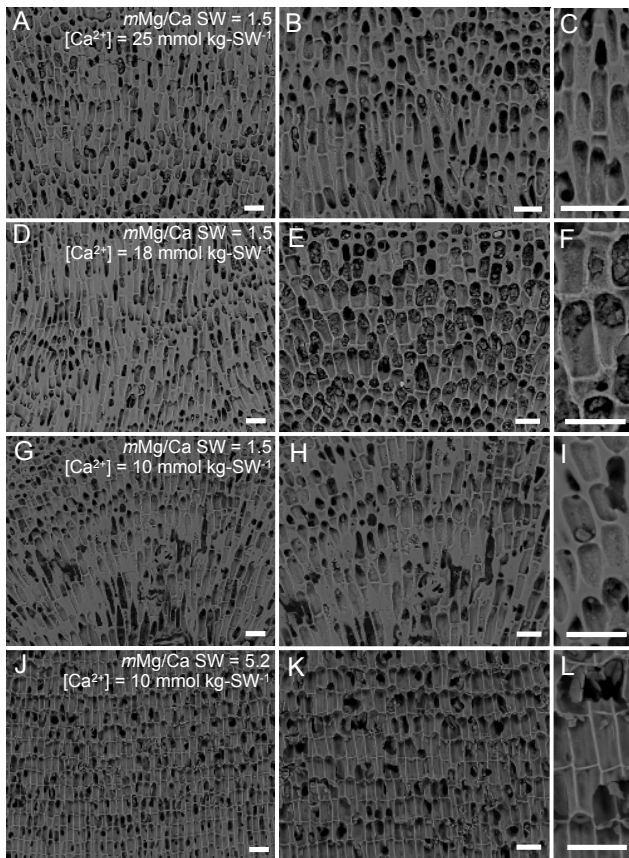
Fig. 23. Backscatter electron images of specimens of the encrusting coralline alga *Neogoniolithon* sp. reared in experimental seawaters with Mg/Ca ratios and absolute Ca^{2+} concentrations (mmol kg-SW^{-1}), respectively, of 1.5 and 25 (**A–C**), 1.5 and 18 (**D–F**), 1.5 and 10 (**G–I**), and 5.2 and 10 (equivalent to modern seawater, **J–L**). Specimens reared in the low Mg/Ca seawaters (1.5, A–I), which favor the algae's inherently calcitic skeletal mineral, produced an apparently more heavily calcified and less organized skeleton than did specimens reared in the modern, high Mg/Ca seawater, which naturally favors the precipitation of aragonite. Changes in the absolute concentration of Ca^{2+}, for specimens reared in experimental seawaters with Mg/Ca ratios fixed at 1.5 (A–I), appear to have little effect on skeletal thickness and organization, suggesting that, for the range of values evaluated in this study, the ambient Mg/Ca ratio is more important than the $CaCO_3$ saturation state of seawater in influencing rates of algal calcification. Scale bar is 20 μm. From Ries (2006b).

layers that were so weakly calcified that some appear to be shattered. The elevated rates of calcification evident for algae grown in the experimental calcite seawaters (Fig. 23a–i) may disrupt their normally well ordered daily growth bands, resulting in a more chaotically organized skeletal ultrastructure. Backscatter images of algae grown in experimental seawaters formulated at a fixed Mg/Ca ratio (1.5) and differing absolute concentrations of Ca^{2+} (10, 18, 25 mmol kg-SW^{-1}; Fig. 23a–i) revealed no major differences in either skeletal organization or thickness.

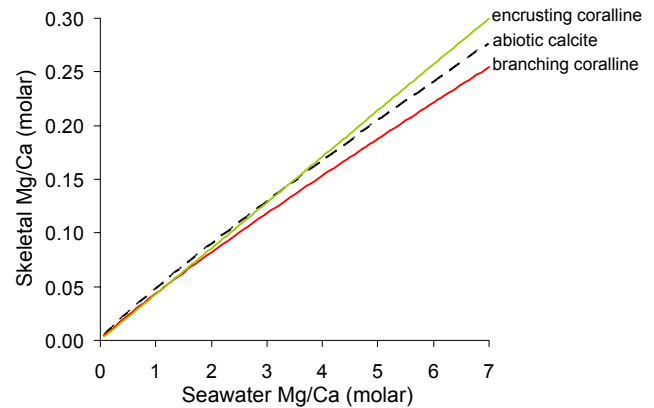**Fig. 24.** Experimentally derived Mg fractionation curves for the encrusting coralline alga *Neogoniolithon* sp. (solid green curve; $Mg/Ca_C = 0.0421 Mg/Ca_{sw}^{1.01}$), for the three species of branching coralline algae *Amphiroa* A, *Amphiroa* B, and *Amphiroa rigida* (averaged; solid red curve; $Mg/Ca_C = 0.0582 Mg/Ca_{sw}^{0.904}$), and for abiotically precipitated calcite (dashed black curve; $Mg/Ca_C = 0.0482 Mg/Ca_{sw}^{0.898}$; Füchtbauer and Hardie, 1976). This reveals that Mg fractionation within coralline algae generally mimics that of abiotic calcification. Mg fractionation curves were calculated using least squares regressions. From Ries (2006b).

The *Neogoniolithon* and *Amphiroa* genera investigated in the studies reviewed here belong to the Corallinacean family, a member of the Rhodophyte phylum that is believed to have originated in Early Cretaceous time (Fig. 1). However, a closely related family of coralline Rhodophytes, known as the Solenoporacean algae, was an important contributor to shelf, reefal, and bioherm carbonates throughout Paleozoic and Mesozoic time. In fact, the Solenoporaceae's similar morphology, environmental distributions, and mineralogy (calcite) relative to the Corallinaceae (Wray, 1977) has led to them being invoked, somewhat controversially (Aguirre et al., 2000), as potential ancestors of the Corallinaceae. Regardless of the phylogenetic relationship between the more recent Corallinaceae and the older Solenoporaceae, their similar morphologies, modes of calcification, and mineralogies suggest that the findings of these experiments on Mg fractionation within the *Amphiroa* and *Neogoniolithon* algae can probably be extrapolated back for most calcite-secreting benthic marine macroalgae, and the limestones that they formed, throughout Phanerozoic time.

6.2 Implications for biomineralogical control within the coralline red algae

The Mg fractionation curves derived for the encrusting (*Neogoniolithon*) and branching coralline red algae (*Amphiroa*) are strikingly similar to that for abiotically produced calcite (Füchtbauer and Hardie 1976; Mucci and Morse 1983; Fig. 24), thereby suggesting that these algae are merely inducing the precipitation of calcite by removing CO_2 via

photosynthesis. However, the algae's precipitation of high Mg calcite from the experimental seawater formulated at a Mg/Ca ratio of 7.0, which favors the abiotic precipitation of the aragonite polymorph (Füchtbauer and Hardie, 1976), suggests that the algae are actively specifying nucleation of the calcite polymorph. However, the algae's abiotic pattern of Mg incorporation suggests that its mineralogical control is limited to polymorph specification and that it is unable to regulate Mg fractionation, which appears to be driven largely by ambient seawater chemistry and temperature.

It is intriguing that the Mg fractionation curve for the branching coralline algae *Amphiroa* sp. (Stanley et al., 2002) is slightly lower than the Mg fractionation curve generated in this study for the encrusting coralline algae (Fig. 24). This suggests that the branching *Amphiroa* algae are slightly more adept at excluding Mg from their skeletal calcite crystal lattice than the encrusting *Neogoniolithon* algae, which is perhaps indicative of enhanced biomineralogical control within the *Amphiroa* genus.

The relationship between Mg/Ca ratios of the coralline algal calcite and the experimental seawater is also generally consistent with the experiments reviewed above regarding Mg fractionation within calcite secreted by the *Halimeda* algae (Stanley et al., 2010), by two species of coccolithophores (Stanley et al., 2005), and by three species of scleractinian corals (Ries et al., 2006). The similarity amongst patterns of Mg-fractionation in calcite secreted by coralline red algae, coccolithophores, calcareous green algae, and scleractinian corals are intriguing given that these organisms employ substantially different modes of calcification (Milliman, 1974). Coralline red algae induce precipitation of $CaCO_3$ within their cell walls, coccolithophores precipitate $CaCO_3$ within intracellular vesicles, and calcareous green algae and scleractinian corals induce precipitation of $CaCO_3$ completely extracellularly (corals precipitate $CaCO_3$ between their skeleton and their inner ectoderm while calcareous green algae precipitate $CaCO_3$ within spaces bounded by their adjacent utricles).

The inverse relationship observed between D_cMg and Mg/Ca$_{sw}$ (when the D_cMg value at Mg/Ca$_{sw}$=1.0 is excluded) is consistent with other studies on Mg fractionation in biogenic calcite (Stanley et al., 2002; Ries, 2004). The inverse nature of this relationship suggests that the algae are less efficient at excluding Mg from their skeletal calcite when the ambient concentration of Mg^{2+} is low relative to Ca^{2+}. As the relative Mg^{2+} concentration increases, the organisms appear to become more efficient at excluding it. However, the identification of this inverse proportionality between D_cMg and Mg/Ca$_{sw}$ in abiogenic Mg-calcite (Füchtbauer and Hardie, 1976; Mucci and Morse, 1983) suggests that the comparable relationship observed in the algae may simply be an abiotic consequence of calcification and, therefore, of little biological significance.

The biological consequences of Mg incorporation in calcite secreted by coralline algae are not well understood

(Milliman et al., 1971). The size differences between the Mg^{2+} and Ca^{2+} cations in the Mg calcite crystal lattice may reduce crack propagation relative to the homogeneous crystal lattice of pure calcite (Magdans and Gies, 2004). However, Mg^{2+} has also been shown to slow abiotic calcite crystal growth and reduce the unit cell volume of skeletal calcite (Bischoff et al., 1983; Mackenzie et al., 1983; Tribble et al., 1995; Davis et al., 2000, 2004), suggesting that Mg-incorporation in biogenic calcite may reduce an organism's rate of skeletal accretion.

6.3 Paleoenvironmental reconstructions from fossil coralline red algae

The branching and encrusting coralline algae's well-defined growth bands, widespread distribution, long life spans, and ubiquity in carbonate rocks throughout Phanerozoic reefal limestones (Wray, 1977) have identified them as potential paleoenvironmental indicators (Halfar et al., 2000). Specifically, the relationship observed in this study between the Mg/Ca ratio of coralline algal calcite and ambient seawater suggests that fossil coralline algae may be an archive of oceanic Mg/Ca.

The relationship between seawater Mg/Ca (Mg/Ca$_{sw}$) and algal Mg/Ca (Mg/Ca$_C$) can be quantified with the following algorithms (Fig. 24):

$$Mg/Ca_C = 0.0582 Mg/Ca_{sw}^{0.904} \text{ (branching coralline algae)} \quad (7)$$

$$Mg/Ca_C = 0.0421 Mg/Ca_{sw}^{1.01} \text{ (encrusting coralline algae)} \quad (8)$$

However, the Mg/Ca of coralline algal calcite is also known to vary as a function of ambient seawater temperature (Chave, 1954). This relationship, when calibrated for *Amphiroa* sp. (branching coralline algae) and *Neogoniolithon* sp. (encrusting coralline algae), can be quantified as follows:

$$Mg/Ca_C = 0.0825 e^{0.0457T} \text{ (branching coralline algae)} \quad (9)$$

$$Mg/Ca_C = 0.0709 e^{0.0457T} \text{ (encrusting coralline algae)} \quad (10)$$

The Mg/Ca$_{sw}$- and T-based Mg fractionation algorithms can be solved simultaneously at Mg/Ca$_{sw}$=5.2 to yield unified Mg fractionation algorithms for the branching and encrusting coralline algae that vary as a function of both temperature and seawater Mg/Ca:

$$Mg/Ca_C = 0.0186 e^{0.0457T} Mg/Ca_{sw}^{0.904}$$

(branching coralline algae) \quad (11)

$$Mg/Ca_C = 0.0134 e^{0.0457T} Mg/Ca_{sw}^{1.01}$$

(encrusting coralline algae) \quad (12)

Therefore, as long as one of these paleoenvironmental variables is know for the fossil alga, then the other variable (temperature or seawater Mg/Ca) can be calculated.

High Mg calcite is notorious for its rapid loss of Mg during even the early stages of diagenesis. Therefore, one of the greatest challenges in using fossil Mg/Ca to infer oceanic Mg/Ca is the identification of carbonate material that has retained its original Mg content. Diagenetic conditions do exist that stabilize high Mg calcite, as demonstrated in recent studies that deduced ancient oceanic Mg/Ca ratios from the Mg content of well preserved fossil echinoderms from throughout Phanerozoic time (Dickson, 2002, 2004). Additionally, the closed-system diagenetic conversion of coralline algae's high Mg calcite to low Mg calcite frequently results in the local precipitation of dolomite rhombs within the fossil algae (Schlanger, 1957). Therefore, assuming that all of the Mg in the original skeleton is retained in the precipitation of the dolomite, the volume of that dolomite relative to the volume of the original fossil should provide an approximation of the original Mg content of the encrusting coralline alga.

It should be noted that the accuracy of ancient chemical and temperature reconstructions from the Mg content of fossil encrusting coralline algae will be reduced by factors such as open system diagenesis (in which Mg is lost from the fossil), species-specific Mg fractionation, fluctuations of other cations in seawater that influence Mg partitioning in the algal calcite, and regional variations in the growth rate of coralline algae (caused by differences in seawater temperature, irradiance, carbonate ion concentration, etc.) that are known to influence Mg-fractionation within algal calcite (Moberly, 1968; Agegian, 1985; and Mackenzie and Agegian, 1989).

6.4　Conclusions – coralline red algae

1. The Mg/Ca ratio of calcite produced by coralline algae of the genera *Neogoniolithon* and *Amphiroa* varies proportionally with the Mg/Ca ratio of ambient seawater. Therefore, the skeletal Mg/Ca ratios of these important reef cementing and carbonate sediment producing algae should have tracked secular changes in the Mg/Ca ratio of seawater throughout the Phanerozoic Eon. First-order reconstructions of oceanic Mg/Ca ratios or paleotemperatures can potentially be made from the Mg content of well-preserved fossils of these coralline algae, given that one of these variables is known for the seawater in which the fossilized algae originally lived.

2. The Mg fractionation curves for calcite produced by the *Neogoniolithon* and *Amphiroa* algae are nearly identical to the Mg fractionation curve for abiotically precipitated calcite. This suggests that the *Neogoniolithon* and *Amphiroa* algae exercise little or no influence over the incorporation of Mg into their skeletons. Their biomineralogical control is apparently limited to the specification of the calcite polymorph over the aragonite polymorph, as evidenced by their exclusive production of calcite even in experimental seawater that favors the abiotic precipitation of aragonite (Mg/Ca=7.0).

3. The coralline algae *Neogoniolithon* and *Amphiroa* begin producing low Mg calcite in experimental seawater formulated with a Mg/Ca ratio of 1.0. This suggests that these coralline algae, which produce exclusively high Mg calcite in modern aragonite seas (Mg/Ca=5.2), probably produced low Mg calcite during calcite seas of middle to Late Cretaceous time, when seawater Mg/Ca ratios were near unity (Hardie, 1996; Lowenstein et al., 2001, 2003). This assertion may also be applicable to the solenoporacean algae, possible ancestors of the Corallinaceae, which have geologic ranges spanning the calcite seas of both the Cretaceous and the Cambrian through middle Mississippian intervals.

7　High Mg calcite-secreting animals

The coralline red algae and coccolithophores are not the only modern, high Mg calcite secreting organisms whose Mg content may have fluctuated in synchroneity with seawater Mg/Ca. Chave (1954) observed that the Mg content of more than twenty species of high Mg calcite secreting marine organisms varied proportionally with seawater temperature, thus revealing that the Mg content of biogenic calcite can be influenced by the physicochemical properties of ambient seawater. Chave's (1954) observations, combined with experimental work showing that the Mg content of abiogenic calcite varies as a function of solution Mg/Ca (e.g., Kitano and Kanamori, 1966; Glover and Sippel, 1967; Katz, 1973; Füchtbauer and Hardie, 1976, 1980; Devery and Ehlmann, 1981; Mucci and Morse, 1983; Rimstidt et al., 1998; De Choudens-Sanchez and Gonzalez, 2009; Lee and Morse, 2010), led Stanley and Hardie (1998, 1999) to hypothesize that the Mg content of most high Mg calcite secreting marine organisms has varied with seawater Mg/Ca throughout the geologic past. Anticipating empirical support for this hypothesis, Dickson (2002, 2004) used the skeletal Mg/Ca of fossil echinoderms to reconstruct seawater Mg/Ca ratios throughout Phanerozoic time. This reconstruction assumed (1) that skeletal Mg/Ca varies with seawater Mg/Ca and (2) that this variation is linear and can therefore be defined with a single fractionation coefficient. Here, I review a series of experiments (Ries, 2004) that were conducted to investigate the relationship between seawater Mg/Ca and skeletal Mg/Ca for four species of high Mg calcite-secreting marine animals.

Four types of marine invertebrates that secrete high Mg calcite in modern seas – echinoids (*Eucidaris tribuloides*), crabs *(Perchon gibbesi)*, shrimps (*Palaemonetes pugio*) and calcareous serpulid worms (*Hydroides crucigera*) – were reared for 160 days in six experimental seawaters (Bidwell and Spotte, 1985) formulated with Mg/Ca ratios of 1.0, 1.5, 2.9, 4.4, 5.4, and 6.7. Temperature of the experimental seawaters was maintained at 25±1 °C. After growth in the experimental seawaters, the Mg/Ca ratios of the spines and
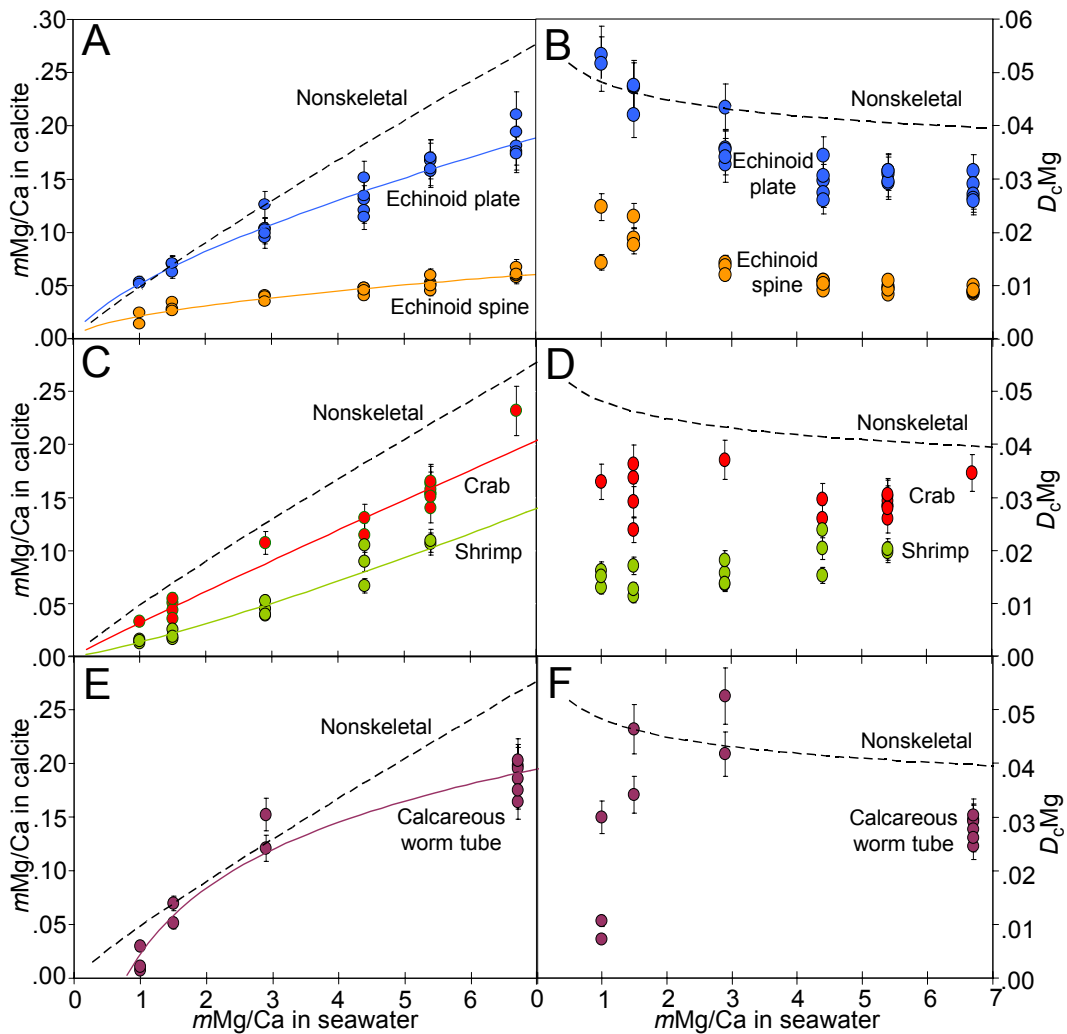
Fig. 25. Mg fractionation data for four calcite-secreting marine animals. **(A)** Mg fractionation curves for echinoid spines (*Eucidaris tribuloides*, closed orange circles, $Mg/Ca_C=0.0213Mg/Ca_{sw}^{0.538}$; $R^2=0.873$, $n=23$) and coronal plates (*Eucidaris tribuloides*, closed blue circles, $Mg/Ca_C=0.0516Mg/Ca_{sw}^{0.668}$; $R^2=0.959$, $n=23$). **(B)** Mg fractionation coefficients for echinoid spines (closed orange circles) and coronal plates (closed blue circles). **(C)** Mg fractionation curves for crabs (*Perchon gibbesi*, closed red circles, $Mg/Ca_C=0.0317Mg/Ca_{sw}^{0.956}$, $R^2=0.964$, $n=16$) and shrimp (*Palaemonetes pugio*, closed green circles, $Mg/Ca_C=0.0134Mg/Ca_{sw}^{1.21}$, $R^2=0.955$, $n=15$). **(D)** Mg fractionation coefficients for crabs (closed red circles) and shrimps (closed green circles). **(E)** Mg fractionation curve for calcareous serpulid worm tubes (*Hydroides crucigera*, closed purple circles, $Mg/Ca_C=0.0883 \ln(Mg/Ca_{sw})+0.0227$, $R^2=0.956$, $n=13$). **(F)** Mg fractionation coefficients for calcareous serpulid worm tubes (closed purple circles). For each of the animals investigated, skeletal Mg/Ca_C increased with Mg/Ca_{sw}. However, D_cMg was not fixed, as it also varied (non-linearly) with Mg/Ca_{sw}. Dashed black lines are Mg fractionation curves and coefficients for nonskeletal calcite (Füchtbauer and Hardie 1976). D_cMg is Mg fractionation coefficient equal to Mg/Ca_C divided by its corresponding Mg/Ca_{sw}. Mg fractionation curves are fit to data using least squares regression. Vertical bars represent uncertainty due to analytical error and specimen variation.

coronal plates of the pencil urchins, claws of the sally lightfoot crabs, tails of the grass shrimp, and tube sections of the serpulid worms (portions grown exclusively in the experimental seawaters) were measured with energy dispersive spectroscopy and confirmed with X-ray diffractometry.

7.1 Mg fractionation within shells of calcitic animals

Each of the four organisms incorporated less Mg into their skeletal calcite as the Mg/Ca of the experimental seawater decreased (Fig. 25a, c, e). Organisms grown in the experimental seawater of lowest Mg/Ca (1.0) changed their mineralogy to low Mg calcite ($Mg/Ca_C < 0.04$), while organisms grown in the experimental seawater of highest Mg/Ca_{sw} (5.2;

"modern" seawater) produced high Mg calcite – remaining within 3% of their pre-experimental Mg/Ca$_C$ ratios.

The production of low Mg calcite by each of the four organisms in the experimental seawater with Mg/Ca=1.0 suggests that these organisms, which produce high Mg calcite in modern seas, probably produced low Mg calcite in middle and Late Cretaceous seas, when Mg/Ca ratios are thought to have been near unity. This trend was also observed in similar studies on coccolithophorids (Stanley et al., 2005), coralline red algae (Stanley et al., 2002; Ries, 2006b), *Halimeda* algae (Stanley et al., 2010) and scleractinian corals (Ries et al., 2006). The wide variety of organisms that exhibit this proportionality between skeletal and seawater Mg/Ca suggests that this is a general trend for modern high Mg calcareous organisms.

Each type of organism investigated in this study produced a unique Mg fractionation curve. Even the spines and coronal plates within the same species of echinoid yielded unique fractionation curves (Fig. 24a). And each of these curves was lower than the experimentally determined curve for abiotic magnesian calcite (Füchtbauer and Hardie, 1976). This deviation of the biotic Mg fractionation curves from the abiotic curve suggests that these organisms influence, to varying degrees, the incorporation of Mg in their calcitic skeletons. However, ranking the organisms by increasing Mg content – echinoid spine, shrimp, crab-echinoid plate-worm – suggests that the degree of Mg fractionation is not, as previously suggested, linked to taxonomic complexity (Chave, 1954).

Calculation of Mg fractionation coefficients [D_cMg=(Mg/Ca$_C$)/(Mg/Ca$_{SW}$)] at various Mg/Ca$_{SW}$ ratios revealed that this coefficient varied with ambient Mg/Ca$_{SW}$ for each of the organisms investigated (Fig. 25b, d, f). D_cMg decreased for the echinoid spines – coronal plates and crabs as Mg/Ca$_{SW}$ increased (Fig. 25b, d). This result is consistent with other experiments on the coralline red algae (Stanley et al., 2002; Ries, 2006b) and abiotic magnesian calcite (Füchtbauer and Hardie, 1976; Mucci and Morse, 1983; De Choudens-Sanchez and Gonzalez, 2009). However, D_cMg values increased for the grass shrimps as Mg/Ca$_{SW}$ increased (Fig. 25d) and were scattered for the serpulid worm tubes (Fig. 25f). The discrepancies amongst the organisms may be attributable to differences amongst the organic templates thought to control crystal growth and/or differences in the mechanisms that transport Mg^{2+} and Ca^{2+} ions into or out of the organisms' calcifying fluids.

The high survival rate for these organisms in each of the seawater treatments suggests that the organisms were not severely stressed by the prescribed variations in concentrations of Mg^{2+} and Ca^{2+}. Bellis et al. (1987) showed that reduced levels of ambient Mg^{2+} (from 50 to 0 mmol kg-SW^{-1}) did not have significant effects on amino acid retention in sea urchin larvae, whereas Hayashi and Motokawa (1986) demonstrated that elevated Mg^{2+} levels increased tissue viscosity in echinoderms. However, this increase was observed at Mg^{2+} concentrations 2–5 times greater than

modern values, well above the range of concentrations evaluated in these experiments.

7.2 Ocean chemistry reconstructions from skeletal Mg/Ca of calcitic animals

The proportionality between the Mg/Ca of these animals' skeletons and the Mg/Ca of the seawater in which they were reared suggests that such animals should have recorded oceanic Mg/Ca throughout Phanerozoic time. Dickson (2002, 2004) innovatively employed a fixed D_cMg, derived from echinoderms in modern seawater at 25 °C, to reconstruct paleoceanic Mg/Ca from the Mg/Ca of fossil crinoid ossicles and echinoid plates. The presently reviewed study showed that this reconstruction can be improved by employing a Mg fractionation curve, instead of a fixed D_cMg, to convert skeletal Mg/Ca to seawater Mg/Ca. The effect of ancient seawater temperature on fossil Mg/Ca can also be corrected for in the reconstruction by using Chave's (1954) observations on the relationship between skeletal Mg fractionation and temperature.

Mg fractionation curves for echinoid plates, echinoid spines, crabs, serpulid worm tubes, coralline algae (Stanley et al., 2002), and nonskeletal calcite (Füchtbauer and Hardie, 1976) were species-normalized with a factor equal to Chave's (1954) average skeletal Mg/Ca of the given higher taxon at Mg/Ca$_{sw}$=5.2 and T=25 °C, divided by the skeletal Mg/Ca of the species in that taxon evaluated in this study at Mg/Ca$_{sw}$=5.2 and T=25 °C (Table 2). The species-normalization factors for the investigated echinoid plates, echinoid spines, crabs, serpulid worm tubes, and coralline algae are 0.913, 1.708, 0.868, 1.140, and 1.3297, respectively.

Temperature-dependent Mg fractionation curves were determined from Chave's (1954) and Füchtbauer and Hardie's (1976) data using least squares regressions (Table 2). The species-normalized Mg/Ca$_{sw}$-dependent Mg fractionation curves and temperature-dependent Mg fractionation curves were solved simultaneously at Mg/Ca$_{sw}$=5.2, thus yielding a single Mg fractionation algorithm varying as a function of temperature and Mg/Ca$_{sw}$ (Table 2). R^2-coefficients for the Mg fractionation algorithms for the echinoid plates, echinoid spines, crabs, serpulid worm tubes, coralline algae, and nonskeletal precipitates are 0.66, 0.77, 0.93, 0.94, 0.88, and 0.98, respectively.

The derived Mg fractionation algorithms can be used to calculate paleoceanic Mg/Ca ratios from well-preserved fossils of the investigated taxa. Although these Mg fractionation algorithms are normalized for the investigated species, they can be calibrated for other extant species with a species coefficient (S) equal to the skeletal Mg/Ca ratio of that species in the wild divided by the skeletal Mg/Ca ratio predicted by the algorithm for the temperature and Mg/Ca ratio (5.2) of the seawater in which the wild specimen lived (Table 2). However, the accuracy of the ancient seawater Mg/Ca calculations will be inherently limited for fossils whose Mg

Table 2. Algorithms relating Mg/Ca$_{sw}$, Mg/Ca$_C$, and temperature.

CaCO$_3$ source	Mg/Ca$_C$=f (Mg/Ca$_{sw}$) (species-normalized, T=25 °C)	Mg/Ca$_C$=$f(T)$ (Mg/Ca$_{sw}$=5.2)	Mg/Ca$_C$=f (Mg/Ca$_{sw}$, T)
Echinoid plate	Mg/Ca$_C$=0.0471 Mg/Ca$_{sw}$$^{0.668}$	Mg/Ca$_C$=0.00216 T+0.0876[a]	Mg/Ca$_C$=S(0.000719 T+0.0292) Mg/Ca$_{sw}$$^{0.668}$
Echinoid spine	Mg/Ca$_C$=0.0364 Mg/Ca$_{sw}$$^{0.538}$	Mg/Ca$_C$=0.00203 T+0.0375[b]	Mg/Ca$_C$=S(0.000837 T+0.0155) Mg/Ca$_{sw}$$^{0.538}$
Crab carapace	Mg/Ca$_C$=0.0275 Mg/Ca$_{sw}$$^{0.956}$	Mg/Ca$_C$=0.00299 T+0.0582[c]	Mg/Ca$_C$=S(0.000619 T+0.0120) Mg/Ca$_{sw}$$^{0.956}$
Serpulid worm	Mg/Ca$_C$=0.101 ln Mg/Ca$_{sw}$+0.0259	Mg/Ca$_C$=0.00463 T+0.0761[d]	Mg/Ca$_C$=S(0.00243 T+0.0399)(ln Mg/Ca$_{sw}$+0.257)
Coralline algae	Mg/Ca$_C$=0.0582 Mg/Ca$_{sw}$$^{0.904}$[e]	Mg/Ca$_C$=0.0825e$^{0.0457T}$[f]	Mg/Ca$_C$=S(0.0186e$^{0.0457T}$ Mg/Ca$_{sw}$$^{0.904}$)
Non-skeletal	Mg/Ca$_C$=0.0482 Mg/Ca$_{sw}$$^{0.898}$[g]	Mg/Ca$_C$=0.00672 T+0.0392[g]	Mg/Ca$_C$=(0.00158 T+0.00924) Mg/Ca$_{sw}$$^{0.898}$

Note: SW is seawater; C is calcite; T is temperature; S is species coefficient.
[a] Algorithm based on Chave's (1954) echinoid and crinoid data (R^2=0.417).
[b] Algorithm based on Chave's (1954) echinoid data (R^2=0.490).
[c] Algorithm based on Chave's (1954) decapod crustacean data (R^2=0.734).
[d] Algorithm based on Chave's (1954) annelid worm data (R^2=0.777).
[e] Algorithm based on Stanley et al.'s (2002) coralline algae data (R^2=0.891).
[f] Algorithm based on Chave's (1954) calcareous algae data (R^2=0.762).
[g] Algorithms based on Fchtbauer and Hardie's (1976) non-skeletal precipitates data (R^2=0.930 for Mg/Ca$_C$=f [Mg/Ca$_{sw}$]; R^2=0.861 for Mg/Ca$_C$=f [T]@Mg/Ca$_{sw}$=5.0).

fractionation algorithms cannot be calibrated with extant representatives. The accuracy of the algorithms may also be limited by other factors that may have influenced biogenic Mg fractionation in the past, yet are not incorporated into the model (e.g., variations in growth rates, fluctuations of other ions in seawater, fluctuations in salinity, fluctuations in salinity; e.g., Borremans et al., 2009).

Dickson's (2002, 2004) paleo-seawater Mg/Ca ratios were recalculated (Fig. 1) using the echinoid plate Mg fractionation algorithm (calibrated for crinoid ossicles when applicable; Table 2; Ries, 2004) that accounts for ambient temperature and variable D_cMg values. Paleotemperatures were estimated by Dickson [see Dickson's (2002) supplementary data] from paleogeographic and paleotemperature maps (Golonka et al., 1994). The resulting Mg/Ca ratios are consistent with other estimates and models of paleoceanic Mg/Ca over Phanerozoic time (Hardie, 1996; Lowenstein et al., 2001; Horita et al., 2002; Siemann, 2003; Demicco et al., 2005).

7.3 Ocean temperature reconstructions from skeletal Mg/Ca of calcitic animals

The correlation between temperature and skeletal Mg incorporation (Chave, 1954) also permits the reconstruction of ancient seawater temperatures from skeletal Mg/Ca ratios. However, such reconstructions must correct skeletal Mg/Ca for the effect of varying Mg/Ca$_{sw}$. A recent temperature reconstruction from the Mg/Ca$_C$ of fossil foraminifera (Lear et al., 2000) has, like the echinoderm reconstruction (Dickson, 2002, 2004), employed a fixed D_cMg to make this correction. This paleotemperature reconstruction can be improved

by using an empirically derived Mg fractionation algorithm, which accounts for D_cMg varying with Mg/Ca$_{sw}$ (Table 2).

7.4 Conclusions – high Mg calcite-secreting animals

1. The Mg/Ca ratio in the calcite secreted by echinoids, shrimp, crabs, and serpulid worms varies proportionally with the Mg/Ca ratio of the seawater in which they are grown. Organisms grown in experimental seawaters formulated with the calcite sea Mg/Ca ratio of 1 began secreting low Mg calcite, as opposed to their normal high Mg calcite. This suggests that the organisms evaluated in this study, which all produce high Mg calcite in modern seas, probably produced low Mg calcite in middle and Late Cretaceous seas, when seawater Mg/Ca values are thought to have been near unity.

2. The Mg/Ca of well-preserved fossils of these organisms may be a reliable monitor of changes in oceanic Mg/Ca throughout Phanerozoic time. However, given the variation in Mg fractionation curves amongst closely related organisms, such as crabs and shrimps, and between different skeletal components within the same organism, such as echinoid spines and coronal plates, these reconstructions should employ only anatomically and taxonomically appropriate Mg fractionation algorithms.

3. Mg fractionation coefficients (D_cMg) were shown to vary with Mg/Ca$_{sw}$ for each of the four organisms. Prior reconstructions of paleoceanic Mg/Ca$_{sw}$ from echinoderms and of temperature from foraminifera, which employed a fixed D_cMg over a range of ambient Mg/Ca$_{sw}$ ratios, would be improved by employing Mg

fractionation algorithms that account for variations in D_cMg with ambient Mg/Ca$_{sw}$ and temperature.

8 Bacterial biofilms

The same mechanism reported to be responsible for secular variation in seawater Mg/Ca ratios throughout Phanerozoic time – ion exchange along zones of newly formed ocean crust driven by global rates of ocean crust production – has also been hypothesized as the primary mechanism controlling this critical ionic ratio throughout Precambrian time (Hardie, 2003). A hydrothermal brine-river water mixing model (Hardie, 1996, 2003) driven by global rates of ocean crust production inferred from secular variation in the frequency of granite-pluton production in North America (Engel and Engel, 1970) predicts that Precambrian seawater Mg/Ca would have been constrained to the same range of values that existed throughout Phanerozoic time (1-to-5.2) and would have caused six intervals of aragonite seas and five intervals calcite seas between late Archean and terminal Proterozoic time (Fig. 26). The observed distribution of aragonite seafloor precipitates in the form of crystal fans, early marine cements, and ooids, as compiled by Hardie (2003, see references therein), is consistent with the predictions of his Precambrian seawater Mg/Ca model (Fig. 26).

Marine calcification throughout Precambrian time – unlike throughout Phanerozoic time – was generally dominated by bacterial biofilms (Riding, 2000). Such bacterially induced calcification is recorded in the geologic record in the form of microbialites, stromatolites, and thrombolites. Although the distribution and abundance of these bacterially induced carbonates have varied substantially throughout Precambrian time, most likely due to fluctuations in the CaCO$_3$ saturation state of seawater (Grotzinger and Knoll, 1999; Arp et al., 2001; Sumner and Grotzinger, 2004; Riding and Liang, 2005) and the evolution of grazing eukaryotes (Awramik, 1971; Riding and Liang, 2005), these deposits are well-represented from late Archean through Cambrian time (Riding, 2000).

Experiments were conducted to investigate the effects of varied seawater Mg/Ca on calcification within marine bacterial biofilms (Ries et al., 2008). The results of these experiments have important implications for our understanding of the mechanisms of calcification within bacterial biofilms, for the history of biofilm calcification throughout Precambrian time, and for the viability of microbial carbonates (e.g., microbialites, stromatolites, thrombolites) as a proxy record of Precambrian ocean chemistry.

Mixed-community marine sedimentary biofilms were cultured in experimental seawaters formulated over the range of Mg/Ca ratios predicted to have occurred since late Archean time (1.5, 2.5, 5.2; Hardie, 2003), corresponding to a calcite sea, a boundary calcite-aragonite sea, and an aragonite sea. Biofilm phylogenetic diversity, CaCO$_3$ polymorph mineralogy and distribution, and Mg fractionation in biofilm calcite were evaluated in response to these modifications in seawater Mg/Ca.

8.1 CaCO$_3$ distribution within biofilms

Backscatter electron images of biofilms cultured in the three experimental seawaters (Fig. 27) reveal that CaCO$_3$ is generally precipitated between the biofilms' bacterial cells. This is particularly evident in Fig. 27c, where bacterial cells were cross-sectioned during sample preparation, thus revealing the intercellular, void-filling CaCO$_3$ matrix. The biofilms, including the control, showed no significant ($p < 0.05$) differences in their percent calcification. Average wt-percent calcification for biofilms grown in the three seawater treatments was 64±4%. SEM imaging revealed that the non-biofilm control plates contained no trace of CaCO$_3$ precipitation.

8.2 Effect of Mg/Ca$_{sw}$ on polymorph mineralogy and Mg content of biofilm CaCO$_3$

Powder X-ray diffraction analysis of CaCO$_3$ precipitated within the biofilms revealed that the calcite:aragonite ratio increased as Mg/Ca$_{sw}$ decreased towards the calcite stability field (Mg/Ca$_{sw} < 2$; Fig. 28a). Biofilms cultured in the modern aragonite seawater (Mg/Ca$_{sw}$=5.2) produced the majority (57±1.0%) of their CaCO$_3$ as aragonite with lesser amounts as magnesian calcite (43±1.0%). Biofilms cultured in the aragonite-calcite boundary seawater (Mg/Ca$_{sw}$=2.5) produced the majority of their CaCO$_3$ as magnesian calcite (85±1.1%) with lesser amounts as aragonite (15±1.1%). Biofilms cultured in the experimental calcite seawater (Mg/Ca$_{sw}$=1.5) produced exclusively magnesian calcite.

The Mg/Ca ratio of the biofilm calcite (Mg/Ca$_C$) varied proportionally with Mg/Ca$_{sw}$ (Fig. 28b). Biofilms cultured in the experimental seawaters formulated at Mg/Ca$_{sw}$ of 5.2, 2.5, and 1.5 yielded Mg/Ca$_C$ of 0.16±0.01, 0.08±0.01, and 0.06±0.01, respectively. The relationship between Mg/Ca$_{sw}$ and Mg/Ca$_C$ observed for the biofilms (0.16<Mg/Ca$_C$ < 0.17 in Mg/Ca$_{sw}$=5.2 at 25 °C) mimics Mg fractionation in abiotically precipitated calcite cements (0.14<Mg/Ca$_C$ < 0.18 in modern shallow seawater; Morse et al., 2006) and is generally consistent with Mg fractionation in calcite produced by corals (Ries et al., 2006), calcareous bryopsidalean algae (Stanley et al., 2010), coralline red algae (Stanley et al., 2002; Ries, 2006b), some species of coccolithophores (Stanley et al., 2005), echinoids, crabs, shrimp, and calcareous serpulid worm tubes (Ries, 2004).

It should also be noted that although Mg fractionation in biofilm calcite appears to mimic that of abiotic calcification, the observation that calcification occurred exclusively on the biofilm plates, and not at all on the non-biofilm control plates, indicates that the calcification observed in the biofilms
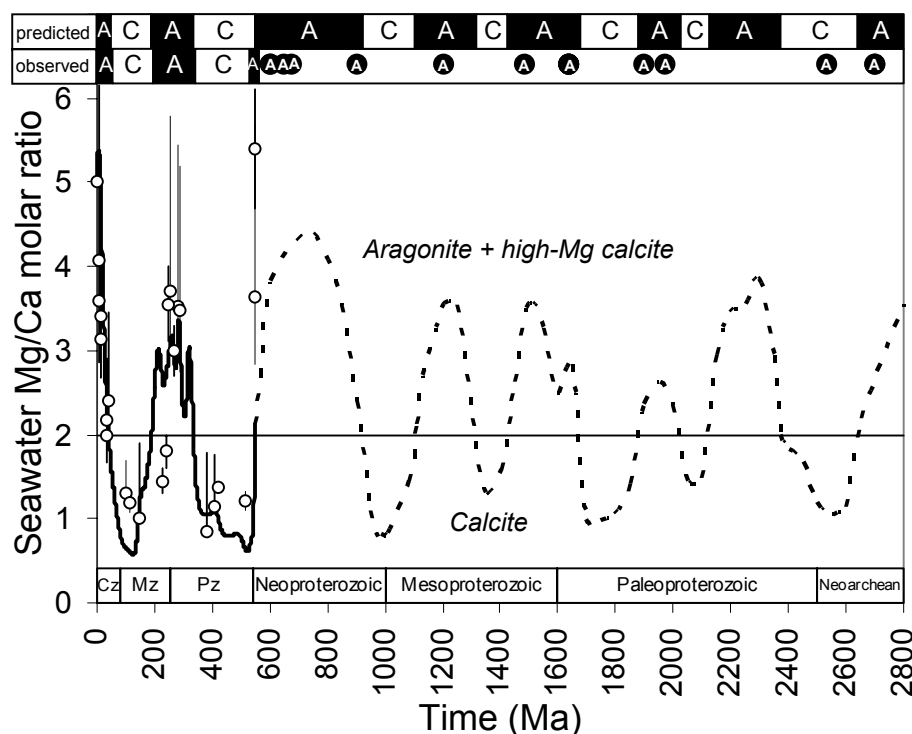
Fig. 26. Secular variation in Mg/Ca$_{SW}$ and the original polymorph mineralogy of nonskeletal CaCO$_3$ precipitates, including ooids, seafloor precipitates, and marine cements, since late Archean time (from Ries et al., 2008). Phanerozoic (solid curve; Hardie, 1996; Demicco et al., 2005) and Precambrian (dashed curve; Hardie, 2003) seawater Mg/Ca is calculated from hydrothermal brine-river water mixing models driven by rates of ocean crust production (Gaffin, 1987) and granite pluton data (Engel and Engel, 1970), respectively. Open circles correspond to Mg/Ca$_{SW}$ estimated from fluid inclusions in primary marine halite (Lowenstein et al., 2001, 2003, 2005; Brennan and Lowenstein, 2002; Brennan, 2002; Horita et al., 2002; Brennan et al., 2004; Timofeeff et al., 2006). Horizontal line divides the calcite (Mg/Ca$_{SW}$ < 2) and aragonite – high Mg calcite (Mg/Ca$_{SW}$ > 2) nucleation fields in seawater at 25 °C (Leitmeier, 1910, 1915; Lippman, 1960; Müller et al., 1972; Berner, 1975; Given and Wilkinson, 1985; Stanley and Hardie, 1999). Temporal distribution of predicted (Hardie, 1996, 2003) and observed (Sandberg, 1983; Hardie, 2003) nonskeletal calcite ("C") and aragonite ("A") precipitates are plotted along top of figure. Closed black circles circumscribing "A" correspond to inferred aragonitic seafloor precipitates observed in Precambrian deposits (cf. Hardie, 2003).

resulted from some degree of biological forcing, and should thus be considered biogenic in nature.

8.3 Effect of seawater Mg/Ca on the bacterial community

Clone library estimates of the microbial diversity (Table 3) and phylogenetic structure of the biofilms cultured in the artificial aragonite (Mg/Ca=5.2) and calcite (Mg/Ca=1.5) sea-waters, and of the control biofilm, were highly similar. The biofilm communities from each of the seawater treatments were dominated by cyanobacteria, alpha proteobacteria, bacteroidetes, and gamma proteobacteria, which collectively comprise greater than 70% of the biofilms' bacterial community. Cyanobacteria were more abundant in the control biofilm than in either of the experimental biofilms that were cultured in the experimental seawaters. This may be attributable to the lower irradiance of the laboratory conditions,

which could have affected the growth of these phototrophs. The biofilms cultured in the experimental seawaters also had greater abundances of gamma proteobacteria than bacteroidetes, while the control biofilm had a greater abundance of bacteroidetes than gamma proteobacteria. There were also slight differences in the representation of the low-abundance bacterial groups, including the planctomycetes, chloroflexi, actinomycetes, verrucomicrobia, legionella, acidobacteria, chlamydiales, delta proteobacteria, and gemmatimonadetes. Such minor differences in the relative abundances of bacterial groups amongst the one control and the two experimental biofilms may be attributable to subtle differences between laboratory and natural conditions and/or stochastic variations in cloning or sampling efficiency.

It is improbable that the minor differences in bacterial diversity and abundance that were observed between the biofilms cultured in the experimental aragonite and calcite seawaters could account for the significant differences in
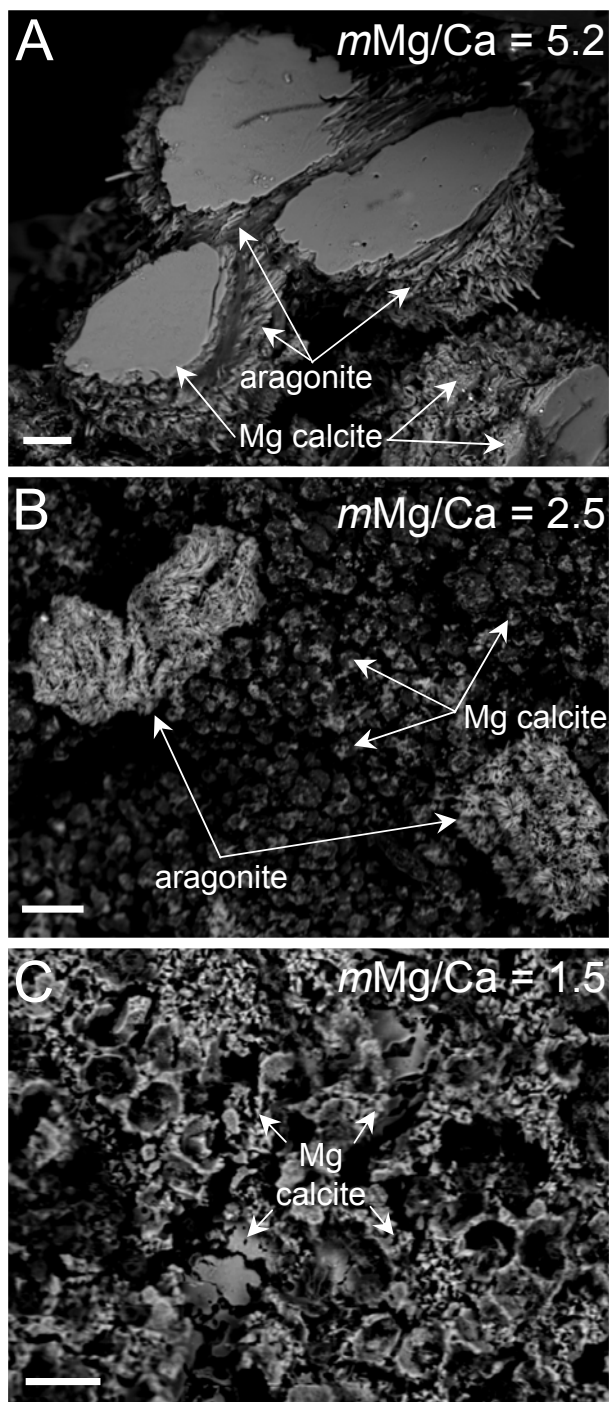
Fig. 27. Backscattered electron images showing distribution of aragonite (large, acicular crystals) and Mg calcite (small, micritic crystals) precipitates within biofilms grown in the three experimental seawaters. **(A)** Mg/Ca$_{sw}$=5.2; 43 mole-% calcite (Mg/Ca$_C$=0.156); 57 mole-% aragonite. **(B)** Mg/Ca$_{sw}$=2.5; 86 mole-% calcite (Mg/Ca$_C$=0.078); 14 mole-% aragonite. **(C)** Mg/Ca$_{sw}$=1.5; 100 mole-% calcite (Mg/Ca$_C$=0.058). Scale bars are 20 μm. Relative abundance of CaCO$_3$ polymorphs was determined by powder X-ray diffraction. From Ries et al. (2008).
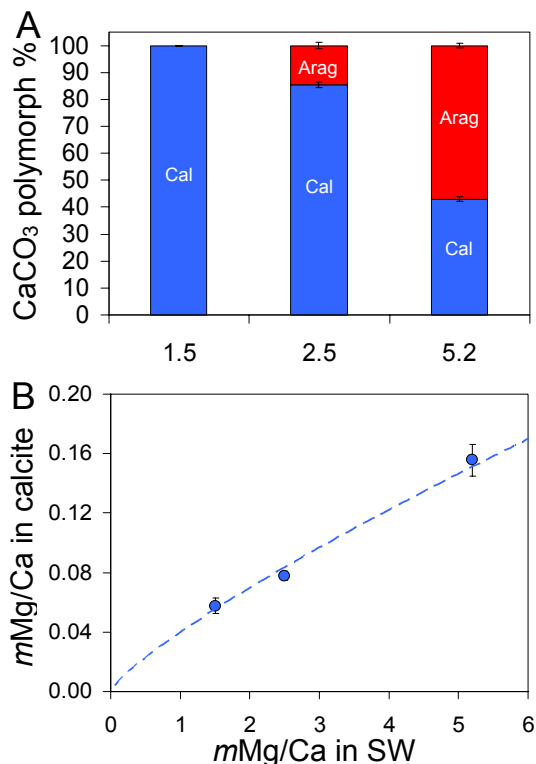

Fig. 28. Mineralogy and geochemistry of CaCO$_3$ precipitated within biofilms grown in the three experimental seawaters (Ries et al., 2008). **(A)** Relative abundance (mole-%) of calcite (blue) and aragonite (red) within biofilm CaCO$_3$, determined by powder X-ray diffraction. **(B)** Mg/Ca of calcite precipitated within biofilms, determined by powder X-ray diffraction and energy dispersive spectrometry. Mg fractionation algorithm (dashed curve) calculated using least squares regression is defined as Mg/Ca$_C$=0.0397Mg/Ca$_{sw}$$^{0.811}$ (R^2=0.99). Error bars represent uncertainty due to instrument error and specimen variation. From Ries et al. (2008).

their CaCO$_3$ polymorph ratios. The more parsimonious explanation for the observed variation in CaCO$_3$ polymorphism and Mg/Ca$_C$ within biofilms cultured in the various seawater treatments is the prescribed difference in seawater Mg/Ca. While specific sulfate reducing bacteria may dictate CaCO$_3$ polymorph mineralogy in pure culture (Van Lith et al., 2003), the results of the present study suggest that this ability is lost in natural, normal-salinity mixed-culture biofilms, where such polymorph-specifiers apparently constitute only a small portion of the total calcifying bacterial community.

Furthermore, the similarity of the composition and structure of the experimental biofilms to that of the control biofilm (Table 3), which was not subjected to the experimental seawater conditions, as well as to other natural calcifying microbial communities (Burns et al., 2004; Lopez-Garcia et al., 2005; Papineau et al., 2005), indicates that the

Table 3. Diversity of bacteria in biofilm communities determined by 16S rRNA gene sequence analysis.

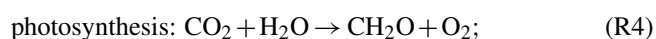| Phylogenetic group	Control[a] (mMg/Ca=5.2)	Aragonite SW (mMg/Ca=5.2)	Calcite SW (mMg/Ca=1.5)
Cyanobacteria	32%	26%	25%
α-Proteobacteria	25%	25%	23%
Bacteroidetes	15%	16%	8%
γ-Proteobacteria	10%	19%	17%
Planctomycetes	8%	6%	2%
Chloroflexi	–	6%	8%
Actinomycetes	5%	–	6%
Verrucomicrobia	–	–	4%
Legionella	–	–	4%
Acidobacteria	–	–	2%
Chlamydiales	2%	–	–
δ-Proteobacteria	2%	–	–
Gemmatimonadetes	–	1%	–
No. of clones analyzed	59	68	48

[a] biofilm processed shortly after removal from lagoon and not grown in experimental seawater

experimental biofilms are essentially representative of natural, calcifying microbial communities and, therefore, reasonable systems from which to extrapolate about microbial calcification throughout the geologic past. Barring phylogenetic reconstruction of fossilized DNA from lithified microbial communities, these modern, normal-salinity, calcifying biofilm systems are the next-best models for investigating the structure and function of the ancient bacterial systems believed to be responsible for the construction of stromatolites, thrombolites, and microbialites throughout the geologic past (Reid et al., 2000).
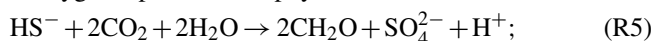
8.4 Mechanisms of calcification within biofilms

Biofilms are highly diverse bacterial communities that can precipitate $CaCO_3$ extracellularly within their mm-to-cm thick matrices. Calcification within these biofilms results from the complex interplay of metabolic and geochemical reactions occurring within and adjacent to the biofilm matrix, often in association with exopolymeric substances (Dupraz and Visscher, 2005; Altermann et al., 2006).
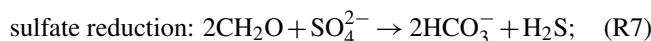
The C, O, S, N, and Fe-based reduction-oxidation reactions that form the basis of microbial metabolisms greatly affect the biofilm system's pH, total alkalinity, and dissolved inorganic carbon, and thus $[CO_3^{2-}]$ and Ω_{CaCO3} of the biofilm's intercellular space, which determines whether calcification will occur (Bosak and Newman, 2005; Dupraz and Visscher, 2005; Visscher and Stolz, 2005; Baumgartner et al., 2006). Simplified examples (Visscher and Stolz, 2005) of such microbial reactions that effectively *increase* $[CO_3^{2-}]$ and Ω_{CaCO3} are:
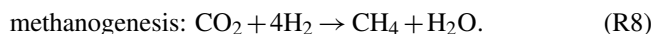
photosynthesis: $CO_2 + H_2O \rightarrow CH_2O + O_2$; (R4)

anoxygenic photoautotrophy:

$HS^- + 2CO_2 + 2H_2O \rightarrow 2CH_2O + SO_4^{2-} + H^+$; (R5)

dissimilatory iron-reduction:

$CH_2O + 4FeOOH + H_2O \rightarrow HCO_3^- + 4Fe^{2+} + 7OH^-$; (R6)

sulfate reduction: $2CH_2O + SO_4^{2-} \rightarrow 2HCO_3^- + H_2S$; (R7)

and

methanogenesis: $CO_2 + 4H_2 \rightarrow CH_4 + H_2O$. (R8)

Examples (Visscher and Stolz, 2005) of microbial reactions that effectively *decrease* $[CO_3^{2-}]$ and Ω_{CaCO3} are:

aerobic respiration: $CH_2O + O_2 \rightarrow CO_2 + H_2O$; (R9)

sulfide oxidation: $HS^- + 2O_2 \rightarrow SO_4^{2-} + H^+$; (R10)
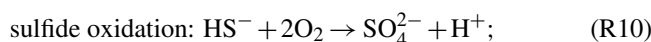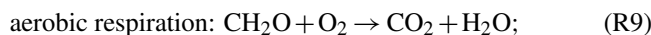
ammonium oxidation:

$2NH_4^+ + 3O_2 \rightarrow 2NO_2^- + 2H_2O + 4H^+$; (R11)
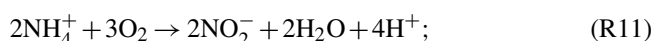
dissimilatory nitrate-reduction:

$5CH_2O + 4NO_3^- \rightarrow 5HCO_3^- + 2N_2 + 2H_2O + H^+$; (R12)

and

fermentation: $3CH_2O + H_2O \rightarrow CO_2 + H_2O + C_2H_6O$. (R13)
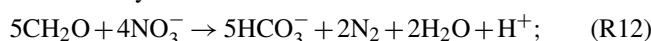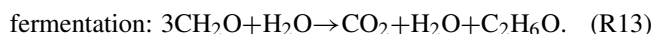
Such primary microbial metabolic reactions within the biofilm are moderated by secondary reactions associated with exopolymeric substance (EPS; Reid et al., 2000; Arp et al., 2001; Bosak and Newman, 2005; Dupraz and Visscher, 2005). EPS is an extension of the microbial cell that maintains biofilm structure, establishes chemical microgradients by reducing rates of diffusion, may regulate intercellular processes, and functions to bind cations, elevate HCO_3^-, and nucleate $CaCO_3$ crystals (Arp et al., 2001; Dupraz and Visscher, 2005).

The observation made in this study that biofilm calcification proceeds nearly abiotically with respect to polymorph distribution and Mg fractionation is consistent with the assertion that calcification in biofilms occurs primarily through the elevation of $[CO_3^{2-}]$ in the biofilm's intercellular space via fundamental microbial reduction-oxidation reactions that remove CO_2 and/or H^+ (McConnaughey and Whelan, 1997; Bosak and Newman, 2005; Dupraz and Visscher, 2005), rather than by elevating $[Ca^{2+}]$ via $CaCO_3$ dissolution and EPS decomposition (Dupraz and Visscher, 2005). The latter scenario of elevated Ca^{2+}, evidence of which was not observed in the presently reviewed study, would decrease the Mg/Ca ratio within the calcifying fluid of the biofilm and cause its patterns of $CaCO_3$ polymorphism and Mg fractionation (Fig. 28), with respect to ambient Mg/Ca$_{sw}$, to deviate from those of abiotically precipitated $CaCO_3$.

8.5 Precambrian ocean chemistry reconstructions

The timing of aragonite and calcite sea intervals is fairly well-constrained for the Phanerozoic Eon (Sandberg, 1983; Hardie, 1996; Stanley and Hardie, 1999; Lowenstein et al., 2001; Horita et al., 2002; Dickson, 2004). However, the distribution of calcite and aragonite seas in Precambrian time is poorly known, primarily because of the scarcity of proxies for seawater chemistry identified in the Precambrian geologic record, such as primary fluid inclusions and calcareous fossils whose skeletons can be chemically calibrated with modern representatives. Our current understanding of Precambrian Mg/Ca$_{sw}$ is derived primarily from Hardie's (2003) hydrothermal brine-river water mixing model driven by ocean crust-productions rates inferred from secular oscillations in granite-pluton production in North America (Engel and Engel, 1970) and from limited observations of aragonite seafloor precipitates (crystal fans, early marine cements, ooids) throughout late Archean to early Cambrian time, compiled by Hardie (2003; see references therein).

The observation that CaCO$_3$ polymorph ratios (aragonite:calcite) and calcite Mg/Ca ratios within the biofilms varied with experimental Mg/Ca$_{sw}$ suggests that well-preserved microbial carbonates may be a reliable monitor of aragonite-calcite sea intervals and Mg/Ca$_{sw}$ throughout Precambrian time. However, an important assumption implicit in the use of the original mineralogy of microbial carbonates as a proxy for seawater Mg/Ca is that the physicochemical properties of Precambrian seawater were such that Mg/Ca$_{sw}$ was the predominant variable influencing the polymorph mineralogy of CaCO$_3$ precipitated from seawater, as it is believed to have been throughout Phanerozoic time (Hardie, 1996; Stanley and Hardie, 1998, 1999; Lowenstein et al., 2001).

Using modern soda lakes associated with volcanic regions as analogs, Kempe and Degens (1985) infer that the Earth's ocean prior to 1 Ga was a soda ocean (HCO$_3^-$ >Ca^{2+}) of high total alkalinity, high pH, and low Ca^{2+} and Mg^{2+} concentrations. They further argue that by 1 Ga, the gradual leaching of chlorine from the oceanic crust and the removal of dissolved carbonates via biotic and abiotic CaCO$_3$ precipitation had transformed the soda ocean into a halite ocean.

Morse and Mackenzie (1998), however, argue that if early seawater was buffered by reactions involving carbonates and silicates, then the composition of post-Hadean seawater may have been comparable to that of today's. In contrast to earlier hypotheses that the Precambrian ocean was a soda ocean prior to 1 Ga (Kempe and Degens, 1985) or even 2 Ga (Grotzinger and Kasting, 1993), Morse and Mackenzie's calculations suggest that the Precambrian ocean had been a halite ocean since late Hadean-early Archean time, with somewhat higher DIC and total alkalinity concentrations, higher CaCO$_3$ saturation states, and possibly lower Ca^{2+} concentrations.

Grotzinger and Kasting (1993) argue that the occurrence of pseudomorphs after CaSO$_4$ minerals in the geologic record back to 2 Ga suggests that the ocean was not alkaline and maintained Ca^{2+} >HCO$_3^-$ over this interval. They further propose that prior to 2 Ga, the absence of evidence for gypsum indicates either (1) such low SO$_4^{2-}$ concentrations that CaSO$_4$ minerals were unable to precipitate or (2) HCO$_3^-$ >Ca^{2+}, such that all Ca^{2+} was depleted during progressive evaporation of seawater via CaCO$_3$ precipitation before the gypsum field could be reached. If the latter scenario (HCO$_3^-$ >Ca^{2+}) occurred, then their assertions would push the soda-to-halite ocean transformation back to 2 Ga. If the former scenario (very low SO$_4^{2-}$) occurred, as supported by the Archean record of stable isotopes of sulphur (Canfield et al., 2000; Habicht et al., 2002), then the transition to a halite ocean could have occurred much earlier, and would not argue for a Precambrian ocean composition that was significantly different from that of today's, at least with respect to the role that Mg/Ca$_{sw}$ played in determining CaCO$_3$ polymorph mineralogy.

Hardie (2003) argues, like Morse and Mackenzie (1998), that the post-Hadean Precambrian ocean was never a soda ocean, but instead was a near-neutral halite ocean with Ca^{2+} >HCO$_3^-$, comparable to modern seawater. Hardie contends that the extreme acidity caused by the high concentrations of dissolved HCl and CO$_2$ in the Earth's primordial ocean (Garrels and Mackenzie, 1971) would have fostered a global scale acid-base titration that would have converted primordial igneous crust into aluminosilicate sediments and yielded a saline ocean with Na^{2+} ~Ca^{2+} >Mg^{2+} >K$^+$ and near neutral pH (Garrels and Mackenzie, 1971; Lafon and Mackenzie, 1974). Hardie (2003) proposes that the elevated production of CaCl$_{2(aq)}$ relative to CaHCO$_{3(aq)}^+$, due to the predominance of HCl over CO$_2$ dissolved in the primordial acid rain, would have yielded Ca^{2+} >HCO$_3^-$ in this primordial ocean. Hardie cites reports of pseudomorphs after gypsum at 2.6 Ga (Simonson et al., 1993) and 3.45 Ga (Lowe, 1983) in support of this line of reasoning.

Temperature, pCO$_2$, and [SO$_4^{2-}$] have also been shown to influence the polymorph mineralogy of CaCO$_3$ precipitated from seawater-based solutions (Bischoff and Fyfe, 1968; Walter, 1986; Burton and Walter, 1991; Morse et al., 1997; De Choudens-Sanchez and Gonzalez, 2009; Lee and Morse, 2010). Experiments on solutions formulated to mimic modern seawater (salinity = 35, 1 atm pressure, modern open seawater total alkalinity, Mg/Ca=5.2, pCO$_2$ =~ 380 ppm) revealed that the kinetically favored polymorph of CaCO$_3$ will switch from aragonite to calcite when temperature falls below 6±3 °C (Morse et al., 1997). Morse et al. (1997) also argue that calcite will be favored over aragonite when pCO$_2$ increases to between ~2600 and 3500 ppm (for T=~25 °C), which represents the range over which modern seawater will be undersaturated with respect to aragonite yet supersaturated with respect to calcite. Because the stoichiometric solubility coefficients (K_{sp}) of aragonite ($10^{-6.19}$) and calcite ($10^{-6.37}$) are relatively close, the range of calcite supersaturation states that yields simultaneous aragonite

undersaturation is narrow ($1 < \Omega_{calcite} < 1.5$), and generally requires that seawater be near undersaturation with respect to calcite.

Given the ubiquity and abundance (Riding, 2000) of nearly abiotically precipitated microbial carbonates from Archean through Neoproterozoic time, it seems improbable that the $CaCO_3$ saturation state of post-Hadean seawater was regularly constrained to such a narrow range that teetered on the edge of total $CaCO_3$ undersaturation ($1 < \Omega_{calcite} < 1.5$), a condition required by the hypothesis that elevated pCO_2 was the primary driver of calcite sea intervals (Morse et al., 1997). To the contrary, it is asserted that Archean and Proterozoic seawater actually maintained $CaCO_3$ saturation states that were much greater than modern seawater (modern seawater $\Omega_{calcite} \sim 5.7$; Kempe and Degens, 1985; Grotzinger, 1989; Grotzinger and Kasting, 1993; Morse and Mackenzie, 1998; Grotzinger and Knoll, 1999; Grotzinger and James, 2000), and thus well above the range ($1 < \Omega_{calcite} < 1.5$) that permits simultaneous aragonite undersaturation and calcite supersaturation. Such assertions cast doubt over the role of pCO_2 as a primary driver of $CaCO_3$ polymorph mineralogy throughout post-Hadean time.

Sulfate has also been shown experimentally to inhibit the precipitation of both calcite and, to a lesser extent, aragonite (Bischoff and Fyfe, 1968; Walter, 1986) in seawater-based solutions. However, the effect of Mg/Ca on $CaCO_3$ polymorph specification (Leitmeier, 1910, 1915; Lippman, 1960; Müller et al., 1972; Berner, 1975; Morse et al., 1997; Stanley and Hardie, 1999; De Choudens-Sanchez and Gonzalez, 2009; Lee and Morse, 2010) supersedes that of $[SO_4^{2-}]$ (Bischoff and Fyfe, 1968) when considered over the geologically realistic ranges of $[SO_4^{2-}]$ and Mg/Ca that stable isotopes of sulfur (Canfield et al., 2000; Habicht et al., 2002), fluid inclusions in halite (Horita et al., 2002; Lowenstein et al., 2003), and various ocean chemistry models (Hardie, 2003; Berner, 2004; Demicco et al., 2005) suggest for Precambrian seawater ($0 < [SO_4^{2-}] < 20$–25 mmol kg-SW^{-1}; $1 < Mg/Ca < 5.2$).

It is more conceivable, however, that temperature (Morse et al., 1997) played a significant role in determining the primary polymorph mineralogy of microbial carbonates throughout Precambrian time. It is therefore important that such reconstructions of seawater Mg/Ca preferentially employ microbial carbonates that were deposited from seawater for which paleotemperature is reasonably well-constrained. Fortuitously, since $CaCO_3$ saturation state increases with temperature, the majority of microbial carbonates preserved in the Precambrian geologic record are thought to be warm-water carbonates.

It should be noted that workers have observed a transition in the mode of accretion of Precambrian microbial carbonates from one that occurs primarily via in situ precipitation in Archean through Mesoproterozoic time, to one involving a combination of in situ calcification and the trapping and binding of loose $CaCO_3$ sediments in Neoproterozoic time and thereafter (Grotzinger and Knoll, 1999; Grotzinger and James, 2000; Sumner and Grotzinger, 2004). However, this transition in mode of accretion should have little bearing on the viability of microbial carbonates as a proxy of seawater Mg/Ca_{sw} throughout Precambrian time, as the polymorph mineralogy of abiotically precipitated $CaCO_3$ sediments that are trapped and bound in the biofilms and microbial mats and the polymorph mineralogy of $CaCO_3$ precipitated in situ should be comparably governed by, and thus equally indicative of, ambient seawater Mg/Ca.

The far greater challenge to using the original mineralogy of Precambrian microbial carbonates as a proxy for understanding secular variation in the major cation composition of Precambrian seawater relates to diagenesis. The aragonite polymorph is less stable than the calcite polymorph at Earth surface conditions and will thus convert to calcite over relatively short geologic timescales. However, various indicators, such as trace element composition (Mg^{2+}, Sr^{2+}), quality of textural preservation, and presence of relic aragonite needles (Grotzinger and Reed, 1983; Brand, 1989; Lasemi and Sandberg, 1984, 1993), have been successfully employed to deduce the precursor mineralogy of micritic carbonates altered in this way.

Diagenesis can also cause the loss of Mg^{2+} from magnesian calcite. Yet despite the effects of diagenesis, the Mg/Ca and dolomite content of well-preserved fossil echinoderms has been shown to generally track seawater Mg/Ca throughout Phanerozoic time (Dickson, 2002, 2004). Thus, the Mg/Ca ratio and dolomite content of well-preserved microbial calcite may similarly track Precambrian Mg/Ca_{sw}.

8.6 Implications for $\delta^{18}O$ and $\delta^{13}C$ isotope stratigraphy

Isotopes of carbon and oxygen are fractionated differently in calcite and aragonite due to differences in the internal vibrational frequencies of the polymorphs' carbonate ions (Rubinson and Clayton, 1969; Tarutani et al., 1969). For $CaCO_3$ precipitated at 25 °C from experimental seawater, $\delta^{18}O$ and $\delta^{13}C$ are enriched in the aragonite polymorph by 0.6‰ and 1.8‰, respectively, relative to the calcite polymorph. $\delta^{18}O$ is also enriched in high Mg calcite (13 mole-% $MgCO_3$) by 1.1‰ relative to pure calcite, indicating a 0.09‰ enrichment in $\delta^{18}O$ per mole-% Mg. Thus, $\delta^{18}O$ and $\delta^{13}C$ isotope records derived from Precambrian microbial carbonates may contain global, threshold excursions of up to 2‰ caused by secular variations in the primary mineralogy of the host carbonates. Workers often make biogeochemical inferences from 2–3‰ excursions in the $\delta^{13}C$ isotope record of Precambrian rocks (e.g., Jacobsen and Kaufman, 1999; Halverson et al., 2005). It is possible that some of these excursions may simply reflect transitions in primary carbonate mineralogy, rather than the biogeochemical perturbations that are often invoked to explain such isotopic excursions.

8.7 Conclusions – bacterial biofilms

1. Reductions in seawater Mg/Ca caused commensurate reductions in the aragonite:calcite ratios of $CaCO_3$ precipitated within biofilms. Biofilms cultured in experimental aragonite seawater (Mg/Ca$_{sw}$=5.2) precipitated primarily aragonite, with lesser amounts of high Mg calcite, while biofilms cultured in experimental calcite seawater (Mg/Ca$_{sw}$=1.5) precipitated exclusively calcite.

2. The Mg/Ca ratios of the calcite precipitated within the biofilms varied proportionally with the Mg/Ca ratios of the experimental seawater. The observation that biofilm calcification mimics abiotic calcification with respect to $CaCO_3$ polymorph specification and Mg fractionation suggests that the elevation in $CaCO_3$ saturation state leading to calcification within the biofilm occurs mainly through the elevation of $[CO_3^{2-}]$, and not through the elevation of $[Ca^{2+}]$, which would inherently change the Mg/Ca ratio of the biofilm's calcifying fluid and cause its $CaCO_3$ polymorph mineralogy to deviate substantially from that of abiotically precipitated $CaCO_3$.

3. The results of the Ries et al. (2008) study suggest that the primary mineralogy and Mg/Ca$_C$ of well-preserved microbial carbonates may be a viable proxy for calcite-aragonite seas throughout Precambrian time, assuming (as discussed above) that the influence of seawater Mg/Ca on $CaCO_3$ polymorph mineralogy in Precambrian seawater was comparable to that in Phanerozoic seawater (i.e., Mg/Ca~2 divided the calcite and aragonite/high Mg calcite nucleation fields). These results invite a systematic study of the primary mineralogy and Mg content of well-preserved Precambrian microbial carbonates aimed at empirically constraining the history of Precambrian seawater Mg/Ca.

9 Implications for ocean acidification research

9.1 Insight into the composition of organisms' calcifying fluids

The anthropogenic elevation of atmospheric pCO$_2$ is predicted to cause portions of the world's surface oceans to become undersaturated with respect to aragonite before the year 2150 (Brewer, 1997). Many experiments have shown that these predicted reductions in carbonate ion concentration impair the ability of calcifying marine organisms to produce their protective shells and skeletons (cf. Hoegh-Guldberg et al., 2007; Kleypas et al., 2006; Langdon and Atkinson, 2005; Langdon et al., 2000; Gattuso et al., 1998). However, multiple studies (Iglesias-Rodriguez et al., 2008; Wood et al., 2008; Ries et al., 2009) have also demonstrated that calcification in some taxa is enhanced by elevated pCO$_2$, most

likely due to the organism's ability to utilize HCO_3^- in calcification, which increases with pCO$_2$. Although the experiments reviewed here were designed to evaluate organisms' response to secular variation in seawater Mg/Ca, the results have important implications for our interpretation of the disparate responses exhibited by calcifying marine organisms investigated in recent ocean acidification experiments.

Calcification within most organisms is catalyzed, in part, by elevating the saturation state of their calcifying fluid with respect to $CaCO_3$, which can be achieved by elevating either the $[Ca^{2+}]$ or $[CO_3^{2-}]$ of this fluid. Organisms whose skeletal mineralogy and calcite Mg-content varied with experimental Mg/Ca$_{sw}$ in a manner that mimics abiotic calcification (i.e., produced high Mg calcite and/or aragonite when Mg/Ca$_{sw}$ > 2 and low Mg calcite when Mg/Ca$_{sw}$ < 2) probably induce calcification primarily by elevating $[CO_3^{2-}]$, since elevating $[Ca^{2+}]$ would reduce the Mg/Ca ratio of the organisms calcifying fluid, causing their skeletal mineral polymorph and calcite Mg-content to deviate from that observed for abiotic calcification.. Although we have limited data about the composition of organisms' calcifying fluids, the elevation of $[CO_3^{2-}]$ within this fluid is believed to result from the elevation of calcifying fluid pH via direct proton pumping, Ca^{2+}-H^+ exchange, secretion of hydroxyl ions, or the removal of CO_2 via photosynthesis (Borowitzka and Larkum, 1976; McConnaughey and Falk, 1991; McConnaughey and Whelan, 1997; De Beer and Larkum, 200; Cohen and McConnaughey, 2003).

Organisms that calcify at high pH relative to ambient seawater (pH=9.0–11.0) will convert a substantial portion of the elevated HCO_3^-, resulting from the CO_2-induced ocean acidification, back into the CO_3^{2-} ion that is used directly in calcification. Thus, it can be reasonably argued that organisms that mimic abiotic calcification with respect to $CaCO_3$ polymorph specification and Mg-incorporation in calcite, an indicator that they induce calcification via the elevation of pH (and, thus, $[CO_3^{2-}]$), will likely be the least negatively impacted by CO_2-induced ocean acidification (Ries et al., 2009).

Conversely, organisms that produce low Mg calcite in seawater that favors nucleation of aragonite and high Mg calcite probably force the precipitation of low Mg calcite by elevating $[Ca^{2+}]$ within their calcifying fluid, which reduces the Mg/Ca ratio of this fluid. If this control over calcifying fluid Mg/Ca ratio comes at the expense of pH control, then these organisms may be less able to convert the elevated HCO_3^- that accompanies CO_2-induced ocean acidification back into CO_3^{2-}, which is required to maintain conditions favorable for biogenic calcification under such acidified conditions. Thus, modern low Mg calcite organisms may be more negatively impacted by CO_2-induced ocean acidification than modern aragonite and high Mg calcite organisms that maintain a high degree of control over the pH and, thus, CO_3^{2-} concentration of their calcifying fluid.
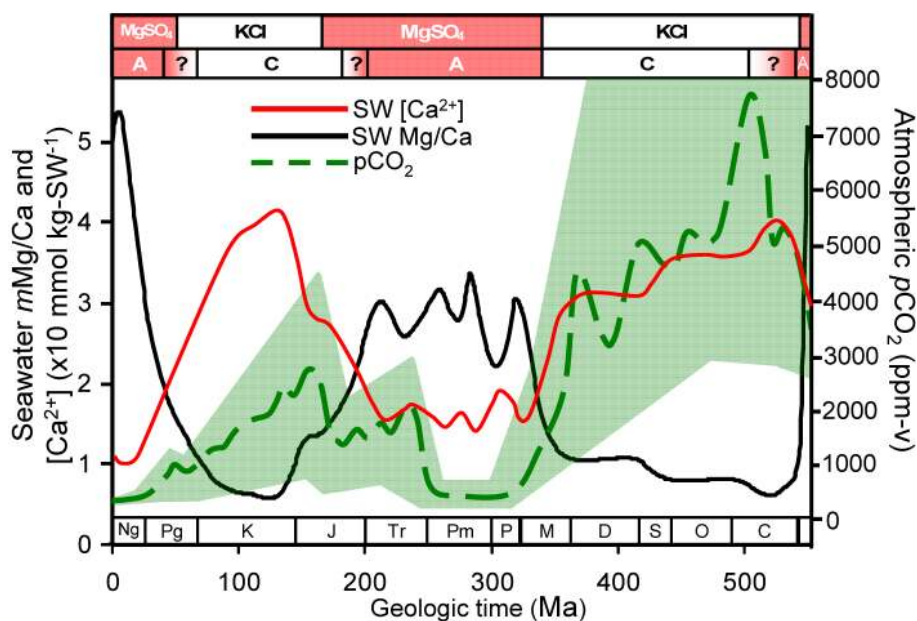
Fig. 29. Models of seawater Mg/Ca (solid black curve; Hardie, 1996; DeMicco et al., 2005), seawater [Ca^{2+}] (solid red curve; Hardie, 1996; DeMicco et al., 2005), and atmospheric pCO$_2$ (dashed green curve – green shading represents model uncertainty; Berner and Kothavala, 2001) throughout Phanerozoic time. Seawater [Ca^{2+}] and atmospheric pCO$_2$ have generally varied in synchroneity with each other because they are both thought to have been largely driven by the global rate of ocean crust production. This results in seawater Mg/Ca and atmospheric pCO$_2$ generally varying inversely with each other throughout Phanerozoic time. Thus, the effect of CO$_2$-induced ocean acidification (i.e., reduced [CO$_3^{2-}$]) on biogenic calcification throughout the geologic past may have been mitigated by corresponding elevations in [Ca^{2+}], which would have (1) partially offset the reduction in CaCO$_3$ saturation state that was associated with the CO$_2$-induced reduction in [CO$_3^{2-}$] and (2) favored the precipitation of the less soluble low Mg calcite polymorph (because of low seawater Mg/Ca) when seawater CaCO$_3$ saturation state was low. Because the modern anthropogenic ocean acidification event is not tectonically driven, there should be no commensurate elevation in seawater [Ca^{2+}] to mitigate the effect of the CO$_2$-induced reduction in [CO$_3^{2-}$] on the calcium carbonate saturation state of seawater.

However, low Mg calcite organisms should be more resistant to dissolution in CO$_2$-acidified seawater than either aragonite or high Mg calcite organisms because their low Mg calcite skeletal mineral is less soluble. Additionally, the elevated concentration of Ca^{2+} within their calcifying fluid (which likely forces precipitation of low Mg calcite in modern, high Mg/Ca seawater) may mitigate the impact of reduced [CO$_3^{2-}$] on calcification rate. Therefore, even though aragonite and high Mg calcite organisms may be more adept at converting the elevated HCO$_3^-$ that accompanies CO$_2$-induced ocean acidification back into CO$_3^{2-}$ within their calcifying fluid, the greater solubility of their skeleton may ultimately render them more vulnerable to dissolution in CO$_2$-enriched aragonite seas, such as those existing today. Of course, this lack of control over calcifying fluid Mg/Ca would have been less of a detriment during calcite sea intervals of the geologic past, when modern high Mg calcite-secreting organisms would have apparently secreted the less soluble low Mg calcite form of CaCO$_3$. Thus, it is reasonable to expect that during calcite seas intervals, organisms that induce calcification primarily by elevating pH and, thus, [CO$_3^{2-}$] of their calcifying fluid would be the most resistant

to CO$_2$-induced ocean acidification, as they would receive the dual benefit of reduced skeletal mineral solubility (low Mg calcite) and elevated [CO$_3^{2-}$] at the site of calcification under these conditions. During aragonite sea intervals – such as the modern one – it is probably the balance of these two mechanisms of calcification (pH vs. Mg/Ca control) within an organism's calcifying fluid that determines its unique response to CO$_2$-induced ocean acidification.

9.2 Calcite-aragonite seas and ocean acidification throughout Phanerozoic time

Over geologic timescales, seawater [Ca^{2+}] is thought to have generally varied inversely with seawater [CO$_3^{2-}$] (Fig. 29; Hardie, 1996; Royer et al., 2004; Demicco et al., 2005). This is because the primary mechanisms responsible for fluctuations in these parameters – hydrothermal brine-basalt reactions ([Ca^{2+}]) and volcanic CO$_2$ outgassing ([CO$_3^{2-}$]) – are both thought to have been largely driven by the global rate of ocean crust production. Thus, tectonically induced reductions in [CO$_3^{2-}$] (via volcanic outgassing of pCO$_2$) would have been partially offset, in terms of CaCO$_3$ saturation state,

by commensurate increases in seawater [Ca^{2+}] driven by enhanced Mg^{2+}-Ca^{2+} exchange along zones of ocean crust production. This is supported by Tyrrell and Zeebe's (2004) observation that the calcium carbonate compensation depth, and thus the saturation state of seawater with respect to calcium carbonate, has varied relatively little since Cretaceous time, compared with the approximately halving of seawater [Ca^{2+}] thought to have occurred over this interval (Hardie, 1996; Lowenstein et al., 2003). Tyrrell and Zeebe (2004) argue that this decline in seawater [Ca^{2+}] since Cretaceous time must have been approximately balanced, in terms of its effect on the calcium carbonate saturation state of seawater, by a near quadrupling of seawater [CO$_3^{2-}$] across this interval.

Additionally, the inverse relationship between seawater [Ca^{2+}] and [CO$_3^{2-}$] (Fig. 29) fortuitously causes low Mg calcite – the least soluble form of CaCO$_3$ – to be the predominant form of CaCO$_3$ (because elevated [Ca^{2+}] causes low seawater Mg/Ca) when the oceans are least saturated with respect to CaCO$_3$ (because of low [CO$_3^{2-}$]). Therefore, the impact of tectonically-induced ocean acidification (via volcanic CO$_2$ outgassing) on hypercalcifying taxa may have been mitigated throughout the geologic past by coeval tectonically-induced calcite sea conditions, which would have favored nucleation of the less soluble low Mg calcite polymorph of CaCO$_3$ and maintained seawater [Ca^{2+}] at an elevated level (Fig. 29).

However, the modern pCO$_2$-induced ocean acidification event, driven by the combustion of fossil fuels, differs from protracted intervals of ocean acidification that were likely associated with rapid rates of global ocean crust production throughout the geologic past in four critical ways: (1) the modern acidification event will not be accompanied by a coincident, tectonically forced elevation in [Ca^{2+}] that mitigates the pCO$_2$-induced reduction in [CO$_3^{2-}$] and, thus, CaCO$_3$ saturation state; (2) the modern acidification event will not be mitigated by a coincident, tectonically forced reduction in seawater Mg/Ca that favors the nucleation of the less soluble low Mg calcite polymorph of CaCO$_3$; (3) the rapidity of the modern acidification event will initially outpace the mitigating effect of rising total alkalinity that accompanies the dissolution of deeper-water carbonates (due to shoaling of the carbonate compensation depth) and enhanced weathering of the continents (due to more acidic rainwater) during intervals of elevated atmospheric pCO$_2$; and (4) the rapidity of the modern acidification event (relative to the gradual ocean acidification that accompanied calcite seas of the geologic past) may preclude evolutionary responses by hypercalcifying taxa. It is for these reasons that the modern anthropogenic ocean acidification event poses an unusually grave threat for hypercalcifying taxa, even when compared with the more protracted and extreme elevations in atmospheric pCO$_2$ that likely accompanied calcite seas of the geologic past (Fig. 29).

It should also be noted here that although shoaling of the carbonate compensation depth is thought to have acted as a natural buffer against rising CO$_2$-induced ocean acidity over geologic timescales (Tyrrell and Zeebe, 2004), Andersson et al. (2009) showed that dissolution of shallow water carbonates in the immediate future would not be sufficient to buffer shallow, carbonate platform marine environments from the effects of CO$_2$-induced ocean acidification over shorter timescales. Andersson et al. (2003) argued that the buffering that would result from the dissolution of metastable forms of shallow water calcium carbonate sediments (Mg-calcite and aragonite; see also Morse et al., 2006; Andersson et al., 2007, 2008) would be limited by relatively slow rates of sediment dissolution and the slow mixing of alkaline pore-waters with the overlying water column.

10 General conclusions

10.1 Tectonic controls on seawater chemistry

Sandberg (1983) observed that the primary mineralogy of ooids and early marine cements has alternated between three aragonite and two calcite intervals over the Phanerozoic Eon. Stanley and Hardie (1998, 1999) observed that major reef-building and sediment-producing organisms have generally shifted mineralogy in phase with these non-skeletal carbonates. Hardie (1996) interprets these shifts in carbonate mineralogy as responses to secular variations in the Mg/Ca ratio of seawater caused by fluctuations in the mixing rate of mid-ocean-ridge (MOR)/large-igneous-province (LIP) hydrothermal brines and river water, which is primarily driven by changes in the global rate of ocean crust production. As upwelling MOR/LIP basalt interacts with hydrothermal brine, the basalt is converted to greenstone, thereby removing Mg^{2+} and SO$_4^{2-}$ from seawater and releasing Ca^{2+} and K$^+$ to it. The rate of MOR/LIP ocean-crust production controls the rate of this ion exchange and, therefore, the respective concentrations of these ions in seawater (Spencer and Hardie, 1990).

Hardie (1996) used this model to calculate Mg/Ca ratios for the entire Phanerozoic Eon from historical rates of ocean crust production (inferred from eustatic sea level change). Füchtbauer and Hardie (1976, 1980) showed experimentally that for earth surface temperatures and pressures, seawater with Mg/Ca ratios greater than 2 precipitate aragonite + high Mg calcite (Mg/Ca in calcite >0.04), while Mg/Ca ratios less than 2 precipitate only low Mg calcite (Mg/Ca in calcite <0.04). The combination of these carbonate nucleation fields with Hardie's (1996) Phanerozoic Mg/Ca curve accurately predicts Sandberg's (1983) and Stanley and Hardie's (1998, 1999) variation in non-skeletal and skeletal carbonates. Hardie's oceanic Mg/Ca model is further supported by synchronized transitions between MgSO$_4$ and KCl evaporites (Hardie, 1996), fluid inclusion data (Lowenstein et al.,

2001, 2003, 2005; Brennan and Lowenstein, 2002; Brennan, 2002; Horita et al., 2002; Brennan et al., 2004; Timofeeff et al., 2006), secular variation in the skeletal Mg/Ca ratio of rugose corals (Webb and Sorauf, 2002), echinoderms (Dickson, 2002, 2004; Hasiuk and Lohmann, 2008), and abiogenic carbonates (Hasiuk and Lohmann, 2008); secular variation in the ratio of aragonite-to-calcite within bi-mineralic calcareous serpulid worm tubes (Railsback, 1993); secular variation in the Sr/Mg ratio of abiogenic marine carbonates (Cicero and Lohmann, 2001); the occurrence of higher seawater Sr/Ca ratios during predicted calcite sea intervals than during predicted aragonite sea intervals (Sr would be depleted in seawater during aragonite sea intervals because Sr is more readily incorporated in aragonite than in calcite; Steuber and Veizer, 2002); and secular variation in the Br concentration of marine halite (Siemann, 2003).

10.2 Fossil evidence for the influence of seawater Mg/Ca on calcareous biomineralization

Stanley and Hardie (1998, 1999) found that the carbonate mineralogy of simple, hypercalcifying organisms has varied in concert with Sandberg's aragonite and calcite seas throughout Phanerozoic time. During Calcite I seas (middle Paleozoic), calcitic corals (tabulate, heliolitid and rugose), and stromatoporoids (possibly calcitic) were the dominant reef builders, while receptaculitids (possibly calcitic) were the dominant sediment producers. During Aragonite II seas (late Paleozoic – early Mesozoic), reefs were dominated by aragonitic groups of sponges, scleractinian corals and phylloid algae and high Mg calcitic red algae, while aragonitic dasycladaceans were the dominant algal sediment producers. During Calcite II seas (Mid-Jurassic-late Paleogene), the bi-mineralic (aragonite and calcite) rudist bivalves replaced the aragonitic scleractinian corals as the dominant benthic marine carbonate producers, while calcitic nannoplankton (coccolithophores) became the major pelagic chalk producers. Finally, during Aragonite III seas, which include the modern ocean, aragonitic scleractinian corals and high Mg calcitic red algae again dominate reef construction while the aragonitic bryopsidalean algae are the major sediment producers.

Stanley and Hardie (1998, 1999) assert that the synchroneity between skeletal and non-skeletal carbonates is most evident for hypercalcifying organisms, including the reef-building corals and sponges and the sediment-producing algae. Kiessling et al. (2008) confirmed that this trend is most evident for reef-building taxa. This is probably because these organisms' characteristically rapid rate of calcification allows them to exercise only limited control over the chemical milieu of their calcifying fluid. However, Porter (2007) showed that the skeletal mineralogies of even non-hypercalcifying taxa track ocean chemistry at the time of skeletal origination – but not necessarily thereafter (Kiessling et al., 2008).

10.3 Experimental evidence for the effect of seawater Mg/Ca on growth and calcification rates

The aragonite-secreting bryopsidalean algae (*Penicillus capitatus*, *Udotea flabellum*, and *Halimeda incrassata*) and the scleractinian corals (*Porites cylindrica*, *Montipora digitata*, and *Acropora cervicornis*) exhibited higher rates of calcification and growth in seawater of Mg/Ca ratios that favored their aragonitic mineralogy. Conversely, the coccolithophores (*Pleurochrysis carterae*, *Ochrosphaera neopolitana*, and *Coccolithus neohelis*) exhibited higher rates of growth and calcification in seawater of Mg/Ca ratios that favored their calcitic mineralogy. It is reasonable, if not expected, that the algae's and corals' precipitation of aragonite in the low Mg calcite nucleation field, and the coccolithophores precipitation of calcite in the aragonite nucleation field, proceeds at a slower rate than it does in seawater that favors the organisms' inherent skeletal mineralogy. It is possible that such reduced rates of calcification within some bryopsidalean and coccolithophorid algae liberate less CO_2 for photosynthesis (Paasche, 1968; Borowitzka and Larkum, 1976b; Borowitzka, 1977; Sikes et al., 1980; Reiskind et al., 1988, 1989; Ries, 2005a, b, 2006a, 2009; Stanley et al., 2005, 2010), thus resulting in the observed concomitant reductions in linear growth and primary productivity for these algae when grown in mineralogically unfavorable seawater.

10.4 Experimental evidence for the effect of seawater Mg/Ca on CaCO$_3$ polymorph mineralogy and Mg incorporation

The bryopsidalean algae (*Halimeda incrassata*, *Udotea flabellum*, and *Penicillus capitatus*) and the scleractinian corals produced approximately one-quarter-to-one-half and one-third, respectively, of their $CaCO_3$ as the calcite polymorph, as opposed to their normal aragonite polymorph, when grown in the experimental calcite seawater (Mg/Ca<2). Bacterial biofilms, which produce a mixture of aragonite and high Mg calcite in modern aragonite seawater, produced exclusively calcite in the experimental calcite seawater. The Mg/Ca of the calcite secreted by the *Halimeda* algae, the corals, and the biofilms varied proportionally with the Mg/Ca of the experimental seawater. The two species of coccolithophores investigated that secrete high Mg calcite in modern aragonite seawater (*Pleurochrysis carterae* and *Ochrosphaera neopolitana*), exhibited reductions in calcite Mg/Ca when grown in experimental seawaters of reduced Mg/Ca. The Mg/Ca ratio of calcite secreted by the third species of coccolithophore (*Coccolithus neohelis*), which secretes low Mg calcite even in modern aragonite seawater, was not affected by the experimental reductions in seawater Mg/Ca. The skeletal Mg/Ca of the calcite-secreting coralline algae (*Neogoniolithon* sp., *Amphiroa fragilissima*, *Amphiroa* sp. A, and *Amphiroa* sp. B) and reef-dwelling animals (the echinoid *Eucidaris tribuloides*, the crab *Perchon gibbesi*, the
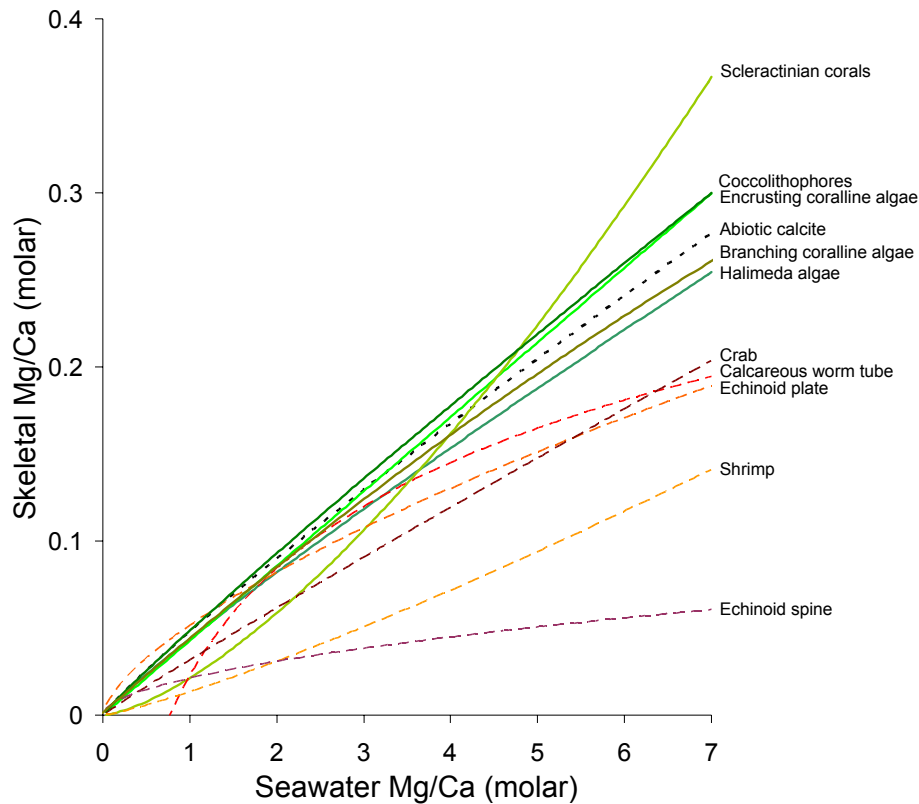
Fig. 30. The relationship between skeletal Mg/Ca and seawater Mg/Ca for organisms that secrete at least part of their skeleton as calcite. Solid lines are Mg fractionation curves for photosynthetic organisms: the two coccolithophores *Pleurochrysis carterae* and *Ochrosphaera neopolitana* (Stanley et al., 2005); the encrusting coralline red algae *Neogoniolithon* sp. (Ries, 2006b); the scleractinian corals *Porites cylindrica*, *Montipora digitata*, and *Acropora cervicornis* (Ries et al., 2006); three species of branching coralline algae of the genus *Amphiroa* (Stanley et al., 2002); and the bryopsidalean alga *Halimeda incrassata* (Stanley et al., 2010). Dotted line is Mg fractionation curve for abiotic calcite (Füchtbauer and Hardie, 1976). Dashed lines are Mg fractionation curves for non-photosynthetic organisms: the echinoid *Eucidaris tribuloides*; the crab *Perchon gibbesi*; the shrimp *Palaemonetes pugio*; and the calcareous serpulid worm *Hydroides crucigera* (Ries, 2004). Photosynthetic organisms appear to be more influenced by ambient seawater Mg/Ca than non-photosynthetic ones. From Ries (2006b).

shrimp *Palaemonetes pugio*, the calcareous serpulid worm *Hydroides crucigera*) varied proportionally with Mg/Ca of the experimental seawater in which these organisms were reared.

10.5 Implications for biomineralogical control

The bryopsidalean algae's and scleractinian corals' precipitation of a mostly aragonitic skeleton, even in seawater that favors the abiotic precipitation of calcite, suggests that these organisms exert significant control over their biomineralization. However, the precipitation of one-quarter to one-half of the algae's CaCO$_3$ and one-third of the corals' CaCO$_3$ as the calcite polymorph, as opposed to the normal aragonite polymorph, suggests that the algae's and corals' biomineralogical control is somewhat limited and can be partially overridden by ambient seawater chemistry (Ries, 2005b).

Likewise, the observed influence of seawater Mg/Ca on the skeletal Mg/Ca of two of the three species of

coccolithophores, the coralline red algae, and the calcite-secreting animals suggests that although these organisms are capable of specifying precipitation of the calcite polymorph, even in seawater that favors the abiotic precipitation of aragonite, their biomineralogical control is limited in its ability to prevent Mg incorporation in that calcite. However, the deviation of many of these organisms' Mg fractionation patterns from that of abiotic calcite, combined with variations in Mg fractionation observed amongst closely related genera and species, and even between different anatomical components within single organisms, suggests that these organisms are exerting substantial biological control over their calcification processes (Ries, 2005b). Although Chave (1954) correlated taxonomic complexity with temperature-driven Mg fractionation in calcifying organisms, a similar correlation could not be unequivocally established here for seawater Mg/Ca-driven Mg fractionation. However, as a general rule, Mg fractionation within the photosynthetic organisms (coccolithophores, corals, coralline algae, bryopsidalean algae)

appears to be more strongly influenced by ambient Mg/Ca than Mg fractionation within the non-photosynthetic ones (echinoids, crabs, shrimp and calcareous serpulid worms; Fig. 30). This increased susceptibility of photosynthetic organisms to seawater Mg/Ca suggests that autotrophic calcifers *induce* precipitation of $CaCO_3$ through the removal of CO_2, thereby resembling abiotic calcification to a greater extent than the more regulated heterotrophic calcifiers, which apparently *control* calcification to a greater extent via ionic pumping and/or organic mineral templates (Ries, 2005b).

10.6 Implications for marine biological calcification throughout Phanerozoic time

The elevated rates of calcification and growth observed for the bryopsidalean algae and scleractinian corals grown in the experimental aragonite seawaters (Mg/Ca>2), and for the coccolithophores grown in the experimental calcite seawaters (Mg/Ca<2), supports the paleontological evidence (Stanley and Hardie 1998, 1999; Porter, 2007; Kiessling et al., 2008) that oceanic Mg/Ca was an important factor in determining the role that these organisms played in sediment production and reef building throughout Phanerozoic time. The elevated primary productivity and calcification of the coccolithophores in the experimental calcite seawater is particularly significant given its occurrence in the experimental treatment (Mg/Ca=1.0) that deviated most from what modern coccolithophores are accustomed (Mg/Ca=5.2). The link between calcification and growth in the photosynthetic organisms – via CO_2 liberation – suggests that autotrophic calcifers would have been most influenced by secular variations in the Mg/Ca ratio of seawater throughout Phanerozoic time (Ries, 2005b).

The correlation observed between skeletal Mg/Ca and seawater Mg/Ca for the coccolithophores, the coralline red algae, and the calcite-secreting animals supports the assertion that the skeletal Mg/Ca of organisms that secrete high Mg calcite in modern seas has varied in synchroneity with oceanic Mg/Ca throughout Phanerozoic time (Stanley and Hardie, 1998, 1999). The secretion of low Mg calcite by each of these organisms in the experimental calcite seawater (Mg/Ca<2) suggests that they would have secreted low Mg calcite in ancient calcite seas, such as those reported for middle Paleozoic and mid-Late Cretaceous time. The wide range of organisms that exhibit this proportionality between skeletal and seawater Mg/Ca suggests that this is a universal trend for organisms that secrete high Mg calcite in modern seas.

10.7 Paleoceanographic reconstructions

The observed relationship between seawater Mg/Ca and skeletal Mg incorporation in the coccolithophores, the coralline algae, the calcite-secreting animals, and the calcitic portions of the scleractinian corals, the bryopsidalean algae,

and the bacterial biofilms suggests that well-preserved fossils of these organisms may be an archive of oceanic Mg/Ca throughout Phanerozoic and Precambrian time. Likewise, the reconstruction of ancient seawater temperatures from skeletal Mg/Ca ratios must correct for the effect of secular variation in the Mg/Ca ratio of seawater. Mg fractionation algorithms that define skeletal Mg/Ca as a function of seawater Mg/Ca and temperature were derived for organisms evaluated in each of the reviewed experiments. Care must be exercised in the application of these proxies for reconstructing paleoseawater Mg/Ca, especially for fossils whose Mg fractionation algorithms cannot be calibrated with extant representatives. The accuracy of these algorithms may also be limited by other factors that may have influenced biogenic Mg fractionation in the past, yet are not incorporated into the proxy model (e.g., variations in growth rates, fluctuations of other ions in seawater). Nevertheless, oceanic Mg/Ca ratios calculated from the Mg content of fossil echinoderms, established paleotemperature data, and the echinoid Mg fractionation algorithm (Ries, 2004) are in general agreement with other independent estimates of oceanic Mg/Ca throughout Phanerozoic time.

Edited by: J.-P. Gattuso

References

Adey, W. H. and Macintyre, I. G.: Crustose coralline algae: a re-evaluation in the geological sciences, Geol. Soc. Am. Bull., 84, 883–904, 1973.

Agegian, C. R.: The biogeochemical ecology of *Porolithon gardineri* (Foslie), PhD thesis, University of Hawaii, 2005.

Aguirre, J. and Riding, R.: Dasycladalean algal biodiversity compared with global variations in temperature and sea level over the past 350 Myr, Palaios, 20, 581–588, 2005.

Aguirre, J., Riding, R., and Braga, J. C.: Diversity of coralline red algae: origination and extinction patterns from the Early Cretaceous to the Pleistocene, Paleobiology, 26, 651–667, 2000.

Alexandersson, T.: Carbonate cementation in Recent coralline algal constructions, in: Fossil Algae: Recent Result and Developments, edited by: Flugel, E., Springer-Verlag, Berlin, 261–269, 1977.

Al-Horani, F. A., Al-Moghrabi, S. M., and De Beer, D.: The mechanism of calcification and its relation to photosynthesis and respiration in the scleractinian coral *Galaxea fascicularis*, Mar. Biol., 142, 419–426, 2003.

Altermann, W., Kazmierczak, J., Oren, A., and Wright, D. T.: Cyanobacterial calcification and its rock-building potential during 3.5 billion years of Earth history, Geobiology, 4, 147–166, 2006.

Andersson, A. J., Mackenzie, F. T., and Bates, N. R.: Life on the margin: implications of ocean acidification on Mg-calcite, high latitude and cold-water marine calcifiers, Mar. Ecol.-Prog. Ser., 373, 265–273, 2008.

Andersson, A. J., Bates, N. R., and Mackenzie, F. T.: Dissolution of carbonate sediments under rising pCO$_2$ and ocean acidification: Observations from Devil's Hole, Bermuda, Aquat. Geochem., 13, 237–264, 2007.

Andersson, A. J., Mackenzie, F. T., and Lerman, A.: Coastal ocean CO$_2$–carbonic acid–carbonate sediment system of the Anthropocene, Global Biogeochem. Cycles, 20, GB1S92, doi:10.1029/2005GB002506, 2006.

Andersson, A. J., Mackenzie, F. T., and Ver, L. M.: Solution of shallow-water carbonates: An insignificant buffer against rising atmospheric CO$_2$, Geology, 31, 513–516, 2003.

Arp, G., Reimer, A., and Reitner, J.: Photosynthesis-induced biofilm calcification and calcium concentrations in Phanerozoic oceans, Science, 292, 1701–1704, 2001.

Awramik, S. M.: Precambrian columnar stromatolite diversity: Reflection of metazoan appearance, Science, 174, 825–827, 1971.

Axelsson, L., Mercado, J. M., and Figueroa, F. L.: Utilization of HCO$_3^-$ at high pH by the brown macroalga *Laminaria saccharina*, Eur. J. Phycol., 35, 53–59, 2000.

Bach, S. D.: Standing crop, growth and production of calcareous Siphonales (Chlorophyta) in a south Florida lagoon, Bull. Mar. Sci., 29, 191–201, 1979.

Badger, M. R. and Price, G. D.: The Role of Carbonic Anhydrase in Photosynthesis, Annu. Rev. Plant Physiol. Plant Mol. Biol., 45, 369–392, 1994.

Barattolo, F.: Mesozoic and Cenozoic marine benthic calcareous algae with particular regard to Mesozoic dasycladaleans, in: Calcareous Algae and Stromatolites, edited by: Riding, R., Springer-Verlag, Berlin, 504–540, 1991.

Barnes, D. J.: Coral skeletons: An explanation of their growth and structure, Science, 170, 1305–1308, 1970.

Bassoullet, E., Bernier, P., Genot, P., Poncet, P., and Roux, A.: Les algues Udoteacees du Paleozoique au Cenozoique, B. Cent. Rech. Expl., 7, 449–621, 1983.

Bates, N. R. and Brand, U.: Secular variation of calcium carbonate mineralogy; an evaluation of ooid and micrite chemistries, Int. J. Earth Sci., 79, 27–46, 1990.

Bathurst, R. G. C.: Carbonate sediments and their diagenesis, Elsevier, Amsterdam, 658 pp., 1975.

Baumgartner, L., Reid, R., Dupraz, C., Decho, A., Buckley, D., Spear, J., Przekop, K., and Visscher, P.: Sulfate reducing bacteria in microbial mats: Changing paradigms, new discoveries, Sediment. Geol., 185, 131–145, 2006.

Baumiller, T. K. and Ausich, W. I.: Crinoid stalk flexibility: theoretical predictions and fossil stalk postures, Lethaia, 29, 47–59, 1996.

Bellis, S., Davis, J. P., and Stephens, G. C.: The lack of an effect of magnesium on the uptake of amino acids by the sea urchin *Strongylocentrotus purpuratus*, J. Exp. Zool., 244, 383–388, 1987.

Bernecker, M.: Upper Triassic reefs of the Oman Mountains: data from the south Tethyan margin, Facies, 34, 41–76, 1996.

Berner, R. A.: The role of magnesium in the crystal growth of calcite and aragonite from sea water, Geochim. Cosmochim. Ac., 39, 489–504, 1975.

Berner, R. A.: The rise of land plants and their effect on weathering and atmospheric CO$_2$, Science, 291, 339–376, 1997.

Berner R. A.: A model for calcium, magnesium, and sulfate in seawater over Phanerozoic time, Am. J. Sci., 304, 438–453, 2004.

Berner, T.: Coral-reef algae, in: Coral Reefs, edited by: Dubinsky, Z., Elsevier, Amsterdam, 253–264, 1990.

Berner, R. A. and Kothavala, Z.: Geocarb III: A revised model of atmospheric CO$_2$ over Phanerozoic time, Am. J. Sci., 301, 182–204, 2001.

Bidwell, J. P. and Spotte, S.: Artificial Seawaters: Formulas and Methods, Jones and Bartlett, Boston, 349 pp., 1985.

Bischoff, W. D., Bishop, F. C., and Mackenzie, F. T.: Biogenically produced magnesian calcite: inhomogeneities in chemical and physical properties: comparison with synthetic phases, Am. Min., 68, 1183–1188, 1983.

Bischoff, J. L. and Fyfe, W. S.: Catalysis, inhibition, and the calcite-aragonite problem: 1. The aragonite-calcite transformation, Am. J. Sci., 266, 65–79, 1968

Blair, S. M. and Norris, J. N.: The deep-water species of *Halimeda Lamouroux* (Halimedaceae, Chlorophyta) from San Salvador Island, Bahamas: species composition, distribution and depth records, Coral Reefs, 6, 227–236, 1988.

Böhm, L., Fütterer, D., and Kaminski, E.: Algal calcification in some Codiaceae (Chlorophyta): ultrastructure and location of skeletal deposits, J. Phycol., 14, 486–493, 1978.

Borowitzka, M. A.: Mechanisms in algal calcification, Phycol. Res., 1, 137–177, 1982a.

Borowitzka, M.: Morphological and cytological aspects of algal calcification, Int. Rev. Cytol., 74, 127–162, 1982b.

Borowitzka, M. A.: Algal calcification, Oceanogr. Mar. Biol., 15, 189–223, 1977.

Borowitzka, M. A.: Calcification in aquatic plants, Plant Cell Environ., 7, 457–466, 1984.

Borowitzka, M. A.: Calcification in algae – mechanisms and the role of metabolism, Crit. Rev. Plant Sci., 6, 1–45, 1987.

Borowitzka, M. A. and Larkum, A. W. D.: Calcification in the green alga *Halimeda*. II. The exchange of Ca^{2+} and the occurrence of age gradients in calcification and photosynthesis, J. Exp. Bot., 27, 864–878, 1976a.

Borowitzka, M. A. and Larkum, A. W. D.: Calcification in the green alga *Halimeda*. III. The sources of inorganic carbon for photosynthesis and calcification and a model of the mechanism of calcification, J. Exp. Biol., 27, 879–893, 1976b.

Borowitzka, M. A. and Larkum, A. W. D.: Calcification in the green alga *Halimeda*. I. An ultrastructure study of thallus development, J. Phycol., 13, 6–16, 1977.

Borowitzka, M. A., Larkum, W. D., and Nockolds, C. E.: A scanning electron microscope study of the structure and organization of the calcium carbonate deposits of algae, Phycologia, 13, 195–203, 1974.

Borremans, C., Hermans, J., Baillon, S., André, L., and Dubois, P.: Salinity effects on the Mg/Ca and Sr/Ca in starfish skeletons and the echinoderm relevance for paleoenvironmental reconstructions, Geology, 37, 351–354, 2009.

Bosak, T. and Newman, D. K.: Microbial kinetic controls on calcite morphology in supersaturated solutions, J. Sediment. Res., 75, 190–199, 2005.

Brand, U.: Aragonite-calcite transformation based on Pennsylvanian molluscs, Geol. Soc. Am. Bull. 101, 377–390, 1989.

Brennan, S. T.: The major-ion evolution of seawater: Fluid inclusion evidence from terminal Proterozoic, Early Cambrian, Silurian, and Tertiary marine halites, Ph.D. thesis, State University of New York, Binghamton, New York, 186 pp., 2002.

Brennan, S. T. and Lowenstein, T. K.: The major-ion composition of Silurian seawater, Geochim. Cosmochim. Ac., 66, 2683–2700, 2002.

Brennan, S. T., Lowenstein, T. K., and Horita, J.: Seawater chemistry and the advent of biocalcification, Geology, 32, 473–476, 2004.

Brewer, P. G.: Ocean chemistry of the fossil fuel CO_2 signal: The haline signal of "business as usual", Geophys. Res. Lett., 24, 1367–1369, 1997.

Bucur, I. I.: Lower Cretaceous Halimedaceae and Gymnocodiaceae from southern Carpatians and Apuseni Mountains (Romania) and the systematic position of the Gymnocodiaceae, Beitrage zur Palaontologie, 13–37, 1994.

Burns, B. P., Goh, F., Allen, M., and Neilan, B. A.: Microbial diversity of extant stromatolites in the hypersaline marine environment of Shark Bay, Australia, Environ. Microbiol., 6, 1096–1101, 2004.

Burton, E. A. and Walter, L. M.: The effect of pCO2 and temperature on magnesium incorporation in calcite in seawater and $MgCl_2$-$CaCl_2$ solutions, Geochim. Cosmochim. Ac., 55, 777–785, 1991.

Canfield, D. E., Habicht, K. S., and Thamdrup, B.: The Archean sulfur cycle and the early history of atmospheric oxygen, Science, 288, 658–661, 2000.

Chalker, B. E.: Calcium-transport during skeletogenesis in hermatypic corals, Comp. Biochem. Physiol., 54, 455–459, 1976.

Chapman, F. and Mawson, D.: On the Importance of Halimeda as a Reef-Forming Organism: with a Description of the Halimeda-Limestones of the New Hebrides, Q. J. Geol. Soc., 62, 702–711, 1906.

Chave, K. E.: Aspects of the biogeochemistry of magnesium, 1. Calcareous marine organisms, J. Geol., 62, 266–283, 1954.

Checa, A. G., Jiménez-López, C., Rodríguez-Navarro, A., and Machado, J. P.: Precipitation of aragonite by calcitic bivalves in Mg-enriched marine waters, Mar. Biol., 150, 819–827, 2007.

Chisholm, J. R. M.: Primary productivity of reef-building crustose coralline algae, Limnol. Oceanogr., 48, 1376–1387, 2003.

Chuvashov, B. and Riding, R.: Principal floras of Palaeozoic marine calcareous algae, Palaeontology, 27, 487–500, 1984.

Cicero, A. D. and Lohman, K. C.: Sr/Mg variation during rock-water interaction: Implications for secular changes in the elemental chemistry of ancient seawater, Geochim. Cosmochim. Ac., 65, 741–761, 2001.

Cloud Jr., P. E.: Environment of calcium carbonate deposition west of Andros Island, Bahamas, US Geological Survey No. 350, 1962.

Cohen, A. L. and McConnaughey, T. A.: A Geochemical Perspective on Coral Mineralization, in: Biomineralization: Reviews in Mineralogy and Geochemistry, edited by: Dove, P. M., Weiner, S., and De Yoreo, J. J., 151–187, 2003.

Colinvaux, L. H.: *Halimeda copiosa* and *Halimeda hederacea*, J. Phycol., 5, 88, 1969.

Colombo, P. M.: An ultrastructural study of thallus organization in *Udotea petiolata*, Phycologia, 17, 227–235, 1978.

Conrad, M. and Rioult, M.: *Halimeda elliottii* nov. sp., algue calcaire (Chlorophyceae) du Turonien des Alpes-maritimes (SE France), Geol. Mediterran., 4, 83–98, 1977.

Cuif, J. P., Dauphin, Y., Doucet, J., Gautret, P., and Zibrowius, H.: Biochemical markers of zooxanthellae symbiosis in soluble matrices of skeleton in scleractinian coral skeletons, Geochim Cosmochim. Ac., 67, 75–83, 1999.

David, T. W. E. and Sweet, G.: The geology of Funafuti, The atoll of Funafuti: Borings into a coral reef and the results, Royal Soc. Lond., Harrison & Sons, 61–124, 1904.

Davis, K. J., Dove, P. M., and De Yoreo, J .J.: The role of Mg^{2+} as an impurity in calcite growth, Science, 290, 1134–1137, 2000.

Davis, K. J., Dove, P. M., Wasylenki, L. E., and De Yoreo, J. J.: Morphological consequences of differential Mg^{2+} incorporation at structurally distinct steps on calcite, Am. Mineral., 89, 714–720, 2004.

De Beer, D. and Larkum, A. W. D.: Photosynthesis and calcification in the calcifying algae *Halimeda discoidea* studied with microsensors, Plant Cell Environ., 24, 1209–1217, 2001.

De Choudens-Sanchez, V. and Gonzalez, L. A.: Calcite and aragonite precipitation under controlled instantaneous supersaturation: elucidating the role of $CaCO_3$ saturation state and Mg/Ca ratio on calcium carbonate polymorphism, J. Sediment. Res., 79, 363–376, 2009.

De Groot, K. and Duyvis, E. M.: Crystal form of precipitated calcium carbonate as influenced by adsorbed magnesium ions, Nature, 212, 183–184, 1966.

Deckker, P. D., Chivas, A. R., and Shelley, J. M. G.: Uptake of Mg and Sr in the euryhaline ostracod *Cyprideis* determined from in vitro experiments, Palaeogeogr., Palaeoclimatol., Palaeoecol., 148, 105–116, 1999.

Demicco, R. V., Lowenstein, T. K., and Hardie, L. A.: Atmospheric pCO_2$ since 60 Ma from records of seawater pH, calcium, and primary carbonate mineralogy, Geology, 31, 793–796, 2003.

Demicco, R. V., Lowenstein, T. K., Hardie, L. A., and Spencer, R. J.: Model of seawater composition for the Phanerozoic, Geology, 33, 877–880, 2005.

Devery, D. M. and Ehlmann, A. J.: Morphological changes in a series of synthetic Mg calcites, Am. Mineral., 66, 592–595, 1981.

Dickson, J. A. D.: Fossil echinoderms as monitor of the Mg/Ca ratio of Phanerozoic oceans, Science, 298, 1222–1224, 2002.

Dickson, J. A. D.: Echinoderm skeletal preservation: calcite-aragonite seas and the Mg/Ca ratio of Phanerozoic oceans, J. Sediment. Res., 74, 355–365, 2004.

Drew, E. A.: *Halimeda* biomass growth rate and sediment generation on reefs in the Central Great Barrier Reef Province, Coral Reefs, 2, 101–110, 1983.

Drew, E. A. and Abel, K. M.: Studies on *Halimeda*: 1. The distribution and species composition of Halimeda meadows throughout the Great Barrier Reef Province, Coral Reefs, 6, 195–205, 1988.

Dupraz, C. and Visscher, P. T.: Microbial lithification in marine stromatolites and hypersaline mats, Trends Microbiol., 13, 429–438, 2005.

Ehrlinger, J. R. and Cerling, T. E.: Atmospheric CO_2 and the ratio of intercellular to ambient CO_2 concentrations in plants, Tree Physiol., 15, 105–111, 1995.

Elliot, G. F.: Ecological significance of post-Paleozoic green calcareous algae, Geol. Mag., 115, 437–442, 1978.

Elliot, G. F.: Climatic tolerance in some aragonitic green algae of the post-Paleozoic, Palaeogeogr., Palaeoclimatol., Palaeoecol., 48, 163–169, 1984.

Elliott, G. F.: Fossil calcareous algal floras of the Middle East with a note on a Cretaceous problematicum *Hensonella cylindrica* gen. et sp. nov, Q. J. Geol. Soc. London, 115, 217–232, 1960.

Elliott, G. F.: The interrelationships of some *Cretaceous codiaceae* (calcareous algae), Palaeontology, 8, 199–203, 1965.

Elliott, G. F.: The Tethyan dispersal of some chlorophyte algae subsequent to the Palaeozoic, Palaeogeogr., Palaeoclimatol., Palaeoecol., 32, 341–358, 1981.

Engel, A. E. J. and Engel, C. G.: Continental accretion and the evolution of North America, in: Adventures in Earth History, edited by: Cloud, P., W.H. Freeman and Co., San Francisco, 293–312, 1970.

Emery, K. O., Tracey Jr., J. I., and Ladd, H. S.: Geology of Bikini and Nearby Atolls: Professional Paper 260 A, US Government Printing Office, 255 pp., 1954.

Enmar, R., Lazar, B., Bar-Matthews, M., Sass, E., Katz, A., and Stein, M.: Diagenesis in live corals from the Gulf of Aqaba. I. The effect on paleo-oceanography tracers, Geochim. Cosmochim. Ac., 64, 3123–3132, 2000.

Feely, R. A., Sabine, C. L., Hernandez-Ayon, J. M., Ianson, D., and Hales, B.: Evidence for upwelling of corrosive "acidified" water onto the continental shelf, Science, 320, 1490–1492, 2008.

Finckh, A. E.: Biology of the reef-forming organisms at Funafuti Atoll, The Atoll of Funafuti: Borings into a coral reef and the results, Report of the Coral Reef Committee of The Royal Society, 125–150, 1904.

Flajs, G.: Skeletal structures of some calcifying algae, in: Fossil Algae, edited by: Flugel, E., Springer-Verlag, Berlin, 225–231, 1977.

Flügel, E.: *Halimeda*: paleontological record and palaeoenvironmental significance, Coral Reefs, 6, 123–130, 1988.

Flügel, E.: Triassic and Jurassic marine calcareous algae: A critical review, in: Calcareous Algae and Stromatolites, edited by: Riding, R., Springer-Verlag, Berlin, 481–503, 1991.

Folk, R. L.: The natural history of crystalline calcium carbonate: effect of magnesium content and salinity, J. Sediment. Petrol., 44, 40–53, 1974.

Freeman, K. H. and Hayes, J. M.: Fractionation of carbon isotopes by phytoplankton and estimates of ancient CO_2 levels, Global Biogeochem. Cycles, 6, 185–198, 1992.

Freile, D. and Hillis, L.: Carbonate Productivity by *Halimeda incrassata* in a land proximal lagoon, Pico Feo, San Blas, Panamá, Proc. 8th Int. Coral Reef Symp., 767–772, 1997.

Freile, D., Milliman, J. D., and Hillis, L.: Leeward bank margin *Halimeda* meadows and draperies and their sedimentary importance on the western Great Bahama Bank slope, Coral Reefs, 14, 27–33, 1995.

Friedman, E. I., Roth, W. C., Turner, J. B., and McEwin, R. S.: Calcium oxalate crystals in the aragonite-producing green alga *Penicillus* and related genera, Science, 177, 891–893, 1972.

Fritsch, F. E.: The Structure and Reproduction of the Algae, Cambridge University Press, Cambridge, 402–413, 1948.

Frost, S. H.: Miocene to Holocene evolution of Caribbean Province reef-building corals, Proc. 3rd Int. Coral Reef Symp., 353–355, 1977.

Frost, S. H.: Oligocene reef coral biofacies of the Vicentin, Northeast Italy in: Fossil Reef Models, edited by: Toomey, D. F., Soc. Econ. Pa., Special Publications, 483–539, 1981.

Füchtbauer, H. and Hardie, L. A.: Experimentally determined homogeneous distribution coefficients for precipitated magnesian calcites: application to marine carbonate cements, Geol. Soc. Am. Abstr. Prog., 8, 877, 1976.

Füchtbauer, H. and Hardie, L. A.: Comparison of experimental and natural magnesian calcites, Int. As. Sed., Bochum, 167–169, 1980.

Gaffin, S.: Ridge volume dependence on seafloor generation rate and inversion using long term sealevel change, Am. J. Sci., 287, 596–611, 1987.

Garrels, R. M. and Mackenzie, F. T.: Evolution of Sedimentary Rocks, Norton, New York, 397 pp., 1971.

Garrigue, C.: Repartition and production organic et minerale de macrophytes benthiques du Lagon de Nouvelle-Caledonie, PhD Thesis, Universite des Sciences et Techniques du Languedoc, 270 pp., 1985.

Gattuso, J. P., Frankignoulle, M., Bourge, I., Romaine, S., and Buddemeier, R. W.: Effect of calcium carbonate saturation of seawater on coral calcification, Global Planet. Change, 18, 37–46, 1998.

Gattuso, J. P., Allemand, D., and Frankignoulle, M.: Photosynthesis and calcification at cellular, organismal and community levels in coral reefs: a review on interactions and control by carbonate chemistry, Integr. Comp. Biol., 39, 160–183, 1999.

Gattuso, J.-P., Reynaud-Vaganay, S., Furla, P., Romaine-Lioud, S., Jaubert, J., Bourge, I., and Frankignoulle, M.: Calcification does not stimulate photosynthesis in the zooxanthellate scleractinian coral *Stylophora pistillata*, Limnol. Oceanogr., 45, 246–250, 2000.

Gaylord, E. H. and Gaylord, C. N.: Structural Engineering Handbook. McGraw-Hill, New York, 600 pp., 1990.

Ginsburg, R. N.: Environmental relationships of grain size and constituent particles in some South Florida carbonate sediments, AAPG Bull., 40, 2384–2427, 1956.

Given, R. K. and Wilkinson, B. H.: Kinetic control of morphology, composition, and mineralogy of abiotic sedimentary carbonates, J. Sediment. Res., 55, 109–119, 1985.

Glover, E. D. and Sippel, R. F.: Synthesis of magnesium calcites. Geochim. Cosmochim. Ac., 31, 603–614, 1967.

Golonka, J., Ros, M. I., and Scotese, C. R.: Phanerozoic paleogeographic and paleoclimatic modeling maps, in: Pangea: Global Environments and Resources, edited by: Embry, A. R., Beaucamp, B., and Glass, D. J., Canadian Society of Petroleum Geologists, Calgary, 1–47, 1994.

Goreau, T. F. and Goreau, N. I.: The ecology of Jamaican coral reefs. II. Geomorphology, zonation, and sedimentary phases, B. Mar. Sci., 23, 399–464, 1973.

Granier, B., Villain, J. M., and Boichard, R.: Biohermes holocènes à *Halimeda* au large du delta de la Mahakam, Kalimantan (Indonésie) – Le concept de section condensée dilatée, Carbonates intertropicaux. Actes de la Réunion spécialisée de Soc. Géol.

France, 3, 225–230, 1997.

Grotzinger, J. P.: Facies and evolution of Precambrian carbonate depositional systems: Emergence of the modern platform archetype, in: Controls on Carbonate Platform and Basin Development, edited by: Crevello, P. D., Wilson, J. L., Saro, J. F., and Read, J. F., Soc. Econ. Pa, 44, 79–106, 1989.

Grotzinger, J. P. and James, N. P.: Precambrian carbonates: Evolution of understanding, in: Carbonate Sedimentation and Diagenesis in the Evolving Precambrian World, edited by: Grotzinger, J. P. and James, N. P., SEPM Spec. P., 67, 3–20, 2000.

Grotzinger, J. P. and Kasting, J. F.: New constraints on Precambrian ocean composition, J. Geol., 101, 235–243, 1993.

Grotzinger, J. P. and Knoll, A. H.: Stromatolites in Precambrian carbonates: evolutionary mileposts or environmental dipsticks?, Annu. Rev. Earth Pl. Sc., 27, 313–358, 1999.

Grotzinger, J. P. and Reed, J. F.: Evidence for Primary Aragonite Precipitation, Lower Proterozoic (1.9 Ga) Rocknest Dolomite, Wopmay Orogen, Northwest Canada. Geology 11, 710–713, 1983.

Habicht, K. S., Gade, M., Thamdrup, B., Berg, P., and Canfield, D. E.: Calibration of sulfate levels in the Archean Ocean, Science, 298, 2372–2374, 2002.

Halfar, J., Zack, T., Kronz, A., and Zachos, J. C.: Growth and high-resolution paleoenvironmental signals of rhodoliths (coralline red algae): A new biogenic archive, J. Geophys. Res.-Oceans, 105, 22107–22116, 2000.

Halligan, G. H.: Report of lagoon borings, The Atoll of Funafuti.Borings into a coral reef and the results. Report of the Coral Reef Committee of The Royal Society, 160–164, 1904.

Halverson, G. P., Hoffman, P. F., Schrag, D. P., Maloof, A. C., and Rice, A. H. N.: Toward a Neoproterozoic composite carbon-isotope record, Geol. Soc. Am. Bull., 117, 1181–1207, 2005.

Hardie, L. A.: Secular variation in seawater chemistry: an explanation for the coupled secular variation in the mineralogies of marine limestones and potash evaporites over the past 600 m.y., Geology, 24, 279–283, 1996.

Harper, E. M., Palmer, T. J., and Alphey, J. R.: Evolutionary response by bivalves to changing Phanerozoic sea-water chemistry, Geol. Mag., 134, 403–407, 1997.

Harris, P. T., Pattiaratchi, C. B., Keene, J. B., Dalrymple, R. W., Gardner, J. W., Barker, E. K., Cole, A. R., Mitchell, D., Gibbs, P., and Schroeder, W. W.: Late Quaternary deltaic and carbonate sedimentation in the Gulf of Papua foreland basin; response to sea-level change, J. Sediment. Res., 66, 801–819, 1996.

Hart, S. R. and Cohen, A. L.: Sr/Ca in corals: An ion microprobe study of annual cycles and microscale coherence with other trace elements, Geochim.Cosmochim. Ac., 60, 3075–3084, 1996.

Hartley, G. and Mucci, A.: The influence of pCO$_2$ on the partitioning of magnesium in calcite overgrowths precipitated from artificial seawater at 25 C and 1 atm total pressure, Geochim. Cosmochim. Ac., 60, 315–324, 1996.

Hasiuk, F. J. and Lohmann, K. C.: Mississippian paleocean chemistry from biotic and abiotic carbonate, Muleshoe Mound, Lake Valley Formation, New Mexico, U.S.A., J. Sediment. Res., 78, 147–164, 2008.

Hattin, D. E.: Cretaceous shelf-sea chalk deposits: a global synthesis, Amer. Assoc. Petr. Geol. B., 72, 195–196, 1988.

Hay, M. E.: Calcified seaweeds on coral reefs: complex defenses, trophic relationships, and value as habitats, Proc. 8th Int. Coral Reef Symp., 713–718, 1997.

Hay, M. E., Kappel, Q. E., and Fenical, W.: Synergism in plant defenses against herbivores: interactions of chemistry, calcification and plant quality, Ecology, 75, 1714–1726, 1994.

Hay, M. E., Paul, V. J., Lewis, S. M., Gustafson, K., Tucker, J., and Trindell, R. N.: Can tropical seaweeds reduce herbivory by growing at night? Diel patterns of growth, nitrogen content, herbivory, and chemical versus morphological defenses, Oecologia, 75, 233–245, 1988.

Hayashi, Y. and Motokawa, T.: Effects of ionic environment on viscosity of catch connective tissue in the Holothurian body wall. J. Exp. Biol., 125, 71–84, 1986.

Heiri, O. O., Lotter, A. F., and Lemcke, G.: Loss on ignition as a method for estimating organic and carbonate content in sediments: reproducibility and comparability of results, J. Paleolimnol., 25, 101–110, 2001.

Hellblom, F., Beer, S., Bjoerk, M., and Axelsson, L.: A buffer sensitive inorganic carbon utilisation system in *Zostera marina*, Aquat. Bot., 69, 55–62, 2001.

Hellblom, F. and Axelsson, L.: External HCO$_3^-$ dehydration maintained by acid zones in the plasma membrane is an important component of the photosynthetic carbon uptake in *Ruppia cirrhosa*, Photosynth. Res., 77, 173–181, 2003.

Heyward, A. J., Pinceratto, E. J., and Smith, L. D.: Big Bank Shoals of the Timor Sea: An Environmental Resource Atlas, Australian Institute of Marine Science and BHP Petroleum, Townsville, Australia, 115 pp., 1997.

Hillis, L. W.: A revision of the genus *Halimeda* (order Siphonales), Publ. Inst. Mar. Sci.., Univ. of Texas, 6, 321–403, 1957.

Hillis, L. W.: The calcareous reef alga *Halimeda* (Chlorophyta, Byropsidales): a cretaceous genus that diversified in the Cenozoic, Palaeogeogr., Palaeoclimatol., Palaeoecol., 166, 89–100, 2001.

Hillis, W. L.: Phylogeny of *Halimeda* (Bryopsidales): Linking paleontolgical, morphological and molecular data, Acta Palaeontol. Rom., 2, 183–189, 2000.

Hillis, L.: Recent calcified halimedaceae, in: Calcareous Algae and Stromatolites, edited by: Riding, R., Springer-Verlag, Berlin, 167–188, 1991.

Hillis-Colinvaux, L.: Ecology and taxonomy of *Halimeda*: Primary producer of coral reefs, in: Advances in Marine Biology 11, edited by: Blaxter, J. H. S, Russell, F. S., and Yonge, M., 1–327, 1980.

Hine, A. C., Hallock, P., Harris, M. W., Mullins, H. T., Belknap, D. F., and Jaap, W. C.: *Halimeda* bioherms along an open seaway: Miskito Channel, Nicaraguan Rise, SW Caribbean Sea, Coral Reefs, 6, 173–178, 1988.

Høeg, O. A.: Preliminary note on a new Codiaceae from the Ordovician of Norway, Avh Nors Vidensk Akad Oslo, Mat. Naturviss, 4, 1–15, 1927.

Hoegh-Guldberg, O., Mumby, P. J., Hooten, A. J., Steneck, R. S., Greenfield, P., Gomez, E., Harvell, C. D., Sale, P. F., Edwards, A. J., Caldeira, K., Knowlton, N., Eakin, C. M., Iglesias-Prieto, R., Muthiga, N., Bradbury, R. H., Dubi, A., and Hatziolos, M. E.: Coral reefs under rapid climate change and ocean acidification, Science, 318, 1737–1742, 2007.

Horita, J., Zimmermann, H., and Holland, H. D.: Chemical evolution of seawater during the Phanerozoic: Implications from the record of marine evaporites, Geochim. Cosmochim. Ac., 66, 3733–3756, 2002.

Hudson, J. H.: Growth rate and carbonate production in *Halimeda opuntia*: Marquesas Keys, Florida, in: Paleoalgology, edited by: Toomey, D. F. and Nitecki, M. H., Springer-Verlag, Berlin, 257–263, 1985.

Iglesias-Rodriguez, M. D., Halloran, P. R., Rickaby, E. E. M., Hall, I. R., Colmenero-Hidalgo, E., Gittins, J. R., Green, D. R. H., Tyrrell, T., Gibbs, S. J., von Dassow, P., Rehm, E., Armbrust, E. V., and Boessenkool, K. P.: Phytoplankton calcification in a high-CO_2 world, Science, 320, 336–340, 2008.

Jacobsen S. B. and Kaufman A. J.: The Sr, C and O isotopic evolution of Neoproterozoic seawater, Chem. Geol. 161, 37–57, 1999.

James, N. P., Wray, J. L., and Ginsburg, R. N.: Calcification of encrusting aragonitic algae (Peyssonneliaceae): implications for the origin of Late Paleozoic reefs and cements, J. Sediment. Petrol., 58, 291–303, 1988.

Johnson, J. H.: Limestone-building algae and algal limestones, PhD Thesis, Colorado School of Mines, 297 pp., 1961.

Jux, U.: Palaeoporella in Boda-Kalk von Dalarne, Palaeontographica, 118, 153–165, 1966.

Kah, L. C., Lyons, T. W., and Frank, T. D.: Low marine sulphate and protracted oxygenation of the Proterozoic biosphere, Nature, 431, 834–838, 2004.

Kangwe, J. W.: Calcareous Algae of a Tropical Lagoon: Primary Productivity, Calcification and Carbonate Production, M.S. Thesis, Stockholm University, Department of Botany, Stockholm, 47 pp., 2006.

Katz, A.: The interaction of magnesium with calcite during crystal growth at 25–90 °C and one atmosphere, Geochim. Cosmochim. Ac., 37, 1563–1586, 1973.

Kauffman, E. G. and Johnson, C. C.: The morphological and ecological evolution of Middle and Upper Cretaceous reef-building rudistids, Palaios, 3, 194–216, 1988.

Kazmierczak, J. and Kempe, S.: Calcium buildup in the Precambrian Sea: A major promoter in the evolution of eukaryotic life, in: Origins, edited by: Seckbach, J., Kluwer Academic Publishers, Netherlands, 329–345, 2004.

Kempe, S. and Degens, E. T.: An early soda ocean?, Chem. Geol., 53, 95–108, 1985.

Kiessling, W., Aberhan, M., and Villier, L.: Phanerozoic trends in skeletal mineralogy driven by mass extinctions, Nat. Geosci., 1, 527–530, 2008.

Kirkland, B. C., Moore, C. H., and Dickson, J. A. D.: Well-preserved aragonitic phylloid algae (*Eugonophyllum*, Udoteaceae) from the Pennsylvanian Holder formation, Sacramento Mountains, NM, Palaios, 8, 111–120, 1993.

Kitano, Y., and Kanamori, N.: Synthesis of magnesium calcites at low temperatures and pressures, J. Geochem., 1, 1–11, 1966.

Kleypas, J. A., Feely, R. A., Fabry, V. J., Langdon, C., Sabine, C. S., and Robbins, L. L.: Impacts of Ocean Acidification on Coral Reefs and Other Marine Calcifiers: A Guide for Future Research, NSF, NOAA, and the US Geological Survey, 89 pp., 2006.

Knoll, A. H. and Semikhatov, M. A.: The genesis and time distribution of two distinctive Proterozoic stromatolite microstructures, Palaios, 13, 408–422, 1988.

Kooistra, W. H. C. F.: Molecular phylogenies of Udoteacea (Bryopsidales, Chlorophyta) reveal nonmonophyly for *Udotea*, *Penicillus* and *Chlorodemsis*, Phycologia, 41, 453–462, 2002.

Kooistra, W. H. C. F., Coppejans, E. G. G., and Payri, C.: Molecular systematics, historical ecology, and phylogeography of *Halimeda* (Bryopsidales), Mol. Phylogenet. Evol., 24, 121–138, 2002.

Kooistra, W. H. C. F. and Verbruggen, H.: Genetic patterns in the calcified tropical seaweeds *Halimeda opuntia*, *H. distorta*, *H. hederacea*, and *H. minima* (Bryopsidales, chlorophyta) provide insights in species boundaries and interoceanic dispersal, J. Phycol., 41, 177–187, 2005.

Lahann, R. W.: Chemical model for calcite crystal growth and morphology control, J. Sediment. Petrol., 48, 337–343, 1978.

Lafon, M. G. and Mackenzie, F. T.: Early evolution of the oceans: A weathering model, in: Studies in Paleoceanography, edited by: Hay, W. W., Soc. Econ. Pa., 20, 205–218, 1974.

Langdon, C. and Atkinson, M. J.: Effect of elevated pCO$_2$ on photosynthesis and calcification of corals and interactions with seasonal change in temperature/irradiance and nutrient enrichment, J. Geophys. Res., 110, C09S07, doi:10.1029/2004JC002576, 2005.

Langdon, C., Takahashi, T., Sweeney, C., Chipman, D., Goddard, J., Marubini, F. Aceves, H., Barnett, H., and Atkinson, M. J.: Effect of calcium carbonate saturation state on the calcification rate of an experimental coral reef, Global Biogeochem. Cycles, 14, 639–654, 2000.

Lasemi, Z. and Sandberg, P. A.: Linked cyclic changes in Phanerozoic ocean atmosphere composition and original mineralogy of micritic limestones, Geol. Soc. Am. Abstr. Prog., 32, A68, 2000.

Lasemi, Z. and Sandberg, P.: Transformation of aragonite-dominated lime muds to microcrystalline limestones, Geology, 12, 420–423, 1984.

Lasemi, Z. and Sandberg, P.: Microfabric and compositional clues to dominant mud mineralogy of micrite precursors, in: Carbonate Microfabrics, edited by: Rezak, R. and Lavoie, D. L., Springer Verlag, New York, 173–185, 1993.

Lasemi, Z. and Sandberg, P.: Temporal trends in the mineralogy of Phanerozoic micrite precursors. SEPM Annual Meeting (abstract), 1994.

Lear, C. H., Elderfield, H., and Wilson, P. A.: Cenozoic deep-sea temperatures and global ice volumes from Mg/Ca in benthic foraminiferal calcite, Science, 287, 269–272, 2000.

Lee, J. and Morse, J. W.: Influences of alkalinity and pCO$_2$ on CaCO$_3$ nucleation from estimated Cretaceous composition seawater representative of "calcite seas", Geology, 38, 115–118, 2010.

Leitmeier, H.: Zur kenntnis der carbonate, die dimorphie des Kohlensauren Kalkes. I. Teil, Neues Jb. Miner. Heft, 1, 49–74, 1910.

Leitmeier, H.: Zur kenntnis der carbonate. II. Teil, Neues Jb. Miner. Beilageband, 40, 655–700, 1915.

Leonardos, N., Read, B., Thake, B., and Young, J. R.: No mechanistic dependence of photosynthesis on calcification in the coccolithophorid *Emiliania huxleyi* (Haptophyta), J. Phycol., 45, 1046–1051, 2009.

Lippman, F.: Versuche zur Aufklarung der Bildungsbedingungen von Calcit und Aragonit, Fortschr. Mineral., 38, 156–161, 1960.

Littler, M. M.: The population and community structure of Hawaiian fringing reef crustose Corallinaceae, J. Exp. Mar. Biol. Ecol., 11, 103–120, 1973.

Lopez-Garcia, P., Kazmierczak, J., Benzerara, K., Kempe, S., Guyot, F., and Moreira, D.: Bacterial diversity and carbonate precipitation in the giant microbialites from the highly alkaline Lake Van, Turkey, Extremophiles, 9, 263–274, 2005.

Lorens, R. B. and Bender, M. L.: The impact of solution chemistry on *Mytilus edulis* calcite and aragonite, Geochim. Cosmochim. Ac., 44, 1265–1278, 1980.

Lowe, D. R.: Restricted shallow-water sedimentation of early Archean stromatolitic and evaporitic strata of the Strelley Pool Chert, Pilbara Block, Western Australia, Precambrian Res., 19, 239–283, 1983.

Loreau, J. P.: Sediments aragonitiques et leur genese, Museum National D'Histoire Naturelle, Memoires, 47, 300 pp., 1982.

Lowenstam, H. A.: Aragonite needles secreted by algae and some sedimentary implications, J. Sediment. Petrol., 25, 270–272, 1955.

Lowenstam, H. A. and Epstein, S.: On the origin of sedimentary aragonite needles of the Great Bahama Bank, J. Geol., 65, 364–375, 1957.

Lowenstein, T. K., Timofeeff, M. N., Kovalevych, V. M., and Horita, J.: The major-ion composition of Permian seawater, Geochim. Cosmochim. Ac., 69, 1701–1719, 2005.

Lowenstein, T. K., Hardie, L. A., Timofeeff, M. N., and Demicco, R. V.: Secular variation in seawater chemistry and the origin of calcium chloride basinal brines, Geology, 31, 857–860, 2003.

Lowenstein, T. K., Timofeeff, M. N., Brennan, S. T., Hardie, L. A., and Demicco, R. V.: Oscillations in Phanerozoic seawater chemistry: evidence from fluid inclusions, Science, 294, 1086–1088, 2001.

Macintyre, I. G.: Reevaluating the role of crustose coralline algae in the construction of coral reefs, Proc. 8th Int. Coral Reef Symp., 1, 725–730, 1997.

Macintyre, I. G. and Reid, R. P.: Comment on the origin of aragonite needle mud; a picture is worth a thousand words, J. Sediment. Res., 62, 1095–1097, 1992.

Macintyre, I. G. and Reid, R. P.: Crystal alteration in a living calcareous alga (*Halimeda*); implications for studies in skeletal diagenesis, J. Sediment. Res., 65, 143–153, 1995.

Mackenzie, F. T. and Agegian, C. R.: Biomineralization and tentative links to plate tectonics, in: Origin, Evolution, and Modern Aspects of Biomineralization in Plants and Animals, edited by: Crick, R. E., Plenum Press, New York, 11–28, 1989.

Mackenzie, F. T. and Pigott, J. D.: Tectonic controls of Phanerozoic sedimentary rock cycling, J. Geol. Soc. Lond., 138, 183–196, 1981.

Mackenzie, F. T., Bischoff, W. B., Bishop, F. C., Loijens, M., Schoonmaker, J., and Wollast, R.: Magnesian calcites: low-temperature occurrence, solubility and solid solution behavior, in: Carbonates: Mineralogy and Chemistry, edited by: Reeder, R. J., Mineralogical Society of America, Michigan, 97–144, 1983.

Magdans, U. and Gies, H.: Single crystal structure analysis of sea urchin spine calcites: Systematic investigations of the Ca/Mg distribution as a function of habitat of the sea urchin and the sample location in the spine, Eur. J. Mineral., 16, 261–268, 2004.

Mamet, B.: Carbonifereous calcareous algae, in: Calcareous Algae and Stromatolites, edited by: Riding, R., Springer-Verlag, Berlin, 370–451, 1991.

Mankiewicz, C.: Occurrence and paleoecologic significance of *Halimeda* in late Miocene reefs, southeastern Spain, Coral Reefs, 6, 271–279, 1988.

Marshall, A. T. and Clode, P. L.: Effect of increased calcium concentration in sea water on calcification and photosynthesis in the scleractinian coral *Galaxea fascicularis*, J. Exp. Biol., 205, 2107–2113, 2002.

Marshall, J. F. and Davies, P. J.: *Halimeda* bioherms of the Great Barrier Reef, Coral Reefs, 6, 139–148, 1988.

Marszalek, D. S.: Skeletal ultrastructure of sediment producing green algae, Proceedings of the Fourth Annual Scanning Electron Microscope Symposium II, Chicago, Illinois, 273–280, 1971.

Martin, J. M., Braga, J. C., and Riding, R.: Late Miocene *Halimeda* alga-microbial segment reefs in the marginal Mediterranean Sorbas Basin, Spain, Sedimentology, 44, 441–456, 1997.

Marubini, F., Ferrier-Pages, C., and Cuif, J. P.: Suppression of skeletal growth in scleractinian corals by decreasing ambient carbonate-ion concentration: a cross-family comparison, Pr. R. Soc. B, 270, 179–184, 2003.

Matthews, R. K.: Genesis of recent lime mud in southern British Honduras, J. Sediment. Petrol., 36, 428–454, 1966.

McConnaughey, T. A. and Whelan, J. F.: Calcification generates protons for nutrient and bicarbonate uptake, Earth Sci. Rev., 42, 95–117, 1997.

McConnaughey, T. A. and Falk, R. H.: Calcium-proton exchange during algal calcification, The Biol. Bull., 180, 185–195, 1991.

Merten, M. J.: Ecological observations of *Halimeda macroloba* Decaisne (Chlorophyta) on Guam, Micronesica, 7, 27–44, 1971.

Milliken, K. L. and Pigott, J. D.: Variation of oceanic Mg/Ca ratio through time: implication of the calcite sea, Geol. Soc. Am. Abstr. Prog.,, 9, 64–65, 1977.

Milliman, J. D.: Marine Carbonates, Springer-Verlag, Berlin, 375 pp., 1974.

Milliman, J. D.: Production and accumulation of calcium carbonate in the ocean: Budget of a nonsteady state, Global Biogeochem. Cycles, 7, 927–957, 1993.

Milliman, J. D.: Role of calcareous algae in Atlantic continental margin sedimentation, in: Fossil Algae, edited by: Flugel, E., Springer-Verlag, Berlin, 232–247, 1977.

Milliman, J. D., Gastner, M., and Muller, J.: Utilization of magnesium in coralline algae, Geol. Soc. Am. Bull., 82, 573–580, 1971.

Mishler, B. D., Lewis, L. A., Buchheim, M. A., Renzaglia, K. S., Garbary, D. J., Delwiche, C. F., Zechman, F. W., Kantz, T. S., and Chapman, R. L.: Phylogenetic relationships of the "green algae" and "bryophytes", Ann. Mo. Bot. Gard., 81, 451–483, 1994.

Mitsuguchi, T., Matsumoto, E., Abe, O., Uchida, T., and Isdale, P. J.: Mg/Ca thermometry in coral skeletons, Science, 274, 961–963, 1996.

Moberly, R.: Composition of magnesian of calcites of algae and pelecypods by electron microprobe analysis, Sedimentology, 11, 61–82, 1968.

Montañez, I. P.: Biological skeletal carbonate records changes in major-ion chemistry of paleo-oceans, P. Natl. Acad. Sci., 99, 15852–15854, 2002.

Moore, C. H., Graham, E. A., and Land, L. S.: Sediment transport and dispersal across the deep fore-reef and island slope (55 m to 305 m), Discovery Bay, Jamaica, J. Sediment. Res., 46, 174–187, 1976.

Morse, J. W., Andersson, A. J., and Mackenzie, F. T.: Initial responses of carbonate-rich shelf sediments to rising atmospheric pCO_2 and "ocean acidification": Role of high Mg-calcites, Geochim. Cosmochim. Ac., 70, 5814–5830, 2006.

Morse, J. W., Arvidson, R. S., and Lüttge, A.: Calcium carbonate formation and dissolution, Chem. Rev., 107, 342–381, 2007.

Morse, J. W. and Bender, M. L.: Partition coefficients in calcite: examination of factors influencing the validity of experimental results and their application to natural systems, Chem. Geol., 82, 265–277, 1990.

Morse, J. W. and Mackenzie, F. T.: Hadean Ocean Carbonate Geochemistry, Aquat. Geochem., 4, 301–319, 1998.

Morse, J. W., Wang, Q., and Tsio, M. Y.: Influences of temperature and Mg:Ca ratio on $CaCO_3$ precipitates from seawater, Geology, 25, 85–87, 1997.

Mu, X.: Fossil udoteaceae and gymnocodiaceae, in: Calcareous Algae and Stromatolites, edited by: Riding, R., Springer-Verlag, Berlin, 146–166, 1991.

Mucci, A.: The solubility of calcite and aragonite in seawater at various salinities, temperatures and 1 atmosphere total pressure, Am. J. Sci., 238, 780–799, 1983.

Mucci, A.: Influence of temperature on the composition of magnesian calcite overgrowths precipitated from seawater, Geochim. Cosmochim. Ac., 51, 1977–1984, 1987.

Mucci, A. and Morse, J. W.: The incorporation of Mg^{2+} and Sr^{2+} into calcite overgrowths: influence of growth rate and solution composition, Geochim.Cosmochim. Ac., 47, 217–233, 1983.

Müller, G., Irion, G., and Förstner, U.: Formation and diagenesis of inorganic Ca-Mg carbonates in the lacustrine environment, Naturwissenschaften, 59, 158–164, 1972.

Multer, H. G.: Growth rate, ultrastructure and sediment contribution of *Halimeda incrassata* and *Halimeda monile*, Nonsuch and Falmouth Bays, Antiqua, W. I., Coral Reefs, 6, 179–186, 1988.

Neumann, A. C. and Land, L. S.: Lime mud deposition and calcareous algae in the Bight of Abaco, Bahamas: A budget, J. Sediment. Petrol., 45, 763–786, 1975.

Okla, S. M.: Permian algae and algal microfacies from Unayzah, Quassim District, Saudi Arabia, Facies, 27, 217–224, 1992.

Orme, G. R., Flood, P. G., and Sargent, G. E. G.: Sedimentation trends in the lee of Outer (Ribbon) Reefs, Northern Region of the Great Barrier Reef Province, 291, 85–99, 1978.

Orme, G. R. and Salama, M. S.: Form and seismic stratigraphy of *Halimeda* banks in part of the northern Great Barrier Reef Province, Coral Reefs, 6, 131–137, 1988.

Orme, G. R., Webb, J. P., Kelland, N. C., and Sargent, G. E. G.: Aspects of the geological history and structure of the Northern Great Barrier Reef, Philos. T. Roy. Soc. A, 291, 23–35, 1978.

Paasche, E.: Biology and physiology of coccolithophorids, Annu. Rev. Microbiol., 22, 77–86, 1968.

Pagani, M., Zachos, J. C., Freeman, K. H., Tipple, B., and Bohaty, S.: Marked decline in atmospheric carbon dioxide concentrations during the Paleogene, Science, 309, 600–603, 2005.

Papineau, D., Walker, J. J., Mojzsis, S. J., and Pace, N. R.: Composition and structure of microbial communities from stromatolites of Hamelin Pool in Shark Bay, Western Australia, Appl. Environ.

Microbiol., 71, 4822–4832, 2005.

Paul, V. J. and Fenical, W.: Bioactive terpenoids from caribbean marine algae of the genera *Penicillus* and *Udotea* (Chlorophyta), Tetrahedron, 40, 2913–2918, 1984.

Paul, V. J. and Hay, M. E.: Seaweed susceptibility to herbivory: chemical and morphological correlates, Mar. Ecol. Prog. Ser., 33, 255–264, 1986.

Paul, V. J. and Van Alstyne, K. L.: Chemical defense and chemical variation in some tropical Pacific species of *Halimeda* (Halimedaceae; Chlorophyta), Coral Reefs, 6, 263–269, 1988.

Paul, V. J. and Fenical, W.: Isolation of halimedatrial: chemical defense adaptation in the calcareous reef-building alga *Halimeda*, Science, 221, 747–749, 1983.

Paul, V. J. and Van Alstyne, K. L.: Activation of chemical defenses in the tropical green algae *Halimeda* spp., J. Exp. Mar. Biol.Ecol., 160, 191–203, 1992.

Payri, C. E.: *Halimeda* contribution to organic and inorganic production in a Tahitian reef system, Coral Reefs, 6, 251–262, 1988.

Payri, C. E.: Carbonate production of some calcifying algae in a French Polynesia coral reef, Oceanograph. Lit. Rev., 42, 77–84, 1995.

Pentecost, A.: Calcification and photosynthesis in *Corallina officinalis* L. using the $^{14}CO_2$ method, Euro. J. Phycol., 13, 383–390, 1978.

Phipps, C. V. G. and Roberts, H. H.: Seismic characteristics and accretion history of Halimeda bioherms on Kalukalukuang Bank, eastern Java Sea (Indonesia), Coral Reefs, 6, 149–159, 1988.

Poncet, J.: Presence du genre *Halimeda Lamouroux*, 1812 (algue verte calcaire) dans le Permien superieur du sud Tunisien, Rev. Micropaleont., 32, 40–44, 1989.

Porter, S. M.: Seawater chemistry and early carbonate biomineralization, Science, 316, 1302, 2007.

Price, G. D. and Badger, M. R.: Inhibition by proton buffers of photosynthetic utilization of bicarbonate in *Chara corallina*, Aust. J. Plant Physiol., 12, 257–267, 1985.

Price, G. D., Badger, M. R., Bassett, M. E., and Whitecross, M. I.: Involvement of plasmalemmasomes and carbonic anhydrase in photosynthetic utilization of bicarbonate in *Chara corallina*, Aust. J. Plant Physiol., 12, 241–256, 1985.

Rao, P. and Veerya, V.: Late Quaternary *Halimeda* bioherms and aragonitic faecal pellet-dominated sediments on the carbonate platform of the western continental shelf of India, Mar. Geol., 121, 293–315, 1994.

Railsback, L. B.: Original mineralogy of carboniferous worm tubes – evidence for changing marine chemistry and biomineralization, Geology, 21, 703–706, 1993.

Rees, S. A., Opdyke, B. N., Wilson, P. A., and Henstock, T. J.: Significance of *Halimeda* bioherms to the global carbonate budget based on a geological sediment budget for the Northern Great Barrier Reef, Australia, Coral Reefs, 26, 177–188, 2007.

Reid, R. P., Visscher, P. T., Decho, A. W., Stolz, J. F., Bebout, B. M., Dupraz, C., Macintyre, I. G., Paerl, H. W., Pinckney, J. L., Prufert-Bebout, L., Steppe, T. F., and Des Marais, D. J.: The role of microbes in accretion, lamination and early lithification of modern marine stromatolites, Nature, 406, 989–992, 2000.

Reiskind, J. B. and Bowes, G.: The role of phosphoenolpyruvate carboxykinase in a marine macroalga with C4-like photosynthetic characteristics, P. Natl. Acad. Sci., 88, 2883–2887, 1991.

Reiskind, J. B., Seamon, P. T., and Bowes, G.: Alternative methods of photosynthetic carbon assimilation in marine macroalgae, Plant Physiol., 87, 686–692, 1988.

Reiskind, J. B., Seamon, P. T., and Bowes, G.: Photosynthetic responses and anatomical features of two marine macroalgae with different CO_2 compensation points, Aquat. Bot., 33, 71–86, 1989.

Riding, R.: Microbial carbonates: The geological record of calcified bacterial-algal mats and biofilms, Sedimentology, 47, 179–214, 2000.

Riding, R. and Guo., L.: Permian marine calcareous algae, in: Calcareous Algae and Stromatolites, edited by: Riding, R., Springer-Verlag, Berlin, 452–480, 1991.

Riding, R. and Liang, L. Y.: Geobiology of microbial carbonates: Metazoan and seawater saturation state influences on secular trends during the Phanerozoic, Palaeogeogr., Palaeoclimatol., Palaeoecol., 219, 101–115, 2005.

Riding, R. and Liang, L.: Seawater chemistry control of marine limestone accumulation over the past 550 million years, Rev. Esp. Micropal., 37, 1–11, 2005.

Ries, J. B.: Effect of ambient Mg/Ca ratio on Mg fractionation in calcareous marine invertebrates: A record of the oceanic Mg/Ca ratio over the Phanerozoic, Geology, 32, 981–984, 2004.

Ries, J. B.: Aragonite production in calcite seas: effect of seawater Mg/Ca ratio on the calcification and growth of the calcareous alga *Penicillus capitatus*, Paleobiology, 31, 445–458, 2005a.

Ries, J. B.: Experiments on the effect of secular variation in seawater Mg/Ca (calcite and aragonite seas) on calcareous biomineralization, PhD thesis, Johns Hopkins University, 235 p., 2005b.

Ries, J. B.: Aragonitic algae in calcite seas: Effect of seawater Mg/Ca ratio on algal sediment production, J. Sediment. Res., 76, 515–523, 2006a.

Ries, J. B.: Mg fractionation in crustose coralline algae: Geochemical, biological, and sedimentological implications of secular variation in the Mg/Ca ratio of seawater, Geochim. Cosmochim. Ac., 70, 891–900, 2006b.

Ries, J. B.: Seawater Mg/Ca controls polymorph mineralogy of microbial $CaCO_3$: a potential proxy for calcite-aragonite seas in Precambrian time, Geobiology, 6, 106–119, 2008.

Ries, J. B.: Effects of secular variation in seawater Mg/Ca ratio (calcite-aragonite seas) on $CaCO_3$ sediment production by the calcareous algae *Halimeda, Penicillus,* and *Udotea* – evidence from recent experiments and the geologic record, Terra Nova, 21, 323–339, 2009.

Ries, J. B., Stanley, S. M., and Hardie, L. A.: Scleractinian corals produce calcite, and grow more slowly, in artificial Cretaceous seawater, Geology, 34, 525–528, 2006.

Ries, J. B., Cohen, A. L., and McCorkle, D. C.: Marine calcifiers exhibit mixed responses to CO_2-induced ocean acidification, Geology, 37, 1131–1134, doi:10.1130/G30210A.1, 2009.

Rimstidt, J. D., Balog, A., and Webb, J.: Distribution of trace elements between carbonate minerals and aqueous solutions, Geochim. Cosmochim. Ac., 62, 1851–1863, 1998.

Roberts, H. H., Aharon, P., and Phipps, C. V.: Morphology and sedimentology of *Halimeda* bioherms from the eastern Java Sea (Indonesia), Coral Reefs, 6, 161–172, 1988.

Ronov, A. B.: General tendencies in evolution of composition of earth crust, ocean and atmosphere, Geochem. Int., 8, 715–743, 1964.

Roux, A.: Ordovician algae and global tectonics, in: Calcareous Algae and Stromatolites, edited by: Riding, R., Springer-Verlag, Berlin, 335–348, 1991a.

Roux, A.: Ordovician to Devonian marine calcareous algae, in: Calcareous Algae and Stromatolites, edited by: Riding, R., Springer-Verlag, Berlin, 349–369, 1991b.

Royer, D. L., Berner, R. A., Montañez, I. P., Tabor, N. J., and Beerling, D. J.: CO_2 as a primary driver of Phanerozoic climate, GSA Today, 14, 4–10, 2004.

Royer, D. L., Berner, R. A., and Beerling, D. J.: Phanerozoic atmospheric CO_2 change: evaluating geochemical and paleobiological approaches, Earth Sci. Rev., 54, 349–392, 2001.

Rushdi, A. I., Pytkowicz, R. M., Suess, E., and Chen, C. T.: The effects of magnesium to calcium ratios in artificial seawater, at different ionic products, upon induction time, and the mineralogy of calcium carbonate: a laboratory study, Geol. Rundsch., 81, 571–578, 1992.

Sandberg, P. A.: New interpretations of Great Salt Lake ooids and of ancient nonskeletal carbonate mineralogy, Sedimentology, 22, 497–538, 1975.

Sandberg, P. A.: An oscillating trend in Phanerozoic nonskeletal carbonate mineralogy, Nature, 305, 19–22, 1983.

Schlanger, S. O.: Dolomite growth in coralline algae, J. Sediment. Petrol., 27, 181–186, 1957.

Scholle, P. A.: A color illustrated guide to carbonate rock constituents, textures, cements, and porosities, Am. Assoc. Petr. Geol. Mem., 27, 241 pp., 1978.

Schupp, P. J. and Paul, V. J.: Calcium carbonate and secondary metabolites in tropical seaweeds: variable effects on herbivorous fishes, Ecology, 75, 1172–1185, 1994.

Scott, R. W.: Evolution of Early Cretaceous reefs in the Gulf of Mexico, Paleont. Americana., 54, 406–412, 1984.

Searle, D. E. and Flood, P. G.: *Halimeda* bioherms of the Swain Reefs—Southern Great Barrier Reef, Proc. 6th Int. Coral Reef Symp., 3, 139–144, 1988.

Segonzak, G.: Aspects concernant les algues de type *Halimeda* (Chlorophycées), actuelles et fossiles, B. Soc. Hist. Naturelle, 122, 125–129, 1986.

Siemann, M. G.: Extensive and rapid changes in seawater chemistry during the Phanerozoic: evidence from Br contents in basal halite, Terra Nova, 15, 243–248, 2003.

Sikes, C. S., Roer, R. D., and Wilbur, K. M.: Photosynthesis and coccolith formation: inorganic carbon sources and net inorganic reaction of deposition, Limnol. Oceanogr., 25, 248–261, 1980.

Simonson, B. M., Schubel, K. A., and Hassler, S. W.: Carbonate sedimentology of the early Precambrian Hamersley Group of Western Australia, Precambrian Res., 60, 287–335, 1993.

Spencer, R. J. and Hardie, L. A.: Control of seawater composition by mixing of river waters and mid-ocean ridge hydrothermal brines, in Fluid-Mineral Interactions: A tribute to H. P. Eugster, edited by: Spencer, R. J. and Chou, I. M., 409–419, 1990.

Smith, A. D. and Roth, A. A.: Effect of carbon dioxide concentration on calcification in the red coralline alga *Bossiella orbigniana*, Mar. Biol., 52, 217–225, 1979.

Spotte, S. H.: Seawater Aquariums: The Captive Environment, Wiley and Sons, New York, 413 pp., 1979.

Stanley, G. D. and McRoberts, C. A.: A coral reef in the Telkwa Range, British Columbia: the earliest Jurassic example, Can. J. Earth Sci., 30, 819–831, 1993.

Stanley, S. M. and Hardie, L. A.: Secular oscillations in carbonate mineralogy of reef-building and sediment-producing organisms driven by tectonically forced shifts in seawater chemistry, Palaeogeogr., Palaeoclimatol., Palaeoecol., 144, 3–19, 1998.

Stanley, S. M. and Hardie, L. A.: Hypercalcification: paleontology links plate tectonics and geochemistry to sedimentology, GSA Today, 9, 1–7, 1999.

Stanley, S. M., Ries, J. B., and Hardie, L. A.: Seawater chemistry, coccolithophore population growth, and the origin of Cretaceous chalk, Geology, 33, 593–596, 2005.

Stanley, S. M., Ries, J. B., and Hardie, L. A.: Low-magnesium calcite produced by coralline algae in seawater of Late Cretaceous composition, P. Natl. Acad. Sci., 99, 15323–15326, 2002.

Stanley, S. M., Ries, J. B., and Hardie, L. A.: Increased production of calcite and slower growth for the major sediment-producing alga *Halimeda* as the Mg/Ca ratio of seawater is lowered to a "calcite sea" level, J. Sediment. Res., 80, 6–16, 2010.

Stanton, R. J. and Flügel, E.: Paleoecology of Upper Triassic reefs in the northern Calcareous Alps: reef communities, Facies, 16, 157–186, 1987.

Steuber, T.: Plate tectonic control on the evolution of Cretaceous platform-carbonate production, Geology, 30, 259–262, 2002.

Steuber, T. and Rauch, M.: Evolution of the Mg/Ca ratio of Cretaceous seawater: Implications from the composition of biological low Mg calcite, Mar. Geol., 217, 199–213, 2005.

Steuber, T. and Veizer, A.: Phanerozoic record of plate tectonic control of seawater chemistry and carbonate sedimentation, Geology, 30, 1123–1126, 2002.

Stockman, K. W., Ginsburg, R. N., and Shinn, E. A.: The production of lime mud by algae in south Florida, J. Sediment. Petrol., 37, 633–648, 1967.

Stolarski, J., Meibom, A., Przenioslo, R., and Mazur, M.: A Cretaceous scleractinian coral with a calcitic skeleton, Science, 318, 92–94, 2007.

Sumner, D. Y. and Grotzinger, J. P.: Implications for Neoarchaean ocean chemistry from primary carbonate mineralogy of the Campbellrand-Malmani Platform, South Africa, Sedimentology, 51, 1273–1299, 2004.

Swart, P.: The effect of seawater chemistry on the growth of some scleractinian corals, in: Development and Cellular Biology of Coelenterates, edited by: Tardent, P. and Tardent, R., Elsevier, Amsterdam, 203–208, 1980.

Tarutani, T., Clayton, R. N., and Mayeda, T. K.: The effect of polymorphism and magnesium substitution on oxygen isotope fractionation between calcium carbonate and water, Geochim. Cosmochim. Ac., 33, 987–996, 1969.

Timofeeff, M. N., Lowenstein, T. K., da Silva, M. A. M., and Harris, N. B.: Secular variation in the major-ion chemistry of seawater: Evidence from fluid inclusions in Cretaceous halites, Geochim.Cosmochim. Ac., 70, 1977–1994, 2006.

Tribble, J. S., Arvidson, R. S., Lane, M., and Mackenzie, F. T.: Crystal chemistry, and thermodynamic and kinetic properties of calcite, dolomite, apatite, and biogenic silica: applications to petrologic problems, Sediment. Geol., 95, 11–37, 1995.

Tyrrell, T. and Zeebe, R. E.: History of carbonate ion concentration over the last 100 million years, Geochim. Cosmochim. Ac., 68, 3521–3530, 2004.

Uku, J., Beer, S., and Björk, M.: Buffer sensitivity of photosynthetic carbon utilisation in eight tropical seagrasses, Mar. Biol., 147, 1085–1090, 2005.

Vail, P. R. and Mitchum, R. M.: Global cycles of relative changes of sea level from seismic stratigraphy, Am. Assoc. Petr. Geol. Mem., 29, 469–472, 1979.

Van de Poel, H. M. and Schlager, W.: Variations in Mesozoic-Cenozoic skeletal carbonate mineralogy, Geologie en Mijnbouw, 73, 31–51, 1994.

Van den Hoek, C.: Chlorophyta: morphology and classification, in: The Biology of Seaweeds, edited by: Lobban, C. S. and Wynne, M. J., University of California Press, Berkeley, 86–132, 1981.

Van Lith, Y., Warthmann, R., Vasconcelos, C., and McKenzie, J. A.: Microbial fossilization in carbonate sediments: A result of the bacterial surface involvement in dolomite precipitation, Sedimentology, 50, 237–245, 2003.

Verbruggen, H., De Clerck, O., Kooistra, W., and Coppejans, E.: Molecular and morphometric data pinpoint species boundaries in *Halimeda* section Rhipsalis (Bryopsidales, Chlorophyta), J. Phycol., 41, 606–621, 2005.

Visscher, P. T. and Stolz, J. F.: Microbial mats as bioreactors: Populations, processes, and products, Palaeogeogr., Palaeoclimatol., Palaeoecol., 219, 87–100, 2005.

Wainwright, S. A., Biggs, W. D., Currey, J. D., and Gosline, J. M. Mechanical Design in Organisms, Edward Arnold, London, 423 pp., 1976.

Walter, L. M.: Relative efficiency of carbonate dissolution and precipitation during diagenesis: A progress report on the role of solution chemistry, in: Roles of Organic Matter in Sediment Diagenesis, edited by: Gautier, D., SEPM Spec. P., no. 38, 1–11, 1986.

Watabe, N. and Wilbur, K. M.: Influence of the organic matrix on crystal type in molluscs, Nature, 188, 334, 1960.

Webb, G. E. and Sorauf, J. E.: Zigzag microstructure in rugose corals: A possible indicator of relative seawater Mg/Ca ratios, Geology, 30, 415–418, 2002.

Wefer, G.: Carbonate production by algae *Halimeda*, *Penicillus* and *Padina*, Nature, 285, 323–324, 1980.

Wilbur, K. M., Hillis-Colinvaux, L., and Watabe, N.: Electron microscope study of calcification in the alga *Halimeda* (order *Siphonales*), Phycologia, 8, 27–35, 1969.

Wilkinson, B. H.: Biomineralization, paleoceanography, and the evolution of calcareous marine organisms, Geology, 7, 524–527, 1979.

Wilkinson, B. H. and Algeo, T. J.: Sedimentary carbonate record of calcium-magnesium cycling, Am. J. Sci., 289, 1158–1194, 1989.

Wilkinson, B. H. and Givens, K. R.: Secular variation in abiotic marine carbonates: Constraints on Phanerozoic atmospheric carbon dioxide contents and oceanic Mg/Ca ratios, J. Geol., 94, 321–333, 1986.

Wolfe, J. A.: A paleobotanical interpretation of Tertiary climates in the Northern Hemisphere, in: Paleontology and Paleoenvironments, William Kaufmann, Inc., Los Altos, CA, 129–138, 1978.

Wood, H. L., Spicer, J. I., and Widdicombe, S.: Ocean acidification may increase calcification rates, but at a cost, P. R. Soc. B, 275, 1767–1773, 2009.

Wray, J. L.: *Archaeolithophyllum*, an abundant calcareous alga in limestones of the Lansing Group (Pennsylvanian), southeastern Kansas, Kansas Geol. Survey Bull., 170, 1–13, 1964.

Wray, J. L.: Calcareous Algae, Elsevier, Amsterdam, 185 pp., 1977.

Yates, K. K. and Robbins, L. L.: Production of carbonate sediments by a unicellular green alga, Am. Mineral., 83, 1503–1509, 1998.

Yan, J., Munnecke, A., Steuber, T., Carlson, E. H., and Xiao, Y.: Marine sepiolite in Middle Permian carbonates of South China: Implications for secular variation of Phanerozoic seawater chemistry, J. Sediment. Res., 75, 328–338, 2005.

Yates, K. K. and Robbins, L. L.: Radioisotope tracer studies of inorganic carbon and Ca in microbially derived $CaCO_3$, Geochim. Cosmochim. Ac., 63, 129–136, 1999.

Yates, K. K. and Robbins, L. L.: Microbial lime-mud production and its relation to climate changes, in: Geological Perspectives of Global Climate Change, edited by: Gerhard, L. C., Harrison, W., and Hanson, B. M., Am. Assoc. Petr. Geol. B., Tulsa, Oklahoma, 47, 267–283, 2001.

Zechman, F. W., Theriot, E. C., Zimmer, E. A., and Chapman, R. L.: Phylogeny of the Ulvophyceae (Chlorophyta): Cladistic analysis of nuclear encoded rRNA sequence data, J. Phycol., 26, 700–710, 1990.

Zhuravlev, A. Y. and Wood, R. A.: Eve of biomineralization: controls on skeletal mineralogy, Geology, 36, 923–926, 2008.

Zhuravlev, A. Y. and Wood, R. A.: Controls on carbonate skeletal mineralogy: Global CO_2 evolution and mass extinctions, Geology, 37, 1123–1126, 2009.